Doctoral Dissertation

Degradation Mechanism and Application of Self-degradable Adhesive Composed of Aldehyde-Functionalized Dextran and Succinic Anhydride-treated ε-poly-L-lysine

Yuki Gen

Supervisor: Professor Kazuaki Matsumura

Japan Advanced Institute of Science and Technology
School of Materials Science
March 2023

Referee-in-chief:

Professor Dr. Kazuaki Matsumura

Japan Advanced Institute of Science and Technology

Referees:

Professor Dr. Tatsuo Kaneko

Japan Advanced Institute of Science and Technology

Professor Dr. Motoichi Kurisawa

Japan Advanced Institute of Science and Technology

Associate Professor Dr. Eijiro Miyako

Japan Advanced Institute of Science and Technology

Associate Professor Dr. Tooru Ooya

Graduate School of Engineering, Faculty of Engineering,

Kobe University

Abstract

Invasive techniques such as sutures and staples are used to join wounds, but have drawbacks such as secondary tissue damage. A promising and attractive option to mitigate this disadvantage and to close and connect tissues is the use of tissue adhesives. Tissue adhesives are not only used as an adjunct during suturing in surgery, but also function as hemostatic agents, sealants, and tissue adhesives that firmly join and secure two surfaces. However, clinically used tissue adhesives do not fully meet the required properties such as low adhesion under wet conditions and low cytocompatibility, and research and development of new tissue adhesives are being actively conducted worldwide.

Our group has also developed a self-degradable dextran-based medical adhesive, LYDEX, with high adhesive performance and flexibility, low toxicity, and no risk of viral infection, to meet the requirements for an ideal tissue adhesive. LYDEX is a hydrogel composed of aldehyde-functionalized dextran (AD) and succinic anhydride-treated ε-poly-L-lysine (SAPL). This hydrogel is being considered for a wide range of medical applications, including hemostatic agents, sealants, and anti-adhesion materials. However, to apply LYDEX as a medical material, it is necessary to elucidate the mechanism of degradation as much as possible, since it is a degradable and absorbable material and a novel substance.

After gelation and adhesion of LYDEX by Schiff base bond formation between the aldehyde group of AD and the amino group of SAPL, molecular degradation associated with the Maillard reaction begins, but the detailed degradation mechanism was unknown. Here, I elucidated the degradation mechanism of LYDEX by analyzing the major degradation products under typical *in vitro* solution conditions. Degradation of LYDEX gels with sodium periodate/dextran content of 2.5/20 was observed using gel permeation high-performance liquid chromatography and infrared and ^{1}H NMR spectroscopy; the AD ratio in the AD-SAPL mixture increased with decreasing molecular weight as degradation time progressed. The discovery of the self-degradability of LYDEX is valuable for elucidating the degradation mechanism of other polysaccharide hydrogels and for the use of LYDEX in medical applications such as hemostatic and sealant materials.

LYDEX applications are being considered for a wide range of medical fields as described above, and its unique potential to control the *in vivo* degradation rate depending on its composition has been confirmed for anti-adhesion applications. The thickness of the gel also plays an important role in determining the degradation rate, but this issue has not been fully explored in previous studies. Therefore, in this study, the optimal LYDEX dose (film thickness) to maximize the performance of anti-adhesion materials was tested using a rabbit colon model, and it was confirmed that gel film thickness affects the degradation period and anti-adhesion efficacy. The results obtained suggest the possibility of designing LYDEX materials applicable to a wider range of *in vivo* treatment sites, which would be extremely beneficial for the development and use of novel anti-adhesion materials with adequate hemostatic and sealing performance.

In conclusion, the elucidation of the degradation mechanism of LYDEX and the investigation of maximizing its anti-adhesion performance obtained in this study will not only enhance the applicability of LYDEX as a polymeric material for medical use, but also contribute to the research and development of polymeric compounds as a whole, for which the degradation mechanism is complex to understand. Specifically, combining the degradation mechanism of polysaccharide hydrogels (polymer compounds) with methods to control degradation by oxidation is expected to contribute to the development of new materials.

Keywords: hydrogel, LYDEX, degradation, dextran, poly-L-lysine, Maillard reaction, anti-adhesion.

Contents

List of Tables and Firures

Chapter 1

General Introduction

1.1. Tissue adhesives

Invasive techniques such as sutures, staples, clips, and wires are commonly used in surgery to join wounds, but they have several drawbacks. For example, suturing for wound closure is not only time consuming, but also results in secondary tissue damage, microbial infection, fluid and/or gas leakage, and cosmetically undesirable outcomes[1]. For staples, their use also tends to cause tissue damage, inflammatory reactions, and scar tissue formation including intraperitoneal adhesions, and is associated with high failure rates[2,3].

A promising and attractive alternative to reduce these invasive techniques and make tissue closure and connection more reliable, practical, and quicker is the use of tissue adhesives. The application of tissue adhesives is a convenient alternative method of wound closure, characterized by a simple implementation procedure, shorter time, less patient pain, and no need for removal. In addition, tissue adhesive spreads over the entire contact area of the applied area, eliminating stress localization and facilitating load transfer between the fracture surfaces[4,5]. Furthermore, tissue adhesives are easy to apply, bond dissimilar materials, increase design flexibility, improve cost-effectiveness, act as sealant materials or hemostatic agents to prevent fluid and/or gas leakage from the anastomosis, and cause minimal or no tissue damage at the application site[6]. A wide variety of medical polymeric materials have been used to achieve this

goal[7]. Table 1.1 summarizes the medical polymeric materials intended for biological tissue adhesion. The main types of polymeric materials for tissue adhesion are liquid and sheet. In order to improve the adhesion of these materials to biological tissues, materials have been designed to introduce molecular interactions such as covalent bond formation or hydrophobic interactions, coordination bonds, electrostatic interactions, and molecular recognition at the interface with the biological tissue. Recently, research and development of adhesive materials based on biomimetic technology is rapidly expanding.

Research and development of tissue adhesives has skyrocketed due to their many attractive advantages over traditional closure methods, and the market for tissue adhesives is currently estimated at about $38 billion[8]. Tissue adhesives are classified as hemostatic agents, sealant materials, and adhesives based on their function, as well as their use as an adjunct during suturing in surgery. Although they are often treated in the same way, they are quite different from each other. Hemostatic agents achieve hemostasis by triggering a coagulation reaction. Sealants form a barrier layer that prevents fluid and/or gas from leaking through the incision, ensuring a watertight seal. Adhesives function to firmly bond and secure two surfaces and are applied to a variety of tissues, including skin, muscle, and intestine[9,10].

Since tissue adhesives are usually used *in vivo*, they must be safe, have strong wet adhesion, stability under physiological conditions, degradation and absorption *in vivo*, stability during sterilization processes, rapid curing and cross-linking without excessive heat generation, cytocompatibility, minimal swelling, and elastic modulus comparable to tissue. Table 1.2 summarizes the properties required for tissue adhesives. Ideally, the product should be able to be stored at refrigerated or room temperature and applied easily intraoperatively.

Tissue adhesives already in clinical application include cyanoacrylate adhesives made from synthetic materials, fibrin glue adhesives made from naturally derived materials, and

biopolymer-aldehyde adhesives made from naturally derived materials and synthetic materials. However, these tissue adhesives do not fully meet the aforementioned required properties, such as low adhesive strength under wet conditions and low cytocompatibility[11-13].

This chapter describes the current status of new adhesives reported in the scientific literature, in addition to tissue adhesives already in clinical application, and discusses their advantages and disadvantages. Specifically, we focus on synthetic polymers, biopolymers, biofunctional mimetic materials, and biostructural mimetic materials, and address them from the perspective of polymer chemistry. This will provide a plot for research on the degradation mechanism and application of a new aldehyde-functionalized dextran-based self-degrading medical adhesive I have been developing, LYDEX.

Table 1.1: Applications of Medical Polymers for Tissue Adhesion

Classification	Materials	Components	Applications	Ref.
Synthetic polymers	Cyanoacrylate-based	· ethyl-2-cyanoacrylate · n-Butyl-2-cyanoarylate · 2-Octyl-2-cyanoacrylate · n-hexyl-2-cyanoacrylate	· Medical Adhesives · Sealants · Hemostatic agents	[25]
	Urethane-based	· fluorinated isocyanate		[28], [29]. [33]
	Polyethylene glycol(PEG)-based	· 4 armed PEG encapped with -NHS or -amin, -thiol		[39], [43], [44]
Bio-polymers	Fibrin-based	· Fibrinogen/thrombin	· Medical Adhesives · Sealants · Hemostatic agents · Anti-adhesive Materials · Scaffolding Materials	[47]
	Alubumin-based	· Human serum albumin · Bovine serum albumin		[54], [56], [57]
	Gelatin-based	· Gelatin/resorcinol/formaldehyde/glutaraldehyde · Gelatin/genipin · Hydrophobically modified gelatin		[60], [68]
	Polysaccharide	· Dextran aldehyde · Hyaluronic acid aldehyde · Chondroichin sulfate aldehyde · Carboxymethyl chitin		[70], [71], [75], [76], [77], [78], [79], [80], [81], [82], [84]
Biofunctional mimetic materials	Mussel adhesion protein	· 3,4-dihydroxyphenylalanine (DOPA)	· Medical Adhesives	[119]
Biostructure-mimetic materials	Gecko foot structure materials	· Poly (dimethylpolysiloxane)	· Medical Adhesives	[136]

Table 1.2: Properties Required of Tissue Adhesives

Safety	No concern of virus infection.
Adhesive strength	Sufficient adhesion to biological tissues even in wet environments.
Pressure resistance	Withstand the pressure of fluid and/or gas leakage from the cut surface.
Biodegradable/absorbable *in vivo*	Absorbed by the living body and the degradation products are harmless.
Sterilization stability	No change in adhesive properties during the sterilization process.
Adhesion time	Adhesion within seconds – minutes.
Mild reactivity	Adhere at around body temperature and do not generate reactive heat that can damage tissue.
Cytocompatibility	To provide a scaffold for cells to enter.
Minimal swelling	The degree of swelling should be such that it does not compress nerves or blood vessels.
Integrative mechanics	Strength and flexibility to prevent damage due to stretching and contraction of soft tissues caused by body movements.
Non-irritant, non-obstructive	Do not cause inflammation at the site of use or unnecessary tissue adhesion around the site of use.
Handling	Good storage stability and easy intraoperative use.

1.2. Elastic sealants based on synthetic polymers

1.2.1. Cyanoacrylate-based

Cyanoacrylate (CA) adhesives are a type of liquid synthetic adhesives based on alkyl α-cyanoacrylate, and their application in medicine was first seen in the Vietnam War, when spray CA adhesives were used to stop bleeding in soldiers[14]. Since then, it has been used for adhesion and reinforcement of living tissues (skin, blood vessels, organs, etc.), wound healing, wound covering, and prevention of contamination.

As with industrial adhesives, CA-based adhesives have the property of rapidly polymerizing and curing by anionic polymerization of monomers in the presence of trace amounts of water in living tissues or weak bases such as blood[15]. Also, functional groups of proteins present on the tissue surface, such as primary amines on lysine side chains, initiate CA polymerization and form tissue-to-tissue The advantages of CA-based adhesives include strong wet adhesion, rapid curing, inherent bactericidal properties, good cosmetic effects, and low cost[11,16-19].

The chemical structural formula of CA is CH_2=C(CN)COOR, and its properties vary greatly depending on the length of the alkyl group (R) in the side chain. Alkyl groups have the general formula C_nH_{2n+1-} and are named according to the number of carbons. Typical examples include methyl group (n=1), ethyl group (n=2), butyl group (n=4), octyl group (n=8) and others. The lower the number of carbons in the alkyl group, the stronger the adhesion, but the decomposition releases cyanoacetic acid and formaldehyde, which are tissue toxic components[20] and their degradation products cause inflammatory reactions and delayed wound healing[21]. Therefore, the use of low-carbon methyl-2-cyanoacrylate (Figure 1.1(A)) and ethyl-2-cyanoacrylate (Figure 1.1(B)) has been almost completely discontinued[22-24], and the use of n-butyl-2-cyanoacrylate (Figure 1.1(C)) and 2-octyl-2-cyanoacrylate(Figure 1.1(D)), which have

complex structures with high carbon numbers, have been mainly continued for medical applications[25] (Table 1.3).

However, CA-based adhesives have limited applications as tissue adhesives because they have caused many problems, including chronic inflammation, *in vivo* tissue necrosis, intimal thickening, arterial eye lesions, occupational asthma, dermatitis, and *in vitro* cytotoxicity to cells in direct contact and to eluted solutions[24,26,27].

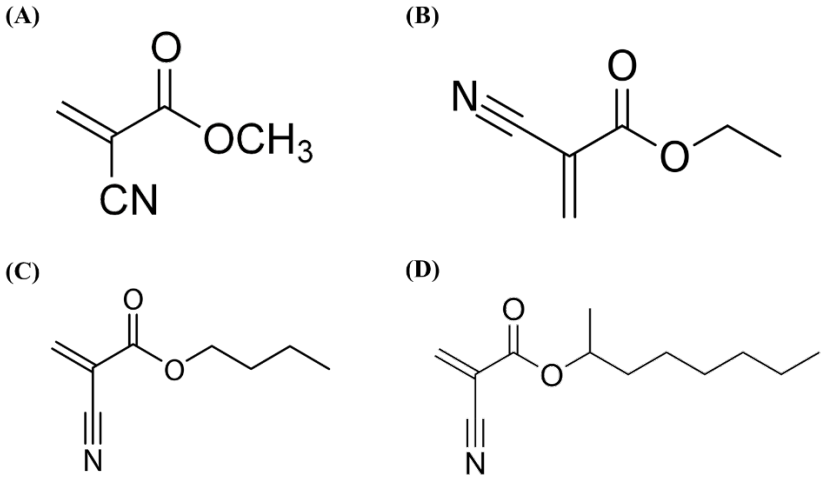

Figure 1.1. Structures of cyanoacrylates with (A) methyl-2-cyanoacrylate, (B) ethyl-2-cyanoacrylate, (C) n-butyl-2-cyanoacrylate and (D) 2-octyl cyanoacrylate.

Table 1.3 Cyanoacrylate adhesives for medical use

Commercial product	Manufacturer	Approced indications	Constituents
Aron Alpha A "Sankyo"	Toagosei	Wound healing of living tissue (skin, blood vessels, organs, etc.)	ethyl-2-cyanoacrylate
Dermabond®	Ethicon	Closure of topical skin incisions and trauma induced skin lacerations Barrier to microbial penetrations	2-octyl-2-cyanoacrylate
Indermil®	Henkel	Closure of topical skin incisions and traumainduced skin lacerations Barrier to microbial penetrations	n-butyl-2-cyanoacrylate
Omnex®	Ethicon	blocking the passage of blood, body fluids or air	n-octyl-2-cyanoacrylate / butyl lactoyl-2-cyano acrylate
Glubran® and Glubran2®	GEM Italy	synthetic surgical glue, CE certified for internal and external use, with haemostatic, adhesive, sealer and bacteriostatic properties	n-butyl-2-cyanoacrylate / methacryloxysulpholane
Leukosan® Adhesive	Terumo BSN	Closure of topical skin incisions and traumainduced skin lacerations	2-octyl-2-cyanoacrylate n-butyl-2-cyanoacrylate
Histoacryl® and Histoacryl® Blue	B. Braun	Closure of topical skin incisions and traumainduced skin lacerations	n-butyl-2-cyanoacrylate
TRUFILL™ n-BCA Liquid Embolic System	Codman & Shurtleff	Blockage or reduction of blood flow in cerebral arteriovenous malformations (AVMs)	n-butyl-2-cyanoacrylate
VenaSeal™ Closure System	Medtronic	Closure of blood vessels for treatment of varicose veins	n-butyl-2-cyanoacrylate
IFABond®	IFA medical	Class III implantable device designed to offer an alternative to staples and sutures (mesh)	n-hexyl-2-cyanoacrylate

1.2.2. Urethane-based

Urethane (PU)-based tissue adhesives have been applied as hemostatic and sealant materials due to their excellent thermal stability at physiological temperatures, lack of hemolytic activity, high elasticity, and strong adhesion to tissue[28]. In Japan, Hydrofit® (Terumo Corporation, Tokyo, Japan) is approved as a hemostatic agent for use at the anastomotic site of thoracic aorta and arch branch artery replacement surgery.

Hydrofit is composed of a polyether fluoropolymer PU prepolymer with reactive isocyanate groups introduced at both ends[29]. The isocyanate groups react with the amino groups of the tissue proteins to form urea bonds, which subsequently promote adhesive strength with the soft tissue[30]. The isocyanate groups also react with the amino groups of the tissue proteins to form urea bonds. And also, isocyanate groups react with water to produce carbon dioxide gas, which forms a gel-like flexible polymerization (film) that adheres closely to the anastomosis. As a result, it has moderate elasticity and strength, and is characterized by excellent follow-up to the beating of the heart and blood vessels. However, although it is derived from non-living material and the risk of infection can be avoided, it is composed only of synthetic components and is not degradable and absorbable in the body. Therefore, when used in surgery, there is a risk of foreign body reaction and increased risk of infection due to residual polymerized material in the body.

This restriction can be synthesized in a biodegradable form by molecular design or modification with natural molecules. For example, Kobayashi et al. introduced highly reactive isocyanate groups at both ends of biodegradable polyesters obtained by D,L-lactide polymerization or D,L-lactide-E-caprolactone (50:50) copolymerization using ethylene glycol or polyethylene glycol as initiators and synthesized biodegradable Biodegradable PU was synthesized[31]. Ferreira et al. synthesized biodegradable PU-based adhesives by modifying castor

oil with isophorone diisocyanate (IPDI)[28]. They also developed photo-crosslinkable They have developed a PU-based adhesive that is slightly hemolytic (within acceptable limits), but the hemolysis is reported to stop when the material is extracted with a PBS solution[32].

Overseas, TissuGlu® Surgical Adhesive (Cohera Medical Inc., Pittsburgh, PA, USA) is approved in the US and Europe as an adhesive for abdominal tissue. It is used to form bonds between tissue layers and reduce voids to prevent seroma due to postoperative fluid retention. The material is a one-component adhesive consisting of a hyperbranched polymer with isocyanate end groups containing approximately 50 wt% lysine[33]. Cross-linking occurs within 25 minutes, allowing sufficient time for closure of the abdominal skin. The gel is biodegradable by hydrolysis and enzymatic degradation of the lysine bonds, yielding a variety of water-soluble degradation products including polyols, lysine, ethanol, and carbon dioxide, all of which are readily excreted from the body.

Despite these improvements in biodegradability and toxicity disadvantages, there are still safety concerns regarding the use of urethane monomolecular isocyanates in surgery, as they are notably sensitizing even in very small amounts, have a high incidence rate, and can cause death with acute or chronic exposure[34,35].

1.2.3. Polyethylene glycol-based

Polyethylene glycol (PEG)-based products are widely used as sealants and hemostatic agents. PEG is a hydrophilic biocompatible polymer that is widely used as a biomaterial in tissue engineering because of its properties suitable for medical applications, including stealth behavior *in vivo*, where it is not easily recognized by the immune system[36-38]. Sealant materials approved by the U.S. Food and Drug Administration include the DuraSeal® Cranial Sealant System (INTEGRA LifeSciences Corporation, New Jersey, USA), the Adherus™ Dural Sealant system

(HyperBranch Medical Technology, North Carolina, USA), and CoSeal® (Cohesion Technologies, Inc., California, USA).

DuraSeal® Cranial Sealant System is a surgical sealant material used in neurosurgery to prevent cerebrospinal fluid leakage after cranial and spinal surgery[39-42]. A tetrabranched PEG with an N-hydroxysuccinimide (NHS)-activated ester at the end is utilized (Figure 1.2A). The NHS active ester reacts with amino groups under physiological conditions to form amide bonds. This cross-linking reaction is used to combine an aqueous solution of PEG with NHS active esters (sodium borate buffer, pH 4.0) with an aqueous solution of trilysineamine (Figure 1.2B) with amino groups (sodium borate buffer, pH 10.2)[42].

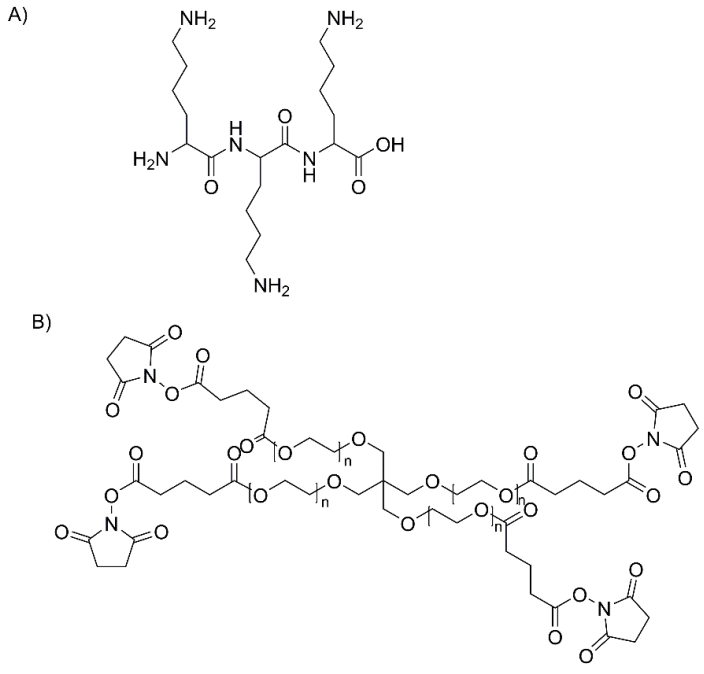

Figure 1.2: Structures of A) trilysine and B) pentaerythritol poly(ethylene glycol) ether tetrasuccinimidyl glutarate. [42]

The Adherus® Dural Sealant system is a new hydrogel sealant designed for use as an adjunct to standard methods of dural repair such as sutures, allowing for watertight closure[43]. One of the main components is a PEG succinimidyl sebacate polymer with two electrophilic ester groups, and the other is a polyethyleneimine polymer with about 17 nucleophilic amine groups (Figure 1.3). When the two precursor solutions are mixed in the provided applicator to prepare the sealant, cross-linking occurs and a solid, absorbable, biocompatible PEG-based hydrogel is formed.

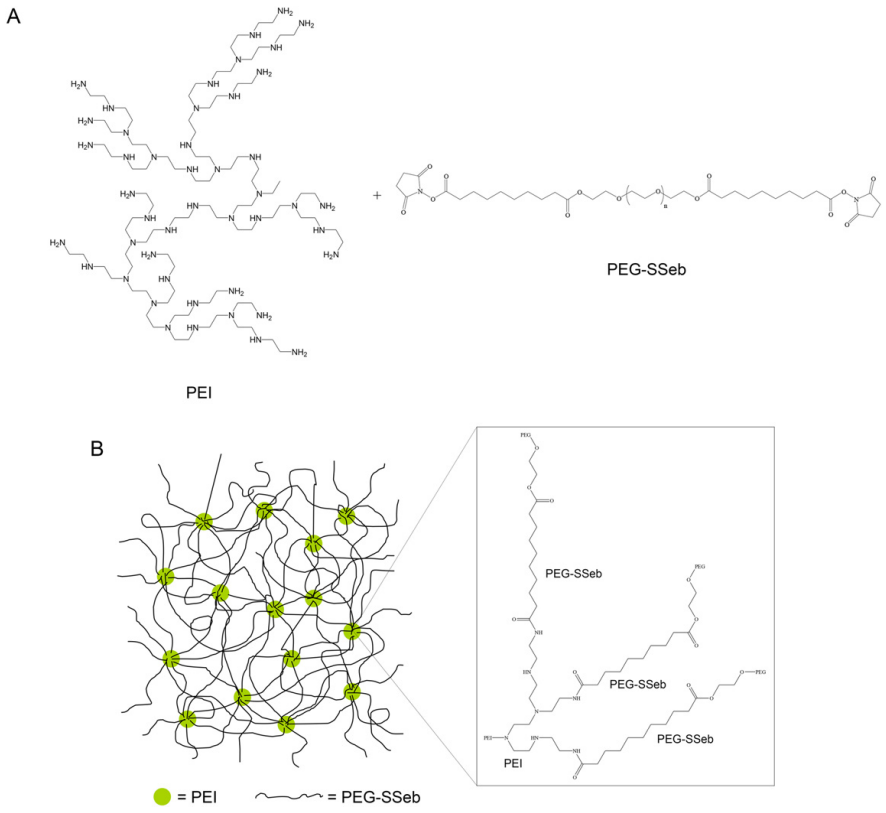

Figure 1.3. A depiction of a novel hydrogel used to provide augmentation to standard methods of dural repair. (A) Schematic of crosslinking components for novel hydrogel including a modified polyethylene glycol (PEG) succinimidyl sebacate polymer with terminal electrophilic ester groups and a polyethyleneimine (PEI)with nucleophilic amine groups. [43]

CoSeal® has been used in vascular surgery to seal sutures and stop bleeding[44]. The carbonyl and thiol (SH) groups of the NHS active ester form covalent bonds between PEG molecules under physiological conditions[45]. This product uses this covalent bond formation and consists of two 4-arm PEGs with a glutaryl-succinimidyl ester and a thiol end group (Figure 1.4)[45].

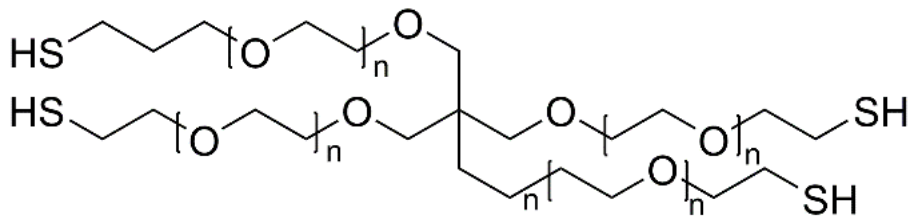

Figure 1.4. Structure of pentaerythritol poly(ethylene glycol) ether tetra thiol. [45]

In addition to causing cross-linking between the two components, these sealant materials also react with amino groups in biological tissues, resulting in high adhesion and tissue following properties. However, PEG-based sealants have a high degree of swelling, which may put pressure on the surrounding tissue at the site of application[46]. In addition, both products require preoperative dissolution of the powder, which is a weakness in terms of handling.

1.3. Sealants based on natural polymers

1.3.1. fibrin-based

Tissue adhesives made from fibrin, a component derived from human blood, were one of the earliest surgical adhesives widely used in medical applications, including medical adhesives, sealant materials, and hemostatic agents[47]. The mechanism of action of fibrin glue is similar to a series of biological reactions during the final stages of blood coagulation *in vivo*[48,49].

Fibrin glue is composed of two major components from human plasma: fibrinogen and thrombin. Fibrinogen is a soluble glycoprotein with a molecular weight of approximately 340,000 present in plasma and plays a central role in hemostasis and thrombus formation. Thrombin cleaves fibrinopeptides A and B from the alpha and beta chains in fibrinogen, respectively, and converts them to fibrin monomers. These fibrin monomers are physically cross-linked via hydrogen bonds to form unstable thrombi (fibrin polymers). In addition, the action of blood coagulation factor XIII (fibrin stabilizing factor) activated by thrombin in the presence of calcium ions results in cross-linking bonds between fibrin polymers. More specifically, factor XIIIa, formed from factor XIII with Ca2+ as a cofactor, acts on the fibrin polymer to form cross-links in the form of amide bonds between glutamate and lysine residues to form insoluble blood clots that are resistant to proteolysis (Figure 1.5). These clots are stable fibrin clots with a three-dimensional fine structure called stabilized fibrin, and the formation of these clots results in tissue adhesion and closure[11]. Note that, as mentioned above, these biological processes are facilitated by calcium ions, so many fibrin glues also contain small amounts of calcium ions to facilitate the reaction[50].

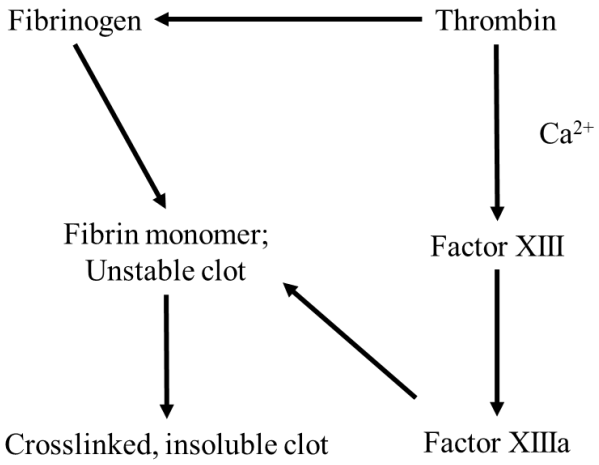

Figure 1.5. Mechanism of clot formation in fibrin glue resembling physiological coagulation.

Fibrin glues are highly biocompatible and versatile because they are composed of biologically derived components[12]. However, they have several drawbacks that limit their use and raise safety concerns. In the former, their low interfacial strength to biological tissue and organ surfaces prevents them from providing an adequate sealing effect[51]. As such, their mechanical properties are not strong enough for many elastic tissues. As a result, fibrin glues are often used in combination with conventional techniques such as sutures and staples[51].

With regard to safety, there is concern about the transmission of diseases that may be associated with blood products (e.g., hepatitis C and HIV viruses) because they are manufactured from human plasma from blood donors. Therefore, fibrin glue components are subjected to virus screening and virus inactivation/reduction treatments such as pasteurization, two-step steam heat treatment, solvent washing, dry heat treatment, nanofiltration, precipitation, pH treatment, and some chromatographic processes. However, no particular treatment is effective against all viruses[52] and medical applications generally require a combination of these treatments[47].

1.3.2. Albumin-based

Albumin is a relatively small protein with a molecular weight of about 66,000, made up of about 600 amino acids. Albumin makes up about 60% of plasma proteins and is available from a variety of animal sources. Medical adhesives containing human serum albumin are composed of albumin reacted with a PEG-based cross-linker[53]. Because of the flexibility afforded by the use of PEG cross-linkers, the first application is air leakage prevention in pulmonary surgery, for which Progel™ Pleural Air Leak Sealant (Bard Davol, Inc., Massachusetts, USA) is commercially available in the United States.

Progel™ Pleural Air Leak Sealant is a composite sealant containing human albumin and a PEG cross-linker with two NHS-activated ester groups[54,55]. When mixed, the primary amine groups on the lysine residues of albumin react rapidly with the succinimidyl succinate groups to form a cross-linked structure within one minute. Progel™ was shown to effectively stop pleural air leakage and to degrade relatively quickly *in vivo* without severe immune response[54,55].

Recently, Tridyne™ Vascular Sealant (Becton, Dickinson and Company, New Jersey, USA) has been marketed as a solution to enhance aortic anastomosis and control bleeding in cardiovascular surgery. This product reportedly combines polyethylene glycol and human serum albumin to form a strong, flexible seal even in anticoagulated patients[56].

BioGlue® (CryoLife Inc., Gerogia, USA), a medical adhesive composed of bovine serum albumin and glutaraldehyde, is commercially available in the United States. This product was approved in Japan in 2010 and is used as an adhesive for the treatment of dissecting aortic aneurysms[57]. The covalent bonding of glutaraldehyde and bovine serum albumin binds to tissue proteins at the repair site by a mechanism other than blood coagulation in the body to form a flexible mechanical bond. Upon mixing, polymerization begins immediately, solidifying within

20~30 seconds and reaching a higher bonding strength in 2 minutes. However, this rapid solidification requires extreme caution during use, as improper dripping can lead to the risk of embolism, causing cerebral embolism, myocardial infarction, or arterial embolism of the extremities[58]. In addition, since concerns about the biological safety of glutaraldehyde arise, caution should also be exercised regarding damage to the transverse nerves and the stimuloconductive system due to tissue toxicity from BioGlue® adhesion. Furthermore, these adhesives use serum-derived albumin, which poses the challenge that the risk of infection cannot be ruled out 100%. For this reason, products using genetically modified albumin have also been developed[59].

1.3.3. Gelatin-based

Gelatin is a protein produced by an irreversible hydrolysis process from collagen, an important component of connective tissue in animal skin and bone. Because of its excellent bioabsorbability and biocompatibility, it is widely applied in the medical field.

Gelatin is water-soluble and is quickly degraded by various proteases present in the body and absorbed by the body, so an intermolecular cross-linking reaction is performed with formamide and glutaraldehyde.

Early studies investigated formaldehyde-based adhesives that react with formaldehyde and the primary amino groups of lysine residues in gelatin to form covalent bonds, and gelatin-resorcinol-glutaraldehyde (GRF) adhesives were developed with the addition of resorcinol to increase bond strength[60]. This adhesive is said to be less toxic than methyl cyanoacrylate adhesives and is characterized by the addition of formaldehyde to a mixed solution of gelatin and resorcinol to cure and bond[61]. However, due to the well-known toxicity of formaldehyde, glutaraldehyde was later used as a cross-linking gelatin-resorcinol-formaldehyde-glutaraldehyde

hide (GRFG) adhesive was developed using glutaraldehyde as the cross-linking agent[60,62,63]. Formaldehyde-based adhesives have stronger initial bond strength, while glutaraldehyde-based adhesives exhibit greater stability *in vivo*. The adhesive strength of GRFG to dry substrates is comparable to cyanoacrylate-based adhesives and significantly stronger than fibrin-based adhesives, but degrades under wet conditions[64]. Despite their high adhesive strength and improved *in vivo* stability, the main concern regarding GRF and GRFG sealants is the toxicity of formaldehyde and glutaraldehyde. In fact, there were scattered reports of re-dissociation in the remote postoperative period and occurrence of anastomotic pseudoaneurysms, which were thought to be caused by the tissue toxicity of the formaldehyde and glutaraldehyde mixture[65], and the products have now been discontinued worldwide.

A gelatin-genipin two-component adhesive using genipin as an additive has also been reported[66]. Genipin is an aglycon of an iridoid glycoside called geniposide, which is found in the fruit of gardenias of the family Acanthaceae,[67] and is known to react with lysine residues in proteins to form cross-links. This genipin has been shown to be less cytotoxic than glutaraldehyde and to have about 50% of the adhesive strength of biopolymer-aldehyde adhesives[66].

Furthermore, research on surgical sealants using hydrophobized gelatin to improve biological tissue adhesion in a wet environment during surgery was also reported[68]. Hydrophobic gelatin, in which cholesteryl groups are introduced to the amino groups in gelatin, has high interaction with proteins and cell membranes in biological tissues, resulting in high interfacial adhesion between the hydrogel made of this hydrophobic gelatin and biological tissues[68]. Hydrophobic gelatin, in which amino groups in gelatin are modified with lipophilic molecules, has been shown to exhibit high adhesion to aortic tissue when combined with

tetrabranched PEG with NHS active esters[68]. Practical applications of bioadhesives based on this gelatin are currently underway.

With regard to the safety of gelatin, since the gelatin is treated with acids and alkalis and at high temperatures during extraction, there is no possibility of viral contamination of the final gelatin[69-72].

1.4. Polysaccharide-based (dextran, hyaluronic acid, chondroitin sulfate, chitosan, chitin)

Polysaccharides are rich in functional groups such as amines, hydroxyls, and carboxylic acids. Adhesives developed from monosaccharide (sugar) building blocks adhere to amine groups on tissue surfaces by N-hydroxysuccinimide activation, Schiff base formation, Michael addition reactions, biaryl formation, imine formation, and covalent bonding through π-π interaction.

As for polysaccharide-based biological tissue adhesion technology, adhesives and sealant materials using aldehydized polysaccharides have been extensively studied. By reacting aldehyde groups introduced into polysaccharides with amino groups in biological tissues or synthetic polymers, excellent adhesion and sealing effects are achieved.

A typical example is a dextran-based medical adhesive with an aldehyde group. Dextran is a relatively complex polysaccharide with several branched structures, synthesized by the enzyme of the heterolactic acid bacteria Leuconostoc mesenteroides. Its linear portion is composed of glucose building blocks via α-1,6-linkages. Unlike chitosan, a polyglucosamine, dextran has no reactive amino groups. There is a modification strategy that relies on selective partial oxidation of dextran to introduce an aldehyde group, which reacts with the amino group

to form an imine bond (Schiff base), resulting in hydrogel formation. Our group have been researching the use of this modification strategy, specifically by mixing aldehyde-functionalized dextran with ε-poly-L-lysine[73]. The adhesive (LYDEX) was successfully applied in lung surgery, laparoscopic partial nephrectomy, eye reconstruction, cartilage and bone regeneration, cardiovascular surgery, drug and gene carrier agents, anti-adhesion, and as an endoscopic wound dressing[74-88]. Research investigations are also underway regarding the degradation mechanism of LYDEX[89,90]. Modification of dextran-based adhesives by introducing methacrylate functional groups for cross-linking with thiol cross-linkers[91] and preparation of enzymatically cross-linkable dextran-tyramine conjugates[92] have been reported by other research teams.

Other polysaccharide-based sealants have also been studied extensively. In the chitosan base, Ishihara et al. reported chitosan derivatives made by reacting chitosan with lactobionic acid in the presence of water-soluble carbodiimides[93,94] and Moratti et al. reported hemostatic and adhesive properties of gels with succinylated chitosan and aldehyde dextran[95]. Imine bonds are formed between amino and aldehyde groups to form gels, and Elisseeff et al. reported a gel-based sealant using chondroitin sulfate with aldehyde groups combined with poly(vinyl alcohol-co-vinylamine)[96]. Other reports include a regenerative medical injectable gel composed of aldehydized hyaluronic acid and chitosan[97] and a medical adhesive of carboxymethylated chitin[98].

1.5. Biofunctional mimetic materials

1.5.1. Mussels mimic adhesion in water

Adhesion enhancement techniques using cross-linked structures in nature have been studied for decades, inspired by the strong adhesive properties of mussels, especially the mussel,

to solid surfaces. Mussels are of particular interest because of their ability to secrete protein mucus threads from their feet that do not lose their adhesive properties in saline solution[99-101].

The main components of this mucus filament are the amino acids lysine and tyrosine, a complex mixture of proteins characterized by a very high content of L-b-3,4-dihydroxyphenyl-a-alanine (DOPA), which is obtained by the translational modification of tyrosine by tyrosine hydroxylase It is known[102]. After modification with DOPA, DOPA is oxidized to produce quinones[103-106]. Although the exact cross-linking mechanism is still unknown, it has been demonstrated that oxidation of DOPA is necessary for adhesion to tissue surfaces, and quinones have been reported to cross-link with other quinones, amines, and thiols[104-107]. Preliminary immunological studies have shown that mussel adhesion proteins are poor antigens and have great potential to be used for biomedical purposes, especially as adhesives for living tissues[108].

Early studies began with the extraction of proteins secreted from mussels[109]. The adhesive properties of mussel adhesive protein (mussel adhesive protein, MAP) extracted from mussels showed satisfactory results on a variety of substrates, including stainless steel, porcine duodenal mucosa, porcine small intestinal submucosa, and porcine skin[110-113]. Although this approach has helped us to understand the formation mechanism of this material, it is very difficult to isolate and purify trace amounts of MAP from natural mussels. In fact, it is said that 10,000 mussels are needed to extract 1 g of MAP, which is not cost-effective.100 Therefore, synthetic mimics of mussel adhesion have been developed using recombinant DNA technology, peptide synthesis, fragment condensation technology, and gene cloning[108,114,115].

For example, DOPA/catechol-functionalized polymeric materials have been designed and hemostatic adhesives such as chitosan/pluronic hydrogel, polyorganophazene-catechol, polyethylene glycol-citrate-catechol, and gelatin-catechol have been reported[116-119]. In addition,

non-covalent cross-linking by adding trivalent iron ions and covalent cross-linking by adding oxidants have been shown as cross-linking structures for adhesion[120-122].

Furthermore, Lee et al. reported that mussel-mimetic polymers containing catechol and amine groups as adhesive components exhibit aggregation of serum proteins upon blood contact[123]. It is worth noting that the phenomenon observed in mussel adhesive-blood contact is very similar to fibrin-mediated coagulation, and that this alternative artificial coagulation process does not require a biological substance such as fibrin. In Korea, this technology was approved as a Class IV medical device by the Korea Food and Drug Administration in October 2019 for InnoSEAL Plus (InnoTherapy, Inc., Seoul, Korea)[124] after its safety and efficacy for patients with bleeding after hepatectomy were confirmed in a randomized clinical trial. approved as a Class IV medical device. This product is a pad type and achieves hemostasis by compression, so the range of indications is limited.

1.6. Biostructure-mimicking materials

1.6.1. Gecko Structure

Geckos can glue and quickly climb up against vertical or inverted surfaces[125,127-132]. This is attributed to the presence of cilia on the surfaces of their feet[126]. They are densely covered with linear hairs (setae) with numerous terminal projections (spatu-lae) of 200-500 nm in length, and this structure allows them to detach while exhibiting strong adhesive properties[125,127]. It is well known that the adhesion of this terminal process to surfaces is controlled by a combination of Vander Waals forces[128] and capillary forces[129] and that it can travel at high speed on almost any surface[125,128]. Fast switching between adherent and detached

states during exercise is achieved by dynamic and reversible mechanical deformation of the toes, a mechanism commonly referred to as the detachment mechanism[133,134].

Inspired by the gecko's characteristic structure, the adhesive uses van der Waals forces by arranging nanostructures on the surface of the substrate. Studies using hierarchical carbon nanotube arrays have demonstrated maximum adhesion to dry surfaces (1000 kPa), which is 10 times stronger than that of geckos[135]. In contrast, studies using nanostructured films composed of polydimethylsiloxane showed little adhesion to hydrophilic surfaces in water[136].

To overcome this problem, adhesives have been developed using multilayer systems that coat the interface region to better adhere in wet environments. For example, an adhesive structural material consisting of a nanostructured film made of polydimethylsiloxane coated with the adhesive protein DOPA has been reported[137]. It exhibits high adhesion in the presence of water and maintains adhesion under dry conditions by mimicking the gecko structure. Mahdavi et al. reported a tissue adhesive using a tough biodegradable elastomer, polyglycerol sebacate acrylate, combined with a thin tissue-reactive biocompatible surface coating[138]. Coating nanomolded pillars of biodegradable elastomers with a thin film of oxidized dextran significantly increased interfacial adhesion strength in porcine intestinal tissue *in vitro* and in the rat abdominal subfascial environment *in vivo*, and *in vivo* experiments when implanted have shown little tissue reaction[138]. Other coatings with various compounds, such as medical cyanoacrylate[139], promote tissue cross-linking under wet physiological conditions and ensure irreversible chemical bonding.

While coatings improve adhesion, they also increase the number of manufacturing steps and complicate the manufacturing procedure. Barton, M. et al. developed a biocompatible sutureless adhesive for peripheral nerve repair as a one-stop manufacturing method[140,141]. The adhesive is based on chitosan, which is photochemically bonded to tissue with a green laser

without thermal damage[140,141]. The fabrication of the nanostructured film requires a simple dry-casting technique, but does not require a coating to stabilize the bond between the adhesive and the tissue in a wet environment. Furthermore, it has been reported that green laser-activated monolayer nanostructured films have increased adhesion to wet tissues due to a combination of van der Waals and electrostatic forces[142].

Thus, the adhesion technique that mimics the gecko structure is effective for biological tissue adhesion and is expected to have clinical applications in wet tissue adhesion.

1.7. Objective of study

As I have introduced, many tissue adhesives have been developed using natural and synthetic materials to reduce invasive wound closure such as sutures. Many tissue adhesives have been approved for clinical use and commercialized due to their advantages such as easy application, strong adhesion, and biodegradability. However, the disadvantages of some materials, such as concerns about viral infection and local application due to cytotoxicity, have created a need to develop alternative tissue adhesives.

Our group have also developed a new aldehyde-functionalized dextran-based self-degrading medical adhesive, LYDEX[73-77], to meet clinical needs. LYDEX is made from natural polymers of dextran and ε-poly-L-lysine, and is not only highly adhesive and flexible, but also safe because it is made from materials that are virus-free. In addition, since various dosage forms (liquid, powder, and sheet/disc) can be selected, application research is underway for many medical uses, including sealant materials[74,143], hemostatic materials[75,144], anti-adhesive materials[83,86,87], and wound dressing materials for endoscopy[88]. However, in order to achieve clinical applications, it is necessary to confirm the biological safety impact of LYDEX by

clarifying its degradation products, degradation mechanism, and *in vivo* kinetics, because LYDEX is a novel substance. Although previous studies have investigated that after the gelation reaction of the aldehyde and amino groups of aldehyde-functionalized dextran, the Maillard reaction proceeds and molecular degradation occurs, the degradation mechanism and degradation products of LYDEX itself have not yet been fully elucidated. Therefore, in Chapter 2 of this study, I will analyze the main degradation products of LYDEX in aqueous media by instrumental measurement in order to clarify the degradation process of LYDEX and attempt to elucidate the degradation mechanism. The elucidation of the reaction mechanism of polysaccharide degradation will be useful for developing new biodegradable polysaccharide substances for biomedical applications as well as for clinical applications of LYDEX.

In Chapter 3 of this study, I report a study focusing on the optimal LYDEX gel thickness (dosage) for anti-adhesion efficacy in order to advance the development stage toward clinical application of anti-adhesion materials, which is one of the applications of LYDEX. In anti-adhesion materials, it has already been reported that LYDEX gel is effective in reducing pleural and intra-abdominal adhesions in a rat model[86,87]. It has also been reported to efficiently reduce adhesions in the posterior portion of the sternum by inhibiting macrophage infiltration and fibrosis progression in a rabbit median sternotomy model[83]. Furthermore, it has been reported that the degradation rate of LYDEX affects the progression of fibrosis in the posterior sternum[145]. On the other hand, although gel thickness (dosage) also plays a significant role in the degradation rate of LYDEX, no studies focusing on dosage have been conducted to date. Therefore, I will examine how the dosage of LYDEX gel affects the physical barrier in intraperitoneal adhesions using a rabbit organ adhesion model, and verify the optimal gel thickness (dosage) to be effective as an anti-adhesion material.

Finally, the purpose of this study is to elucidate the mechanism of polysaccharide

degradation and thereby contribute to the development of not only LYDEX but also, by extension, new biodegradable polysaccharide materials for biomedical applications. The goal is also to promote the clinical application of a novel anti-adhesive material with both hemostatic and sealing properties, and to apply LYDEX as an extremely versatile material, which has not been possible with other anti-adhesive materials. In other words, I hope that this study will help provide insight into the development of new bioadhesives with advanced features for surgical applications.

1.8. References

1. Lauto, A., Mawad, D., Foster, L. J. R. Adhesive biomaterials for tissue reconstruction. *J. Chem. Technol. Biotechnol*. **2008**, 83, 464−472. https://doi.org/10.1002/jctb.1771
2. Lloyd, J. D., Marque, M. J., Kacprowicz, R. F. Closure techniques. *Emerg. Med. Clin. North Am*. **2007**, 25, (1), 73-81. https://doi.org/10.1016/j.emc.2007.01.002
3. Tajirian, A. L., Goldberg, D. J. A review of sutures and other skin closure materials. *J. Cosmet. Laser. Ther*. **2010**, 12, (6), 296-302. https://doi.org/10.3109/14764172.2010.538413
4. Schreader, K. J., Bayer, I. S., Milner, D. J., Loth, E., Jasiuk, I. A polyurethane-based nanocomposite biocompatible bone adhesive. *J. Appl. Polym. Sci*. **2013**, 127, 4974−4982. https://doi.org/10.1002/app.38100
5. Wistlich, L., Rucker, A., Schamel, M., Kubler, A. C., Gbureck, U., Groll, J. A bone glue with sustained adhesion under wet conditions. *Adv. Healthcare Mater*. **2017**, 6, 1600902. https://doi.org/10.1002/adhm.201600902
6. Waite, J. H. Nature's underwater adhesive specialist. *Int. J. Adhes. Adhes*. **1987**, 7, 9−14. https://doi.org/10.1016/0143-7496(87)90048-0
7. Annabi, N., Tamayol, A., Shin, S.R., Ghaemmaghami, A.M., Peppas, N.A., Khademhosseini, A. Surgical Materials: Current Challenges and Nano-enabled Solutions. *Nano Today*. **2014**, 574–589. https://doi.org/10.1016/j.nantod.2014.09.006
8. Brennan, M. J., Kilbride, B. F., Wilker, J. J., Liu, J. C. A bioinspired elastin-based protein for a cytocompatible underwater adhesive. *Biomaterials*. **2017**, 124, 116−125. https://doi.org/10.1016/j.biomaterials.2017.01.034
9. Spotnitz, W. D., Burks, S. Hemostats, sealants, and adhesives: components of the surgical toolbox. *Transfusion*. **2008**, 48, (7), 1502-16. https://doi.org/10.1111/j.1537-2995.2008.01703.x

10. Spotnitz, W. D., Burks, S. State-of-the-art review: Hemostats, sealants, and adhesives II: Update as well as how and when to use the components of the surgical toolbox. *Clin. Appl. Thromb. Hemost*. **2010**, 16, (5), 497-514. https://doi.org/10.1177/1076029610363589
11. Petersen, B., Barkun, A., Carpenter, S., Chotiprasidhi, P., Chuttani, R., Silverman, W., Hussain, N., Liu, J., Taitelbaum, G., Ginsberg, G. G., Technology Assessment Committee., American Society for Gastrointestinal Endoscopy. Tissue adhesives and fibrin glues. *Gastrointest Endosc*. **2004**, 60, (3), 327−333. https://doi.org/10.1016/S0016-5107(04)01564-0
12. Spotnitz, W. D. Fibrin sealant: The only approved hemostat, sealant, and adhesive-a laboratory and clinical perspective. *ISRN Surg*. **2014**, 2014, 203943. https://doi.org/10.1155/2014/203943
13. Chivers, R. A., Wolowacz, R. G. The strength of adhesivebonded tissue joints. *Int. J. Adhes. Adhes*. **1997**, 17, 127−132. https://doi.org/10.1016/S0143-7496(96)00041-3
14. Champagne, C. Serendipity, super glue and surgery: Cyanoacrylates as hemostatic aids in the Vietnam war. The proceedings of the 18th annual history of medicine days, March 6th and 7th, 2009 University of Calgary, Faculty of Medicine, Calgary, AB. 155–176. http://dx.doi.org/10.11575/PRISM/33383
15. Vinters, H. V., Galil, K. A., Lundie, M.J., Kaufmann, J.C. The histotoxicity of cyanoacrylates. A selective review. *Neuroradiology*. **1985**, 27, (4), 279–291. https://doi.org/10.1007/BF00339559
16. Singer, A.J., Quinn, J.V., Hollander J. E. The cyanoacrylate topical skin adhesives. *Am. J. Emerg. Med*. **2008**, 26, (4), 490-6. https://doi.org/10.1016/j.ajem.2007.05.015
17. Bré, L. P., Zheng, Y., Pêgo, A. P., Wang, W. Taking tissue adhesives to the future: from traditional synthetic to new biomimetic approaches. *Biomater. Sci*. **2013**, 1, (3), 239−253.

https://doi.org/10.1039/C2BM00121G

18. Leonard, F., Kulkarni, R. K., Brandes, G., Nelson, J., Cameron, J. J. Synthesis and degradation of poly (alkyl α-cyanoacrylates). *J. Appl. Polym. Sci*. **1966**, 10, 259−272. https://doi.org/10.1002/app.1966.070100208
19. Eiferman, R. A., Snyder, J. W. Antibacterial effect of cyanoacrylate glue. *Arch. Ophthalmol*. **1983**, 101, (6), 958−960. https://doi.org/10.1001/archopht.1983.01040010958022
20. Bhatia, S. K., Traumatic Injuries Chapter 10 Traumatic Injuries. *Biomater. Clini. Applications*. **2010**, 213-258. https://doi.org/10.1007/978-1-4419-6920-0_10
21. Novotný, K., Rohn, V. Cyanoacrylate glue in treatment of varicose veins. *Cor. et Vasa*. **2019**, 61, (3), 290–293. https://doi.org/10.33678/cor.2019.029
22. Trott, A. T. Cyanoacrylate tissue adhesives. An advance in wound care. *Jama*. **1997**, 277, (19), 1559-1560. https://doi.org/10.1001/jama.1997.03540430071037
23. Ronis, M. L., Harwick, J. D., Fung, R., Dellavecchia, M. Review of cyanoacrylate tissue glues with emphasis on their otorhinolaryngological applications. *Laryngoscope*. **1984**, 94, (2 Pt 1), 210-213. https://doi.org/10.1288/00005537-198402000-00012
24. Leggat, P. A., Smith, D. R., Kedjarune, U. Surgical applications of cyanoacrylate adhesives: a review of toxicity. *ANZ J. Surg*. **2007**, 77, (4), 209-213. https://doi.org/10.1111/j.1445-2197.2007.04020.x
25. Kull, S., Martinelli, I., Briganti, E., Losi, P., Spiller, D., Tonlorenzi, S., Soldani, G. Glubran2 surgical glue: *in vitro* evaluation of adhesive and mechanical properties. *J. Surg. Res*. **2009**, 157, (1), 15−21. https://doi.org/10.1016/j.jss.2009.01.034
26. Quirce, S., Baeza, M. L., Tornero, P., Blasco, A., Barranco, R., Sastre, J. Occupational asthma caused by exposure to cyanoacrylate. *Allergy*. **2001** May;56(5):446-9. https://doi.org/10.1034/j.1398-9995.2001.056005446.x

27. Bruze, M., Björkner, B., Lepoittevin, J.-P. Occupational allergic contact dermatitis from ethyl cyanoacrylate. *Contact Dermatitis*. **1995**, 32, (3), 156−159. https://doi.org/10.1111/j.1600-0536.1995.tb00806.x

28. Ferreira, P., Pereira, R., Coelho, J. F., Silva, A. F., Gil, M. H. Modification of the biopolymer castor oil with free isocyanate groups to be applied as bioadhesive. *Int. J. Biol. Macromo*l. **2007**, 40, (2), 144-152. https://doi.org/10.1016/j.ijbiomac.2006.06.023

29. Eto, M., Morita, S., Sugiura, M., Yoshimura, T., Tominaga, R., Matusda, T. Elastomeric surgical sealant for hemostasis of cardiovascular anastomosis under full heparinization. *Eur. J. Cardiothorac. Surg*. **2007**, 32, (5), 730-734. https://doi.org/10.1016/j.ejcts.2007.06.046

30. Ferreira, P., Silva, A. F. M., Pinto, M. I., Gil, M. H. Development of a biodegradable bioadhesive containing urethane groups. *J. Mater. Sci. Mater. Med*. **2008**, 19, (1), 111–120. https://doi.org/10.1007/s10856-007-3117-3

31. Kobayashi, H., Hyon, S. H., Ikada, Y. Water-curable and biodegradable prepolymers. *J. Biomed. Mater. Res*. **1991**, 25, (12), 1481-1494. https://doi.org/10.1002/jbm.820251206

32. Ferreira, P., Coelho, J. F. J., Gil, M. H. Development of a new photocrosslinkable biodegradable bioadhesive. *Int. J. Pharm*. **2008**, 352, (1-2), 172–181. https://doi.org/10.1016/j.ijpharm.2007.10.026

33. Gilbert, T. W., Badylak, S. F., Gusenoff, J., Beckman, E. J., Clower, D. M., Daly, P., Rubin, J. P. Lysine-derived urethane surgical adhesive prevents seroma formation in a canine abdominoplasty model. *Plast. Reconstr. Surg*. **2008**, 122, (1), 95–102. https://doi.org/10.1097/PRS.0b013e31817743b8

34. Bernstein, I. L. Isocyanate-induced pulmonary diseases: a current perspective. *J. Allergy. Clin. Immunol*. **1982**, 70, (1), 24-31. https://doi.org/10.1016/0091-6749(82)90197-x.

35. Karol, M. H. Respiratory effects of inhaled isocyanates. *Crit. Rev. Toxicol*. **1986**, 16, (4), 349-379. https://doi.org/10.3109/10408448609037467

36. Klibanov, A. L., Maruyama, K., Torchilin, V. P., Huang, L. Amphipathic polyethyleneglycols effectively prolong the circulation time of liposomes. *FEBS Lett*. **1990**, 268, (1), 235-237. https://doi.org/10.1016/0014-5793(90)81016-H

37. Knop, K., Hoogenboom, R., Fischer, D., Schubert, U. S. Poly(ethylene glycol) in drug delivery: pros and cons as well as potential alternatives. *Angew. Chem. Int. Ed. Engl*. **2010**, 49, (36), 6288-6308. https://doi.org/10.1002/anie.200902672

38. Caliceti, P., Veronese, F. M. Pharmacokinetic and biodistribution properties of poly(ethylene glycol)-protein conjugates. *Adv. Drug. Deliv. Rev*. **2003**, 55, (10), 1261-1277. https://doi.org/10.1016/S0169-409X(03)00108-X

39. Kim, K. D., Wright, N.M. Polyethylene glycol hydrogel spinal sealant (DuraSeal Spinal Sealant) as an adjunct to sutured dural repair in the spine: results of a prospective, multicenter, randomized controlled study. *Spine (Phila Pa 1976)*. **2011**, 36 (23), 1906-1912. https://doi.org/10.1097/BRS.0b013e3181fdb4db

40. Fransen, P. Reduction of postoperative pain after lumbar microdiscectomy with DuraSeal Xact Adhesion Barrier and Sealant System. *Spine J*. **2010**, 10, (9), 751–761. https://doi.org/10.1016/j.spinee.2010.05.001

41. Lee, G., Lee, C.K., Bynevelt, M. DuraSeal-hematoma: concealed hematoma causing spinal cord compression. *Spine (Phila Pa 1976)*, **2010**, 35, (25), E1522-E1524. https://doi.org/10.1097/BRS.0b013e3181edfe2c

42. Preul, M.C., Bichard, W.D., Spetzler, R.F. Toward optimal tissue sealants for neurosurgery: use of a novel hydrogel sealant in a canine durotomy repair model. *Neurosurgery*. **2003**, 53, (5), 1189–1199. https://doi.org/10.1227/01.neu.0000089481.87226.f7

43. Strong, M. J., Carnahan, M. A., D'Alessio, K., Butlin, J. D. G., Butt, M. T., Asher, A. L. Preclinical characterization and safety of a novel hydrogel for augmenting dural repair. *Mater. Res. Express 2*. **2015**, 095401. https://doi.org/10.1088/2053-1591/2/9/095401

44. Hill, A., Estridge, T. D., Maroney, M., Monnet, E., Egbert, B., Cruise, G., Coker, G.T. Treatment of suture line bleeding with a novel synthetic surgical sealant in a canine iliac PTFE graft model. *J. Biomed. Mater. Res*. **2001**, 58, (3), 308–312. https://doi.org/10.1002/1097-4636(2001)58:3<308::AID-JBM1022>3.0.CO;2-P

45. Wallace, D.G., Cruise, G.M., Rhee, W.M., Schroeder, J.A., Prior, J.J., Ju, J., Maroney, M., Duronio, J., Ngo, M.H., Estridge, T., Coker, G.C. A tissue sealant based on reactive multifunctional polyethylene glycol. *J. Biomed. Mater. Res*. **2001**, 58, (5), 545–555. https://doi.org/10.1002/jbm.1053

46. Wheat, J.C., Wolf Jr, J.S. Advances in bioadhesives, tissue sealants, and hemostatic agents. *Urol. Clin. North. Am*. **2009**, 36, (2), 265–275. https://doi.org/10.1016/j.ucl.2009.02.002

47. Jackson, M.R. Fibrin sealants in surgical practice: An overview. *Am. J. Surg*. **2001**, 182, S1–S7. https://doi.org/10.1016/S0002-9610(01)00770-X

48. Alving, B. M., Weinstein, M. J., Finlayson, J. S., Menitove, J. E., Fratantoni, J.C. Fibrin sealant: summary of a conference on characteristics and clinical uses. *Transfusion*. **1995**, 35, (9), 783–790. https://doi.org/10.1046/j.1537-2995.1995.35996029166.x

49. Martinowitz, U., Saltz, R. Fibrin sealant. *Curr Opin Hematol*. **1996**, 3, (5), 395–402. https://doi.org/10.1097/00062752-199603050-00011

50. Busuttil, R.W. A comparison of antifibrinolytic agents used in hemostatic fibrin sealants. *J. Am. Coll. Surg*. **2003**, 197, (6), 1021–1028. https://doi.org/10.1016/j.jamcollsurg.2003.07.002

51. Mandell, S.P., Gibran, N.S. Fibrin sealants: surgical hemostat, sealant and adhesive. *Expert Opin. Biol. Ther*. **2014**, 14, (6), 821–830. https://doi.org/10.1517/14712598.2014.897323

52. Hino, M., Ishiko, O., Honda, K. I., Yamane, T., Ohta, K., Takubo, T., Tatsumi, N. Transmission of symptomatic parvovirus B19 infection by fibrin sealant used during surgery. *Br. J. Haematol*. **2000**, 108, (1), 194-195. https://doi.org/10.1046/j.1365-2141.2000.01818.x

53. Kjihian, A. A novel approach to control air leaks in complex lung surgery: a retrospective review. *J. Cardiothorac. Surg*. **2012**, 7, 49. https://doi.org/10.1186/1749-8090-7-49

54. Fuller, C. Reduction of intraoperative air leaks with Progel in pulmonary resection: a comprehensive review. *J. Cardiothorac. Surg*. **2013**, 8, 90. https://doi.org/10.1186/1749-8090-8-90

55. Kobayashi, H., Sekine, T., Nakamura, T., Shimizu, Y. *In vivo* evaluation of a new sealant material on a rat lung air leak model. *J. Biomed. Mater. Res*. **2001**, 58, (6), 658–665. https://doi.org/10.1002/jbm.1066

56. Khoynezhad, A., DelaRosa, J., Moon, M. R., Brinkman, W. T., Thompson, R. B., Desai, N. D., Malaisrie, S. C., Girardi, L. N., Bavaria, J. E., Reece, T. B., PROTECT Investigators. Facilitating hemostasis after proximal aortic surgery: Results of the PROTECT trial. *Ann. Thorac. Surg*. **2018**, 105, (5), 1357-1364. https://doi.org/10.1016/j.athoracsur.2017.12.013

57. Coselli, J. S., Bavaria, J. E., Fehrenbacher, J., Stowe, C. L., Macheers, S. K., Gundry, S. R. Prospective randomized study of a protein-based tissue adhesive used as a hemostatic and structural adjunct in cardiac and vascular anastomotic repair procedures. *J. Am. Coll. Surg*. **2003**, 197, (2), 243-252. https://doi.org/10.1016/s1072-7515(03)00376-4

58. Furukawa, H., Masaki, H., Tanemoto, K. Late limb embolization of biological glue after repair of aortic dissection. *Eur. J. Cardiothorac. Surg*. **2015**, 48, (4), 633. https://doi.org/10.1093/ejcts/ezv002

59. Allen, M. S., Wood, D. E., Hawkinson, R. W., Harpole, D. H., Mckenna, R. J., Walsh, G. L., Vallieres, E., Miller, D. L., Nichols 3rd, F. C., Smythe, W. R., Davis, R. D., 3M Surgical Sealant Study Group. Prospective randomized study evaluating a biodegradable polymeric sealant for sealing intraoperative air leaks that occur during pulmonary resection. *Ann. Thorac. Surg*. **2004**, 77, (5), 1792-1801. https://doi.org/10.1016/j.athoracsur.2003.10.049

60. Albes, J. M., Krettek, C., Hausen, B., Rohde, R., Haverich, A., Borst, H. G. Biophysical properties of the gelatin-resorcin-formaldehyde/glutaraldehyde adhesive. *Ann. Thorac. Surg*. **1993**, 56, (4), 910-915. https://doi.org/10.1016/0003-4975(93)90354-k

61. Boncek, L. I., Braunwald, N. S. Experimental evaluation of a cross-linked gelation adhesive in gastrointestinal surgery. *Ann. Surg*. **1967**, 165, (3), 420-424. https://doi.org/10.1097/00000658-196703000-00013

62. Nomori, H., Horio, H., Morinaga, S., Suemasu, K. Gelatin-resorcinol-formaldehyde-glutaraldehyde glue for sealing pulmonary air leaks during thoracoscopic operation. *Ann. Thorac. Surg*. **1999**, 67, (1), 212-216. https://doi.org/10.1016/s0003-4975(98)01184-9

63. Nomori, H., Horio, H., Suemasu, K. The efficacy and side effects of gelatin-resorcinol formaldehyde-glutaraldehyde (GRFG) glue for preventing and sealing pulmonary air leakage. *Surg. Today*. **2000**, 30, (3), 244-248. https://doi.org/10.1007/s005950050053

64. Albes, J. M., Krettek, C., Hausen, B., Rohde, R., Haverich, A., Borst, H.G. Biophysical properties of the gelatin-resorcin-formaldehyde/glutaraldehyde adhesive. *Ann. Thorac. Surg*. **1993**, 56, (4), 910-915. https://doi.org/10.1016/0003-4975(93)90354-k

65. Kazui, T., Washiyama, N., Bashar, A. H., Terada, H., Suzuki, K., Yamashita, K., Takinami, M. Role of biologic glue repair of proximal aortic dissection in the development of early and midterm redissection of the aortic root. *Ann. Thorac. Surg*. **2001**, 72, (2), 509-514. https://doi.org/10.1016/s0003-4975(01)02777-1

66. Sung, H. W., Huang, D. M., Chang, W. H., Huang, R. N., Hsu, J. C. Evaluation of gelatin hydrogel crosslinked with various crosslinking agents as bioadhesives: *in vitro* study. *J. Biomed. Mater. Res*. **1999**, 46, (4), 520-30. https://doi.org/10.1002/(sici)1097-4636(19990915)46:4%3C520::aid-jbm10%3E3.0.co;2-9

67. Ramos-de-la-Peña, A. M., Renard, C. M. G. C., Montañez, J., de la Luz Reyes-Vega, M., Contreras-Esquivel, J. C. A review through recovery, purification and identification of genipin. *Phytochemistry Reviews*, **2016**, 15, 37-49. https://doi.org/10.1007/s11101-014-9383-z

68. Taguchi, T., Mizuta, R., Ito, T., Yoshizawa, K., Kajiyama, M., Robust sealing of blood vessels with cholesteryl group modified, alaska pollock-derived gelatin-based biodegradable sealant under wet conditions. *J. Biomed. Nanotechnol*. **2016**, 12, (1), 128-134. https://doi.org/10.1166/jbn.2016.2210

69. Taylor, D.M., Somerville, R.A., Steele, P.J., Grobben, A.H. Validation of the clearance of TSE agent by the initial steps of the alkaline gelatine manufacturing process. Ref.No.0667/alkaline 263K. **2003**, 1-73.

70. Grobben, A.H., Steele, P. J., Somerville, R.A., Taylor, D.M. Inactivation of the bovine-spongiform-encephalopathy(BSE) agent by the acid and alkaline processes used in the manufacture of bone gelatine. *Biotechnol. Appl. Biochem*. **2004**, 39:329-338. https://doi.org/10.1042/ba20030149

71. Rohwer, R.G., Grobben, A.H., MacAuley, C.M. Intermediate data on the removal and inactivation of TSE agents by the individual process steps of the finishing unit operations of the gelatine manufacturing process. (provided in confidence). 2001.

72. Grobben, A.H., Steele, P.J. Validation of the clearance of TSE infectivity by the initial steps of the acid bone gelatine manufacturing prosess with an additional short NaOH treatment. **2003**, 1-14.

73. Nakajima, N., Sugai, H., Tsutsumi, S., Hyon, S.-H. Self-degradable bioadhesive. *Key Eng. Mater*. **2007**, 342-343, 713-716. https://doi.org/10.4028/www.scientific.net%2FKEM.342-343.713

74. Araki, M., Tao, H., Nakajima, N., Sugai, H., Sato, T., Hyon, S.-H., Nagayasu, T., Nakamura, T. Development of new biodegradable hydrogel glue for preventing alveolar air leakage. *J. Thorac. Cardiovasc. Surg*. **2007**, 134, (5), 1241-1248. https://doi.org/10.1016/j.jtcvs.2007.07.020

75. Naitoh, Y., Kawauchi, A., Kamoi, K., Soh, J., Okihara, K., Hyon, S.-H., Miki, T. Hemostatic effect of new surgical glue in animal partial nephrectomy models. *Urology.* **2013**, 81, (5), 1095-1100. https://doi.org/10.1016/j.urology.2013.01.002

76. Hyon, S.-H., Nakajima, N., Sugai, H., Matsumura, K. Low cytotoxic tissue adhesive based on oxidized dextran and epsilon-poly-l-lysine. *J. Biomed. Mater. Res. A*. **2014**, 102, (8), 2511-2520. https://doi.org/10.1002/jbm.a.34923

77. Matsumura, K., Nakajima, N., Sugai, H., Hyon, S.-H. Self-degradation of tissue adhesive based on oxidized dextran and poly-l-lysine. *Carbohydr. Polym*. **2014**, 113, 32-38. https://doi.org/10.1016/j.carbpol.2014.06.073

78. Takaoka, M., Nakamura, T., Sugai, H., Bentley, A. J., Nakajima, N., Fullwood, N. J., Yokoi, N., Hyon, S.-H., Kinoshita, S. Sutureless amniotic membrane transplantation for ocular

surface reconstruction with a chemically defined bioadhesive. *Biomaterials*. **2008**, 29, (19), 2923-2931. https://doi.org/10.1016/j.biomaterials.2008.03.027

79. Takaoka, M., Nakamura, T., Sugai, H., Bentley, A. J., Nakajima, N., Yokoi, N., Fullwood, N. J., Hyon, S.-H., Kinoshita, S. Novel sutureless keratoplasty with a chemically defined bioadhesive. *Invest. Ophthalmol. Vis. Sci*. **2009**, 50, (6), 2679-2685. https://doi.org/10.1167/iovs.08-2944
80. Tsujita, H., Brennan, A. B., Plummer, C. E., Nakajima, N., Hyon, S.-H., Barrie, K. P., Sapp, B., Jackson, D., Brooks, D. E. An ex vivo model for suture-less amniotic membrane transplantation with a chemically defined bioadhesive. *Curr. Eye Res*. **2012**, 37, (5), 372-380. https://doi.org/10.3109/02713683.2012.663853
81. Kazusa, H., Nakasa, T., Shibuya, H., Ohkawa, S., Kamei, G., Adachi, N., Deie, M., Nakajima, N., Hyon, S. -H., Ochi, M. Strong adhesiveness of a new biodegradable hydrogel glue, lydex, for use on articular cartilage. *J. Appl. Biomater. Funct. Mater*. **2013**, 11, (3), e180-186. https://doi.org/10.5301/jabfm.5000164
82. Yamamoto, T., Fujibayashi, S., Nakajima, N., Sugai, H., Hyon, S.-H., Nakamura, T. Biodegradable adhesive (lydex) with hydroxyapatite granules. *Key Eng. Mater*. **2008**, 361-363, 575-578. https://doi.org/10.5301/jabfm.5000164
83. Kamitani, T., Masumoto, H., Kotani, H., Ikeda, T., Hyon, S. -H., Sakata, R. Prevention of retrosternal adhesion by novel biocompatible glue derived from food additives. *J. Thorac. Cardiovasc. Surg*. **2013**, 146, (5), 1232-1238. https://doi.org/10.1016/j.jtcvs.2013.02.001
84. Takeda, T., Shimamoto, T., Marui, A., Saito, N., Uehara, K., Minakata, K., Miwa, S., Nakajima, N., Ikeda, T., Hyon, S.-H., Sakata, R. Topical application of a biodegradable disc with amiodarone for atrial fibrillation. *Ann. Thoracic. Surg*. **2011**, 91, (3), 734-739. https://doi.org/10.1016/j.athoracsur.2010.10.022

85. Togo, Y., Takahashi, K., Saito, K., Kiso, H., Huang, B., Tsukamoto, H., Hyon, S. -H., Bessho, K. Aldehyded dextran and epsilon -poly(l-lysine) hydrogel as nonviral gene carrier. *Stem Cells Int*. **2013**, 2013, 634379. https://doi.org/10.1155/2013/634379

86. Takagi, K., Tsuchiya, T., Araki, M., Yamasaki, N., Nagayasu, T., Hyon, S. -H., Nakajima, N. Novel biodegradable powder for preventing postoperative pleural adhesion. *J. Surg. Res*. **2013**, Jan;179, (1), e13-e19. https://doi.org/10.1016/j.jss.2012.01.056

87. Takagi, K., Araki, M., Fukuoka, H., Takeshita, H., Hidaka, S., Nanashima, A., Sawai, T., Nagayasu, T., Hyon, S. -H., Nakajima, N. Novel powdered anti-adhesion material: preventing postoperative intra-abdominal adhesions in a rat model. *Int. J. Med. Sci*. **2013**, 10, (4), 467-474. https://doi.org/10.7150/ijms.5607

88. Bang, B, Lee, E., Maeng, J., Kim, K., Hwang, J. H., Hyon, S. -H., Hyon, W., Lee, D. H. Efficacy of a novel endoscopically deliverable muco-adhesive hemostatic powder in an acute gastric bleeding porcine model. *PLoS One*. **2019**, 14, (6), e0216829. https://doi.org/10.1371/journal.pone.0216829

89. Chimpibul, W., Nagashima, T., Hayashi, F., Nakajima, N., Hyon, S. -H., Matsumura, K. Dextran oxidized by a malaprade reaction shows main chain scission through a maillard reaction triggered by schiff base formation between aldehydes and amines. *J. Polym. Sci. A Polym. Chem*. **2016**, 54, 2254-2260. https://doi.org/10.1002/pola.28099

90. Nonsuwana, N., Matsugamic, A., Hayashic, F., Hyon, S. -H., Matsumura, K. Controlling the degradation of an oxidized dextran-based hydrogel independent of the mechanical properties, *Carbohydr. Polym*. **2019**, 204, 131-141. https://doi.org/10.1016/j.carbpol.2018.09.081

91. Hiemstra, C., van der Aa, L. J., Zhong, Z., Dijkstra, P. J., Feijen, J. Novel in situ forming, degradable dextran hydrogels by michael addition chemistry: synthesis, rheology, and degradation. *Macromolecules*. **2007**, 40, 1165-1173. https://doi.org/10.1021/ma062468d

92. Jin, R., Hiemstra, C., Zhong, Z., Feijen, J. Enzyme-mediated fast in situ formation of hydrogels from dextran-tyramine conjugates. *Biomaterials*. **2007**, 28, (18), 2791–2800. https://doi.org/10.1016/j.biomaterials.2007.02.032

93. Ono, K., Saito, Y., Yura, H., Ishikawa, K., Kurita, A., Akaike, T., Ishihara, M. Photocrosslinkable chitosan as a biological adhesive. *J. Biomed. Mater. Res*. **2000**, 49, (2), 289-295. https://doi.org/10.1002/(sici)1097-4636(200002)49:2%3C289::aid-jbm18%3E3.0.co;2-m

94. Ishihara, M. Photocrosslinkable chitosan hydrogel as a wound dressing and a biological adhesive. *Trends Glycosci. Glycotechnol*. **2002**, 14, 331-341. https://doi.org/10.4052/TIGG.14.331

95. Liu, G., Shi, Z., Kuriger, T., Hanton, L. R., Simpson, J., Moratti, S.C., Robinson, B.H., Athanasiadis, T., Valentine, R., Wormald, P.J., Robinson, S. Synthesis and characterization of chitosan/ dextran-based hydrogels for surgical use. *Macromol. Symp*. **2009**, 279, 151–157. https://doi.org/10.1002/masy.200950523

96. Reyes, J.M.G., Herretes, S., Pirouzmanesh, A., Wang, D.A., Elisseeff, J.H., Jun, A., McDonnell, P.J., Chuck, R.S., Behrens, A. A modified chondroitin sulfate aldehyde adhesive for sealing corneal incisions. *Invest. Ophthalmol. Vis. Sci*. **2005**, 46, (4), 1247-1250. https://doi.org/10.1167/iovs.04-1192

97. Tan, H., Chu, C. R., Payne, K. A., Marra, K. G. Injectable in situ forming biodegradable chitosan-hyaluronic acid based hydrogels for cartilage tissue engineering. *Biomaterials*. **2009**, 30, (13), 2499-2506. https://doi.org/10.1016/j.biomaterials.2008.12.080

98. Wiltsey, C., Christiani, T., Williams, J., Scaramazza, J., Van Sciver, C., Toomer, K., Sheehan, J., Branda, A., Nitzl, A., England, E., Kadlowec, J., Iftode, C., Vernengo, J. Thermogelling bioadhesive scaffolds for intervertebral disk tissue engineering : Preliminary *in vitro* comparison of aldehyde-based versus alginate microparticle-mediated adhesion. *Acta Biomater*. **2015**, 16, 71-80. https://doi.org/10.1016/j.actbio.2015.01.025

99. Smyth, J. D. A technique for the histochemical demonstration of polyphenol oxidase and its application to egg-shell formation in helminths and byssus formation in mytilus. *Q. J. Microsc. Sci*. **1954**, s3-95, (30), 139-152. https://doi.org/10.1242/jcs.s3-95.30.139

100. Yonge, C. M. On the primitive significance of the byssus in the bivalvia and its effects in evolution. *J. Mar. Biol. Assoc. U. K*. **1962**, 42, 113-125. https://doi.org/10.1017/S0025315400004495

101. Waite, J. H., Tanzer, M. L. Polyphenolic substance of mytilus edulis: novel adhesive containing l-dopa and hydroxyproline. *Science*. **1981**, 212, (4498), 1038-1040. https://doi.org/10.1126/science.212.4498.1038

102. Waite, J.H. Evidence for a repeating 3,4-dihydroxyphenylalanine- and hydroxyproline-containing decapeptide in the adhesive protein of the mussel, mytilus edulis l. *J. Biol. Chem*. **1983**, 258, (5), 2911-2915. https://doi.org/10.1016/S0021-9258(18)32805-9

103. Strausberg, R. L., Link, R. P. Protein-based medical adhesives. *Trends Biotechnol*. **1990,** 8, (2), 53-57. https://doi.org/10.1016/0167-7799(90)90134-j

104. Waite, J. H. Nature's underwater adhesive specialist. *Int. J. Adhes. Adhes*. **1987**, 7, 9−14. https://doi.org/10.1016/0143-7496(87)90048-0

105. Vreeland, V., Waite, J. H., Epstein, L. Polyphenols and oxidases in substratum adhesion by marine algae and mussels. *J. Phycol*. **1998**, 34, (1), 1-8. https://doi.org/10.1046/j.1529-8817.1998.340001.x

106. Matos-Perez, C. R., White, J. D., Wilker, J. J. Polymer composition and substrate influences on the adhesive bonding of a biomimetic, cross-linking polymer. *J. Am. Chem. Soc*. **2012**, 134, (22), 9498-9505. https://doi.org/10.1021/ja303369p

107. Lee, B. P., Dalsin, J. L., Messersmith, P. B. Synthesis and gelation of DOPA-modified poly(ethylene glycol) hydrogels. *Biomacromolecules*. **2002**, 3, (5), 1038-1047. https://doi.org/10.1021/bm025546n

108. Sáez, C., Pardo, J., Gutierrez, E., Brito, M., Burzio, L. O. Immunological studies of the polyphenolic proteins of mussels. *Comp. Biochem. Physiol. B*. **1991**, 98, 569−572. https://doi.org/10.1016/0305-0491(91)90255-C

109. Crisp, D.J., Walker, G., Young, G.A., Yule, A.B. Adhesion and substrate choice in mussels and barnacles. *J. Colloid Interface Sci*. **1985**, 104, 40–50. https://doi.org/10.1016/0021-9797(85)90007-4

110. Hansen, D. C., Luther, G. W., Waite, J. H. The adsorption of the adhesive protein of the blue mussel mytilus edulis l onto type 304l stainless steel. *J. Colloid Interface Sci*. **1994**, 168, 206-216. https://doi.org/10.1006/jcis.1994.1410

111. Schnurrer, J., Lehr, C.-M. Mucoadhesive properties of themussel adhesive protein. *Int. J. Pharm*. **1996**, 141, 251-256. https://doi.org/10.1016/0378-5173(96)04625-X

112. Ninan, L., Monahan, J., Stroshine, R. L., Wilker, J. J., Shi, R. Adhesive strength of marine mussel extracts on porcine skin. *Biomaterials*. **2003**, 24, 4091-4099. https://doi.org/10.1016/s0142-9612(03)00257-6

113. Ninan, L., Stroshine, R. L., Wilker, J. J., Shi, R. Adhesive strength and curing rate of marine mussel protein extracts on porcine small intestinal submucosa. *Acta Biomater*. **2007**, 3, (5), 687-694. https://doi.org/10.1016/j.actbio.2007.02.004

114. Strausberg, R.L., Link, R. P. Protein-based medical adhesives. *Trends Biotechnol*.

1990, 8, 53-57. https://doi.org/10.1016/0167-7799(90)90134-j

115. Silverman, H. G., Roberto, F. F. Understanding marine mussel adhesion. *Mar. Biotechnol (NY)*. **2007**, 9, (6), 661-681. https://doi.org/10.1007/s10126-007-9053-x

116. Ryu, J. H., Lee, Y., Kong, W. H., Kim, T. G., Park, T. G., Lee, H. Catechol-functionalized chitosan/pluronic hydrogels for tissue adhesives and hemostatic materials. *Biomacromolecules*. **2011**, 12, (7), 2653-2659. https://doi.org/10.1021/bm200464x

117. Kim, Y. -M., Kim, C. -H., Park, M. -R., Song, S. -C. Development of an injectable dopamine-conjugated poly(organophophazene) hydrogel for hemostasis. *Bull. Korean. Chem. Soc*. **2016**, 37, 372-377. https://doi.org/10.1002/bkcs.10686

118. Mehdizadeh, M., Weng, H., Gyawali, D., Tang, L., Yang, J. Injectable citrate-based mussel-inspired tissue bioadhesives with high wet strength for sutureless wound closure. *Biomaterials*. **2012**, 33, (32), 7972-7983.

119. Fan, C., Fu, J., Zhu, W., Wang, D. -A. A mussel-inspired double-crosslinked tissue adhesive intended for internal medical use. *Acta Biomater*. **2016**, 33, 51-63. https://doi.org/10.1016/j.biomaterials.2012.07.055

120. Kim B. J., Oh, D. X., Kim, S., Seo, J. H., Hwang, D. S., Masic, A., Han, D. K., Cha, H. J. Mussel-mimetic protein-based adhesive hydrogel. *Biomacromolecules*. **2014**, 15, (5), 1579-1585. https://doi.org/10.1021/bm4017308

121. Liu, Y., Meng, H., Konst, S., Sarmiento, R., Rajachar, R., Lee, B. P. Injectable dopamine-modified poly(ethylene glycol) nonocomposite hydrogel with enhanced adhesive property and bioactivity. *ACS Appl. Mater. Interfaces*. **2014**, 6, (19), 16982-16992. https://doi.org/10.1021/am504566v

122. Zhang, H., Bré, L. P., Zhao, T., Zheng, Y., Newland, B., Wang, W. Mussel-inspired hyperbranched poly(amino ester) polymer as strong wet tissue adhesive. *Biomaterials*.

2014, 35, (2), 711-719. https://doi.org/10.1016/j.biomaterials.2013.10.017

123. Kim, K., Ryu, J. H., Koh, M. -Y., Yun, S. P., Kim, S., Park, J. P., Jung, C. -W., Lee, M. S., Seo, H. -I, Kim, J. H., Lee, H. Coagulopathy-independent, bioinspired hemostatic materials: a full research story from preclinical models to a human clinical trial. *Sci. Adv*. **2021**, 7, (13), eabc9992. https://doi.org/10.1126/sciadv.abc9992

124. Choi, G. -S., Kim, S. H., Seo, H I., Ryu, J. H., Yun, S. P., Koh, M. -Y., Lee, M. S., Lee, H., Kim, J. H. A multicenter, prospective, randomized clinical trial of marine mussel-inspired adhesive hemostatic materials, innoseal plus. *Ann. Surg. Treat. Res*. **2021**, 101, (5), 299-305. https://doi.org/10.4174/astr.2021.101.5.299

125. Autumn, K., Liang, Y. A., Hsieh, S. T., Zesch, W., Chan, W. P., Kenny, T. W., Fearing, R., Full, R. J. Adhesive force of a single gecko foot-hair. *Nature*. **2000**, 405, (6787), 681-685. https://doi.org/10.1038/35015073

126. Bartlett, M. D., Croll, A. B., King, D. R., Paret, B. M., Irschick, D. J., Crosby, A. J. Looking beyond fibrillar features to scale gecko-like adhesion. *Adv. Mater*. **2012**, 24, (8), 1078-1083. https://doi.org/10.1002/adma.201104191

127. Pennisi, E. Biomechanics. Geckos climb by the hairs of their toes. *Science*. **2000**, 288, (5472), 1717-1718. https://doi.org/10.1126/science.288.5472.1717a

128. Autumn, K., Sitti, M., Liang, Y. A., Peattie, A. M., Hansen, W. R., Sponberg, S., Kenny, T. W., Fearing, R., Israelachvili, J. N., Fullet, R. J. Evidence for van der waals adhesion in gecko setae. *Proc. Natl .Acad. Sci. U. S. A*. **2002**, 99, (19), 12252-12256. https://doi.org/10.1073/pnas.192252799

129. Hansen, W. R., Autumn, K. Evidence for self-cleaning in gecko setae. *Proc. Natl. Acad. Sci. U. S. A*. **2005**, 102, (2), 385–389. https://doi.org/10.1073/pnas.0408304102

130. Sun, W., Neuzil, P., Kustandi, T. S., Oh, S., Samper, V. D. The nature of the gecko lizard adhesive force. *Biophys. J*. **2005**, 89, (2), L14 -17. https://doi.org/10.1529/biophysj.105.065268

131. Huber, G., Mantz, H., Spolenak, R., Mecke, K., Jacobs, K., Gorb, S. N., Arztet, E. Evidence for capillarity contributions to gecko adhesion from single spatula nanomechanical measurements. *Proc. Natl. Acad. Sci. U. S. A*. **2005**, 102, (45), 16293-16296. https://doi.org/10.1073/pnas.0506328102

132. Autumn, K., Hansen, W. Ultrahydrophobicity indicates a non-adhesive default state in gecko setae. *J. Comp. Physiol*. **2006**, 192, (11), 1205-1212. https://doi.org/10.1007/s00359-006-0149-y

133. Tian, Y., Pesika, N., Zeng, H., Rosenberg, K., Zhao, B., McGuiggan, P., Autumn, K., Israelachvili, J. Adhesion and friction in gecko toe attachment and detachment. *Proc. Natl. Acad. Sci. U. S. A*. **2006**, 103, (51), 19320-19325. https://doi.org/10.1073/pnas.0608841103

134. Hu, S., Lopez, S., Niewiarowski, P. H., Xia, Z. Dynamic self-cleaning in gecko setae via digital hyperextension. *J. R. Soc. Interface*. **2012**, 9, (76), 2781-2790. https://doi.org/10.1098/rsif.2012.0108

135. Qu, L., Dai, L., Stone, M., Xia, Z., Wang, Z. L. Carbon nanotube arrays with strong shear binding-on and easy normal lifting-off. *Science*. **2008**, 322, (5899), 238–242. https://doi.org/10.1126/science.1159503

136. Vajpayee, S., Jagota, A., Hui, C.-Y. Adhesion of a fibrillar interface on wet and rough surfaces. *J. Adhes*. **2010**, 86, 39-61. https://doi.org/10.1080/00218460903417834

137. Lee, H., Lee, B. P., Messersmith, P. B. A reversible wet/dry adhesive inspired by mussels and geckos. *Nature*. **2007**, 448, (7151), 338-341. https://doi.org/10.1038/nature05968

138. Mahdavi, A., Ferreira, L., Sundback, C., Nichol, J. W., Chan, E. P., Carter, D. J. D., Bettinger, C. J., Patanavanich, S., Chignozha, L., Ben-Joseph, E., Galakatos, A., Pryor, H., Pomerantseva, I., Masiakos, P. T., Faquin, W., Zumbuehl, A., Hong, S., Borenstein, J., Vacanti, J., Langer, R., Karp, J. M. A biodegradable and biocompatible gecko-inspired tissue adhesive. *Proc. Natl. Acad. Sci. U. S. A*. **2008**, 105, (7), 2307-2312. https://doi.org/10.1073/pnas.0712117105

139. Pereira, M. J., Sundback, C. A., Lang, N., Cho, W. K., Pomerantseva, I., Ouyang, B., Tao, S. L., McHugh, K., Mwizerwa, O., Vemula, P. K., Mochel, M. C., Carter, D. J., Borenstein, J. T., Langer, R., Ferreira, L. S., Karp, J. M., Masiakos, P. T. Combined surface micropatterning and reactive chemistry maximizes tissue adhesion with minimal inflammation. *Adv. Healthc. Mater*. **2014**, 3, (4), 565-571. https://doi.org/10.1002/adhm.201300264

140. Barton, M., Morley, J. W., Stoodley, M. A., Ng, K. -S., Piller, S. C., Duong, H., Mawad, D., Mahns, D. A., Lauto, A. Laser-activated adhesive films for sutureless median nerve anastomosis. *J. Biophotonics*. **2013**, 6, (11-12), 938-949. https://doi.org/10.1002/jbio.201300054

141. Barton, M. J., Morley, J. W., Stoodley, M. A., Shaikh, S., Mahns, D. A., Lauto, A. Long term recovery of median nerve repair using laser-activated chitosan adhesive films. *J. Biophotonics*. **2015**, 8, (3), 196-207. https://doi.org/10.1002/jbio.201300129

142. Frost, S. J., Mawad, D., Higgins, M. J., Ruprai, H., Kuchel, R., Tilley, R. D., Myers, S., Hook, J. M., Lauto, A. Gecko-inspired chitosan adhesive for tissue repair. *NPG Asia Mater*. **2016**, 8, e280. https://doi.org/10.1038/am.2016.73

143. Araki, M., Tao, H., Sato, T., Nakajima, N., Sugai, H., Hyon, S.-H., Nagayasu, T., Nakamura, T. Creation of a uniform pleural defect model for the study of lung sealants. *J.*

Thorac. Cardiovasc. Surg. **2007**, 134, (1), 145–151.

https://doi.org/10.1016/j.jtcvs.2007.01.007

144. You KE, et al., : The effective control of a bleeding injury using a medical adhesive containing batroxobin. Biomed Mater. 2014 Apr;9(2):025002.

https://doi.org/10.1088/1748-6041/9/2/025002

145. Takai, F., Takeda, T., Yamazaki, K., Ikeda, T., Hyon, S. -H., Minatoya, K., Masumoto, H. Management of retrosternal adhesion after median sternotomy by controlling degradation speed of a dextran and ε-poly (l-lysine)-based biocompatible glue. *Gen. Thorac. Cardiovasc. Surg*. **2020**, 68, (8), 793-800.

https://doi.org/10.1007/s11748-020-01297-3

Chapter 2

Elucidating the degradation mechanism of a self-degradable dextran-based medical adhesive

2.1 Introduction

Surgical tissue adhesives are commonly used as sealants to stop bleeding from organs and tissue sutures and prevent air leakage from cut surfaces during thoracic surgery. Tissue adhesives composed of natural or synthetic polymers, or a combination, have been developed[1].

Fibrin-based sealants are highly biocompatible due to their blood coagulation properties, but weak adhesive strengths[2] limit their applications, with the risk of viral infection also reported[3-7]. Conversely, cyanoacrylate, a synthetic adhesive, exhibits high stiffness and adhesive strength, but inhibits *in vivo* healing of the diseased area due to systemic inflammatory reactions[8] and high cytotoxicity[9]. This is because of the involvement of aldehyde compounds in the gelation and degradation of the adhesive. Hence, their areas of application are limited, and they cannot be used in direct contact with the central nervous system or blood vessels. The combination of natural and synthetic polymers is represented by adhesives that contain gelatin cross-linked with formaldehyde and glutaraldehyde. Although the adhesive strength is sufficiently high, the preparations of these adhesives include toxic aldehyde compounds as cross-linking agents (curing components), with their use limited by their biotoxicities[10-12].

As none of these are ideal tissue adhesives for repairing damaged elastic and soft

tissues, extensive research and development has recently been conducted to design biocompatible, biodegradable, flexible sealants to form leak-free seals in soft tissues.

Elvin et al. reported that a photocrosslinked fibrinogen-based hydrogel based on Ru-catalyzed photooxidation of tyrosine residues[13] showed improved adhesion strength, extensibility, and tensile strength compared to those of previously approved products[14, 15]. Elvin et al. synthesized a photocrosslinkable gelatin sealant via a similar reaction and observed the blood and air leak prevention effects in lung tissue using a sheep model[16]. Taguchi et al. reported an improvement in the pressure resistance by introducing dodecyl groups into pollock-derived gelatin to increase hydrophobic interactions[17]. Several types of sealants have been developed using albumin, such as gelatin, from various animal sources. For example, the United States Food and Drug Administration approved BioGlue (CryoLife, Inc.)[18] consisting of bovine albumin and glutaraldehyde, and Progel (Daboll, Inc.)[19, 20], a composite sealant containing human albumin and a polyethylene glycol (PEG) cross-linker with two NHS-activated ester groups. When the two components are mixed, the primary amine group of the albumin lysine residue reacts rapidly with the succinimidyl succinate group to form a cross-linked structure within 1 min.

Research regarding sealants containing polysaccharides, which are widely used in medicine and food as natural polymers, is also active. As sealants, chitosan derivatives were prepared by reacting chitosan with lactobionic acid in the presence of water-soluble carbodiimide[21, 22]. Moratti et al. reported the hemostatic and adhesive properties of gels consisting of succinylated chitosan and dextran aldehyde[23]. Imine bonds are formed between amino and aldehyde groups, yielding gels. Elisseeff et al. reported a gel-based sealant consisting of chondroitin sulfate with aldehyde groups combined with poly(vinyl alcohol-*co*-vinylamine)[24].

Polyurethane-[25], PEG-[26,27], and polyester-based[28] synthetic sealants have been

developed as wound closure technologies suitable for clinical applications, owing to their excellent adhesion strengths and tunable mechanical properties.

Additionally, our group developed a novel dextran-based self-degradable medical adhesive, LYDEX, which exhibits high adhesive performance and flexibility, low toxicity, and no risk of viral infection, to meet clinical requirements[29-32]. LYDEX is prepared using natural dextran and ε-poly-L-lysine (ε-PLL) polymers. In addition, as various dosage forms (liquid, powder, sheet, and disc) may be selected, numerous medical applications have been studied, including hemostatic[33, 34], sealant [29, 30], and anti-adhesion materials[35-37], and endoscopic wound dressing[38].

Dextran within LYDEX predominantly consists of α-1,6-linked glucose polymers synthesized by the heterolactic acid bacteria *Leuconostoc mesenteroides*. Dextran is widely applied in the biomedical field because of its biocompatibility[39,40], low toxicity[31], simple modification[41], and enzyme-mediated degradability *in vivo*[42]. In addition, dextran contains numerous hydroxyl groups, which provide high hydrophilicity and may be used in chemical functionalization[41,43-46].

To develop LYDEX, our group employed a modification strategy wherein sodium periodate was used to introduce aldehyde groups into dextran, which reacted with amino groups to form imine bonds (Schiff base), leading to hydrogel formation (Figure 2.1). Specifically, aldehyde-functionalized dextran (AD) was mixed with ε-PLL[29,30]. This hydrogel showed *in vitro* degradation without degradable cross-linking points[32]. In addition, the development of hydrogels as biomedical adhesives and scaffolds using aldehyde-modified polysaccharides by periodate oxidation (Malaprade reaction)[47] has been previously reported[48].

Studies on LYDEX degradation are underway. The oxidative cleavage of dextran using sodium periodate (Malaprade reaction)[47] is long-known, with the ring cleaved to form two

aldehyde groups accompanied by partial degradation of the main chain[44]. The structure of oxidized dextran is diverse, not unitary, and an intermolecular hemiacetal model between three types of molecules was proposed, using NMR structural analysis[44,49,50]. Our group investigated the possibility of an intramolecular hemiacetal model based on the assumption that the aldo–enol transition occurred, as the proton of the aldehyde group of oxidized dextran was undetected using NMR spectroscopy[51]. In addition, oxidized dextran undergoes irreversible reactions with amino groups, resulting in cross-linking and gelation due to imine bond formation; when the Amadori rearrangement occurs, the 1,6-glycosidic bond becomes unstable and rapidly cleaves the C–O bond of the main chain adjacent to the imino group, resulting in a decrease in molecular weight (Mw) within an hour and swelling of the gel[31,44,50]. Subsequently, the partial hemiacetal structure generated by periodate oxidation reacts with amino groups and undergoes Amadori rearrangement, leading to the cleavage of the glucose unit ring and molecular degradation[51] (Figure 2.2.).

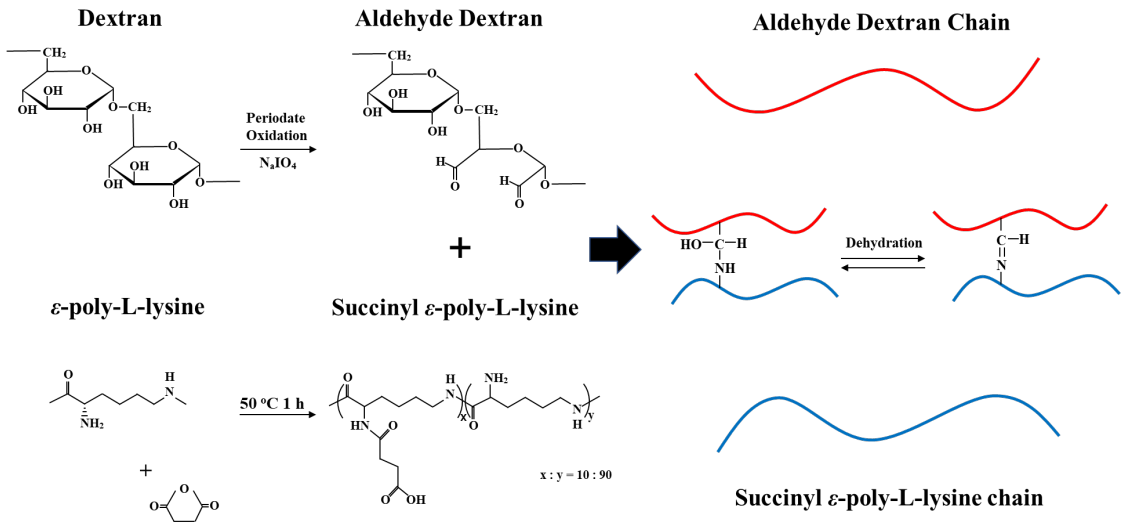

Figure 2.1. LYDEX hydrogel formation.

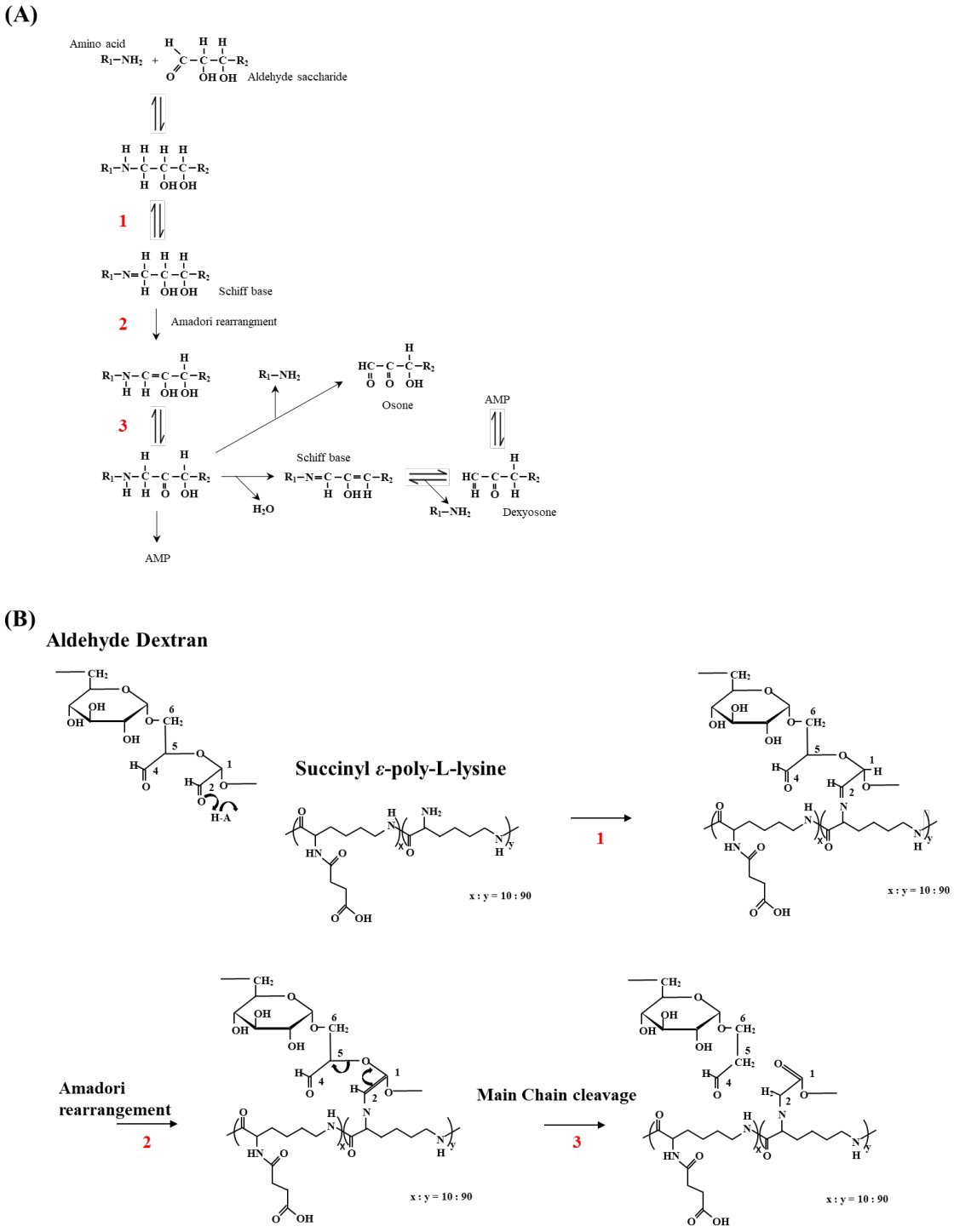

Figure 2.2. (A) Maillard reaction pathway of aldehyde saccharides with amino acids. (B) Molecular scission mechanism of oxidized dextran via reaction with an amine.

A hydrogel exhibiting controlled degradation of dextran derivatives via this degradation mechanism was designed and showed potential as a drug-releasing substrate[52,53]. Furthermore, this degradation mechanism may be applied to induce molecular degradation of cellulose; oxidized cellulose is useful as a low-toxicity biodegradable scaffold[54].

Although the gelation of the aldehyde of oxidized dextran and the amino groups is followed by the Maillard reaction and molecular degradation, the degradation mechanism and products of LYDEX have not been fully elucidated. For clinical application, clarification of the degradation products, mechanisms, and *in vivo* kinetics is necessary to confirm their effects on biological safety. Furthermore, clarification of the *in vitro* degradation behavior of LYDEX is useful for elucidating the *in vivo* degradation and absorption mechanisms. Therefore, in this study, the main degradation products of LYDEX in aqueous media are analyzed experimentally to elucidate the degradation mechanism.

2.2 Material and methods

2.2.1 Materials

Dextran (70 kDa) was obtained from Meito Sangyo (Nagoya, Japan) and ε-PLL (4 kDa, 25 wt.% aqueous solution, free base) from JNC (Tokyo, Japan). Sodium periodate, succinic anhydride (SA), and other chemicals were purchased from Nacalai Tesque (Kyoto, Japan). All chemicals were used without further purification unless otherwise stated.

2.2.2 Preparation of AD

AD (oxidant/dextran ratio: 2.5/20 w/w) was prepared by oxidizing dextran with sodium periodate according to the method reported[55].

2.2.3 Preparation of SA-treated PLL (SAPL)

AD reacts with the primary amino group of ε-PLL at a neutral pH to form a hydrogel. To control this reactivity and due to its low toxicity[18], SA was used to synthesize SAPL. ε-PLL is an oligomer of the amino acid L-lysine with 25–35 primary amino groups per molecule, but SAPL consists of an α-carboxyl group bonded to an ε-amino group. Several amino groups of ε-PLL were acylated by SA addition according to a previously reported method[31].

2.2.4 Characterization of AD and SAPL

2.2.4.1 Aldehyde content determination

The aldehyde content of AD was evaluated using a simple iodometric titration method used in a previous study[31]. Briefly, *ca*. 1% w/v aqueous AD solution (10 mL) was added to an I_2 solution (20 mL, 0.05 M), followed by NaOH addition (20 mL, 1 M). The oxidation reaction proceeded for 15 min. After H_2SO_4 addition (15 mL, 6.25% v/v), the I_2 consumption was determined by titration with 0.1 M $Na_2S_2O_3$ using one drop of 20% w/w starch solution as an indicator. The aldehyde group reacts with 1 mol of I_2 under alkaline conditions to form a carboxylic acid, and 1 mol of I_2 reacts with 2 mol of $S_2O_3^{2-}$ ions. Three readings were obtained for each titration (n = 3). The aldehyde content (mol/ Aldehyde Glucose Unit (AGU)) was calculated using Equation 1.

$$\text{Aldehyde content} = \frac{C_{Na2S2O3} \times ([V_B] - [V_S]) \times Mw_{AGU} \times [D]}{[W] \times 2 \times 1000} \ (\text{mol/AGU}) \quad (1)$$

where [VB] is the titration volume of the blank, [VS] is the titration volume, [D] is the dilution rate of the sample, and [W] is the anhydrous-equivalent sample volume.

2.2.4.2 Carboxyl group content determination

The carboxyl group content in ε-PLL was evaluated using the ninhydrin method[56]. The acylated ε-PLL solution (10% w/v) was diluted 400-fold using distilled water, and subsequently, 0.1 mL of the dilution, 1 mL of ninhydrin solution (0.8 g ninhydrin and 0.12 g anhydrous hydrindantin in 30 mL 2-methoxyethanol), and 2 mL of acetic acid buffer solution (0.1 M acetic acid and 0.2 M sodium acetate, pH 5.5) were added to glass tubes, which were heat-sealed. After coloring at 100 °C for 3 min, the absorbance at 570 nm was recorded at 25 °C using an ultraviolet (UV)-visible spectrophotometer (UVmini-1240; Shimadzu, Kyoto, Japan). Three readings were obtained for each sample (n = 3). Separately, polylysine solution was colored using a ninhydrin solution and measured in the same manner. A calibration curve (aλ, bλ) was prepared using the obtained absorbances, and the residual amino group content is calculated using Equation 2.

$$R_{\mathrm{amino}} = \left(\frac{A_\lambda - b_\lambda}{a_\lambda}\right) / c_{\mathrm{SAPL}} \times 11 \div 10 \times 100 \quad (\%) \qquad (2)$$

2.2.4.3 Preparation and degradation of LYDEX

LYDEX was prepared using AD powder, with an oxidant/dextran ratio of 2.5/20 (w/w), and SAPL powder in a 4:1 mass ratio. To prepare a LYDEX gel, 40 mg of LYDEX powder was added to the well of a silicone mold (φ: 10 mm, LADD Research Industries, Williston, VT, USA) with 60 μL of saline solution, and 120 μL of saline solution was added to form a hydrogel, which was allowed to stand for 3 min. To degrade the gel, the gel was removed from the silicone mold and placed in a brown glass bottle (30 mL, Nichiden-Rika Glass, Kobe, Japan) containing 12 mL of saline solution, and shaken for 1 d, or 1, 2, or 4 wk in a water bath shaker (37 °C, 100 rpm). This solution was then separated into filtrate and residue using a

membrane filter (0.45 μm A045A047A, Advantech, Tokyo, Japan). The residue was washed with approximately 1 mL of water and dried under reduced pressure. The residue was weighed, and the filtrate was subjected to absorption spectroscopy using a Shimadzu UV-1800 spectrophotometer.

2.2.4.4 Degradation product analysis using gel permeation chromatography (GPC) fractionation and spectroscopy

LYDEX gels were subjected to degradation for 2 wk and filtered. The fraction of each GPC peak was collected and analyzed. The sample volume used for preparative GPC was 5 mL, the injection volume was 100 μL per injection, and the number of preparative GPC runs was 50. TSKgel G4000PW_{XL} and TSKgel G2500PW_{XL} columns were used. Two milliliters of the obtained fractions were placed in dialysis tubes (Biotech CE Trial Kit, Repligen, Waltham, MA, USA; MWCO: 100–500D), immersed in approximately 1 L of ion exchange water at 4 °C, and gently agitated for approximately 20 h (during the ion exchange, the water was changed once). The dialyzed samples were placed in eggplant flasks, frozen in a freezer, placed in a desiccator (5 L capacity), and sublimated under vacuum (approximately 6 h). The remaining solids were collected and subjected to infrared (IR) and ^{1}H NMR spectroscopy. IR was performed using the KBr tablet method (4 mm φ) using an IRPrestige-21 (Shimadzu, resolution: 4 cm^{-1}, measurement range: 400–4000 cm^{-1}, cumulative number: 64 times), and ^{1}H NMR spectroscopy was conducted using a JNM-ECA 400 (400 MHz, JEOL, Tokyo, Japan). The lyophilized sample was dissolved in approximately 0.75 mL of D_2O (internal standard: none). Mw fractionation was performed using Shimadzu Prominence LC-20AD HPLC LC-Solution TSKgel G4000PW_{XL} and TSKgel G2500PW_{XL} columns, and absorption at 323 and 210 nm was measured using a UV detector, whereas refraction was measured using a differential

refractometer. The Mw fractionation ranges of the columns ranged from 2000 to 300 000 Da for G4000PW$_{XL}$ and <3000 Da for G2500PW$_{XL}$ for PEG. Therefore, G4000PW$_{XL}$ was used to examine the degradation products of the high-molecular-weight LYDEX, and G2500PW$_{XL}$ was used to examine oligomers, smaller monosaccharides, and amino acids, which were the higher-degradation products. GPC measurement conditions were as follows: mobile phase, 0.9% NaCl; flow rate, 0.6 mL/min; column temperature, 35 °C. Pullulan (STANDARD P-82, Showa Denko, Tokyo, Japan) was used as the reference standard.

2.3 Results and discussion

2.3.1 AD and SAPL characterization

Dextran was oxidized using sodium periodate. The reagents were added in predetermined amounts to establish an oxidant:dextran ratio of 2.5/20 (w/w). The aldehyde content of the produced AD was determined using iodine titration. The desired product was obtained, with an aldehyde content of 0.28 mol/AGU.

Several of the amino groups of ε-PLL were acylated with SA. The reagents were added in predetermined amounts to establish a reaction rate of 10 ± 5 mol%. According to ninhydrin measurement, the desired product was obtained, with an SA reaction rate of 12 mol%. These results are consistent with those of previous studies[31,32], and these parameters were utilized in this study because polymers with these parameters showed good degradabilities and low cytotoxicities.

2.3.2 Degradation product analysis using GPC and gel degradation over time

The degradation of the LYDEX gel in physiological saline was analyzed using GPC. Figure 2.3 shows the gel degradation with time. The gel degrades rapidly on the first day of degradation to 35% residual, and degradation slows thereafter. The residual is 15% after 4 wk. The gel is not visually confirmed after 5 d.

The absorption spectra of the filtrates of SAPL, AD, and LYDEX after 1 d of degradation are shown in Figure 2.4. A 210 nm absorption peak is observed for SAPL, whereas AD shows almost no absorption, with only a slight absorption maximum at approximately 240 nm. The 240 nm peak is due to a pH-dependent enol[49]. In addition, LYDEX immediately after gelation shows absorption only at 210 nm. Conversely, the LYDEX gel after 1 d of degradation shows absorption at approximately 210 and 323 nm. It gradually turns yellow due to the Maillard reaction[32,51], and 323 nm is the absorption of this yellowing. Therefore, I conducted UV detection following GPC at 210 and 323 nm.

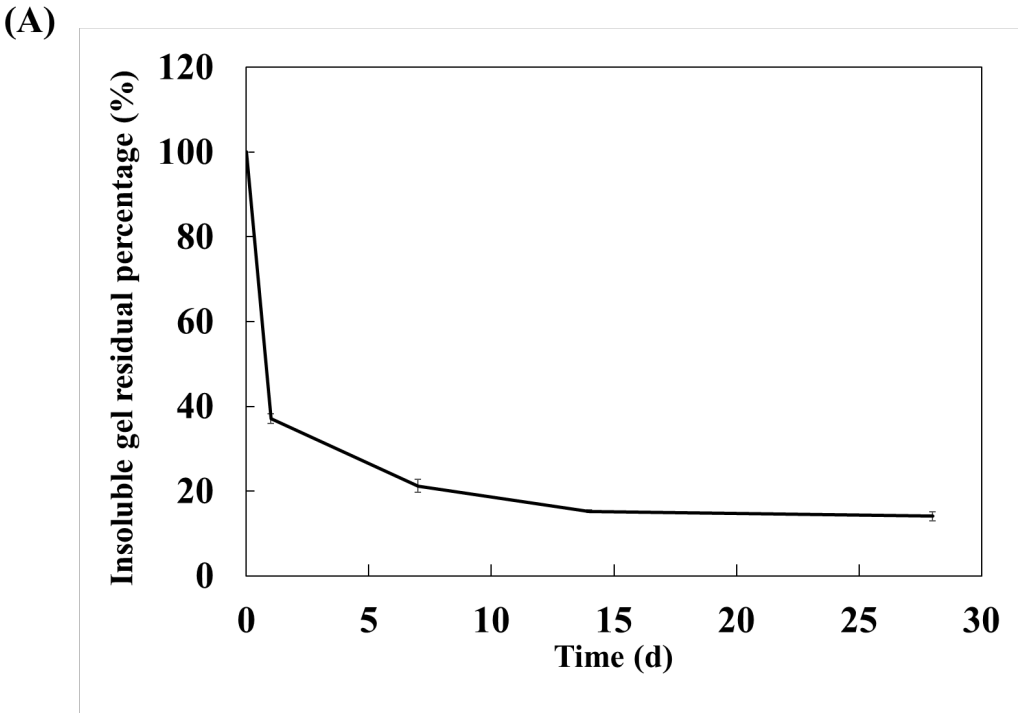

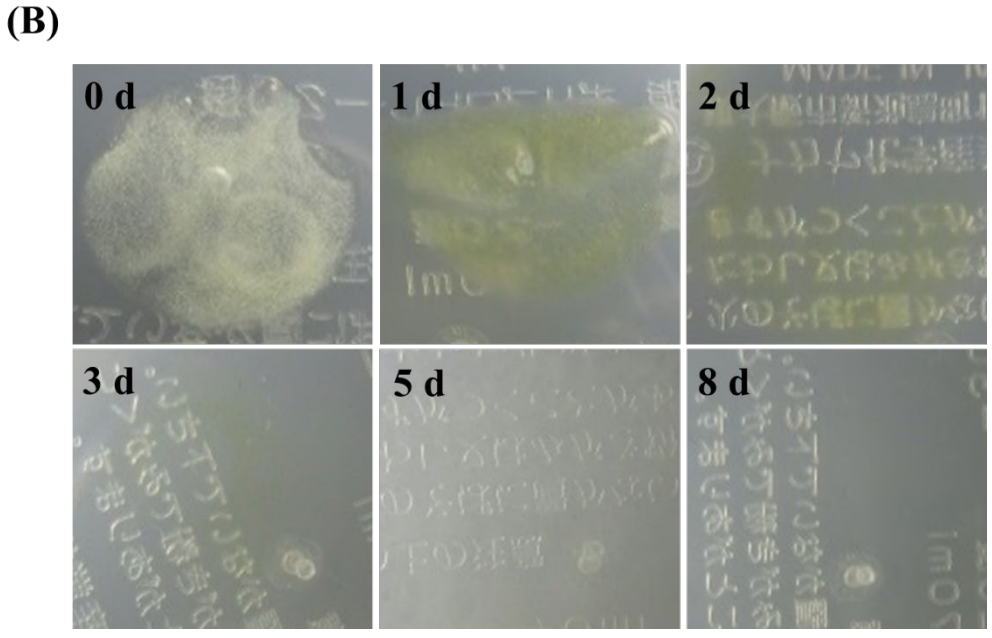

Figure 2.3. (A) Residual rate of LYDEX gel over time, (B) Degradation of LYDEX gel at 0, 1, 2, 3, 5, and 8 d at 37 °C in saline solution.

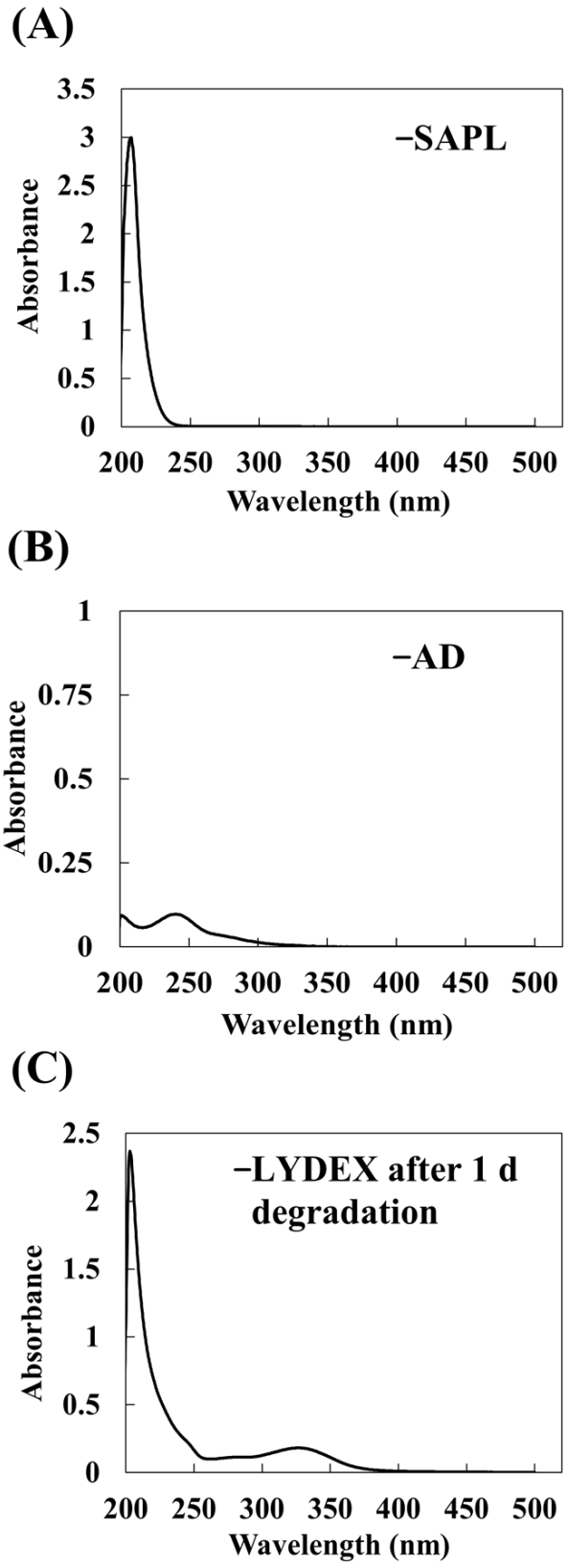

Figure 2.4. Absorption spectra of SAPL, AD, and the LYDEX gel degradation products.

The GPC chromatograms detected using refractive index (RI) detection are shown in Figure 2.5A. There is a small peak at a retention time (RT) of 10.4 min (Mw = more than several million grams per mole), a peak at 12.5 min RT (Mw = 145 900 g/mol), a large peak at 17.0 min RT (Mw = 11 200 g/mol), and a sharp peak at 19.6 min RT (Mw ≤ 2300 g/mol). All peak areas increase with time. For UV detection following GPC at 323 (Figure 2.5B) and 210 nm (Figure 2.5C), the peaks at 10.4, 12.5, and 17.0 min RT are observed at both wavelengths, but not the peak at 19.6 min RT. The peak at 10.4 min RT represents degradation products of Mw = more than several million grams per mole that are not separated by the TSKgel G4000PW$_{XL}$ column and appear in the exclusion limit. However, the peak at 17.0 min RT is much broader than that at 10.4 min RT, and as shown in Figure 3, LYDEX gel degrades rapidly and then slowly, suggesting that the degradation of LYDEX gel occurs as soon as the gel collapses and solubilizes, up to the Mw peak at 17.0 min RT (Mw = 11 200 g/mol). Meanwhile, there is an increase in the peak at 19.6 min RT (Mw ≤ 2300 g/mol) with time, and the fraction represented by this peak exhibits no UV absorption, suggesting that the compositions of the fractions with RTs of 19.6 and 17.0 min are different. The Mws of the degradation products are not uniformly distributed, and after 17.0 min RT, no degradation products with Mw = 3000 g/mol are observed up to RT 19.6 min (Mw ≤ 2300 g/mol).

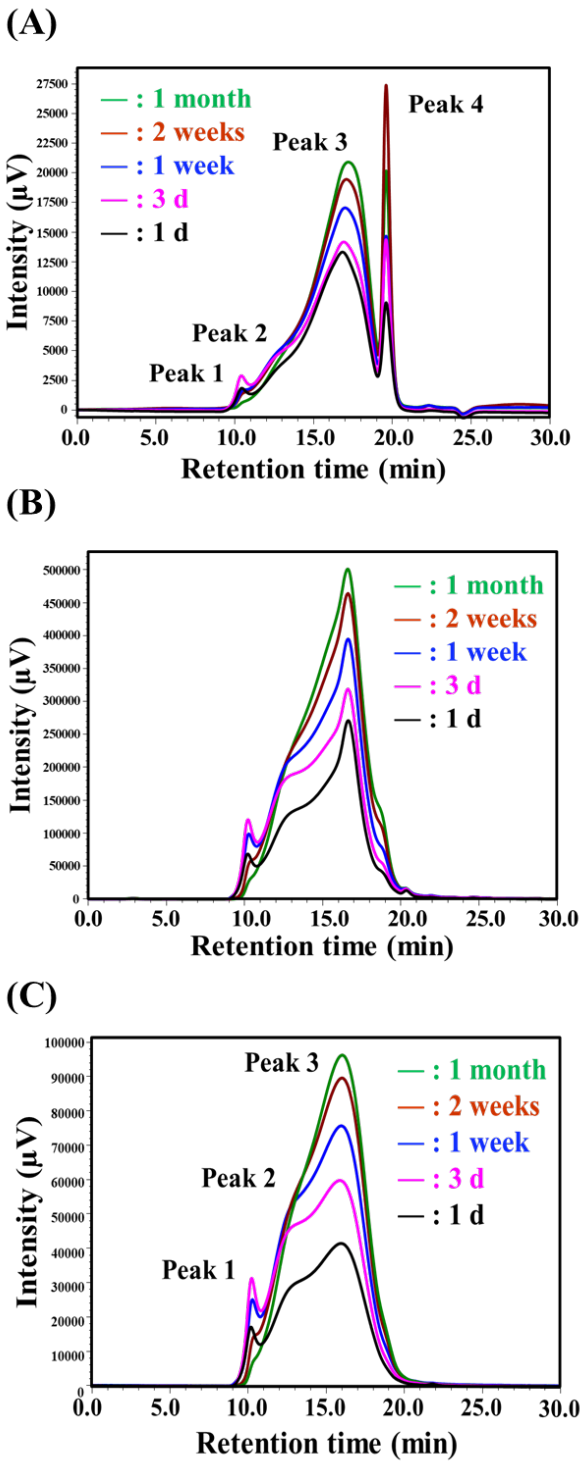

Figure 2.5. Gel permeation chromatograms obtained using G4000PW$_{XL}$ columns, of the products within the LYDEX degradation treatment solution; (A) refractive index detection, (B) ultraviolet (UV) detection at 323 nm, (C) UV detection at 210 nm.

2.3.3 GPC detection value ratio of each component

To observe the change in the formation behaviors of the LYDEX degradation products over time, the ratios of the three GPC detection values of LYDEX gel are compared with those of the raw materials AD and SAPL (Table 2.1). Differential refractometry of AD shows a single peak at 15.9 min RT (Mw = 73 000 g/mol, Figure 2.6), but almost no UV absorption is observed at 323 and 210 nm. AD is a polysaccharide, despite aldehyde group introduction, and the Mw of the starting material, dextran, is 70 000 g/mol, and hence these results are reasonable. The RI of SAPL (Figure 2.7) displays bimodal peaks at 17.3 (Mw = 11 000 g/mol) and 18.5 min RT (Mw = 3800 g/mol), in addition to UV absorption at 210 nm (Table 2.1). At 323 nm, very small bimodal peaks are observed. GPC was performed in the same manner for ε-PLL without the introduction of carboxyl groups (COOH 0% PLL) and polylysine with an increased carboxylation rate of 65% (COOH 65% PLL). The chromatograms reveal single peaks at 18.3 min RT (Mw = 4300 g/mol) for COOH 0% PLL and 16.9 min RT (Mw = 12 000 g/mol) for COOH 65% PLL. COOH 65% PLL is used as a cryoprotectant for cells[57]. ε-PLL is a polyamino acid consisting of 25–35 lysine amino acids that are ε-linked. SAPL is prepared by carboxylating 10% of these amino groups using SA. In COOH 65% PLL, 65% of the amino groups are carboxylated by increasing the amount of SA in the reaction. In COOH 65% PLL, the amino and carboxyl groups form aggregates via ionic bonding, and the Mw suggests that it is a trimer. In SAPL, 10% of the amino groups are carboxylated to form approximately 1/3 of the aggregate; thus, it exhibits bimodal peaks. For the degradation products of LYDEX gel, detection of the small peaks at 10.4 min RT using UV at 323 and 210 nm is more sensitive than RI detection. Even at 17.0 min RT, UV is more sensitive than RI, but less sensitive than UV at 10.4 min RT. At 19.6 min RT, no UV absorption is observed at 323 nm, and even at 210 nm, the sensitivity is lower than that at 10.4- and 17.0-min RT.

Table 2.1. Gel permeation chromatography detection value ratios of aldehyde-functionalized dextran (AD), succinic anhydride-treated poly-L-lysine (SAPL), and LYDEX against refractive index (RI) intensity.

		RI detection	*Ultraviolet (UV, 323 nm)*	*UV (210 nm)*
AD		1	0.0	0.2
SAPL (front peak)		1	0.1	70
Gel degradation peak	RT 10.4 min	1	13	54
	RT 12.5 min	1	13	54
	RT 17.0 min	1	4	21
	RT 19.6 min	1	0.0	2

RT, retention time.

The peak area of each component is expressed as a relative value when the RI value is set to 1, calculated using UV intensity / RI intensity (unit: mv).

Comparing AD and SAPL, only the degradation product of LYDEX gel exhibits UV absorption at 323 nm, suggesting that UV absorption occurs following the Maillard reaction of the Schiff base. As there is no UV absorption at 323 nm at 19.6 min RT, there is therefore no Maillard reaction component from the imine bond (Schiff base) in the fraction represented by this peak. In addition, because the Mw of SAPL is 4000 g/mol, the degradation product is an oligodextran structure, similar to a degradation product of AD undergoing the Maillard reaction. Although the initial reaction pathway of the Maillard reaction is long known[58,59], the Schiff bases are isomerized via Amadori rearrangement to ketoamines, which are likely connected to the side chains of SAPL.

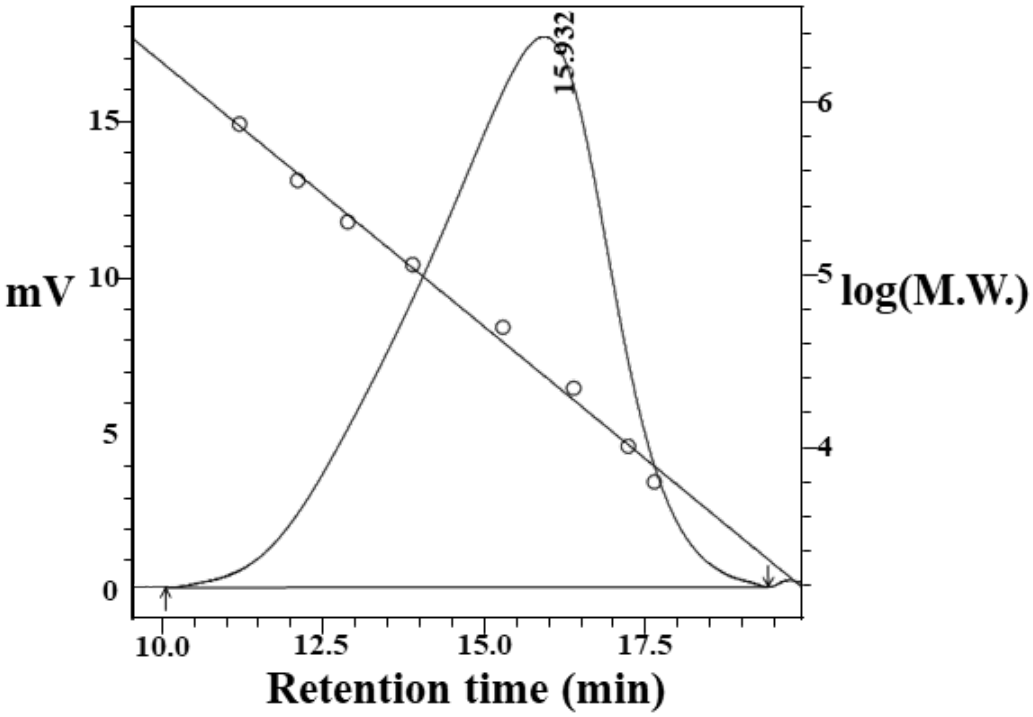

Figure 2.6. Differential refractometry profile of aldehyde-functionalized dextran using a G4000PW$_{XL}$ column. M.W., molecular weight. mV, millivolt.

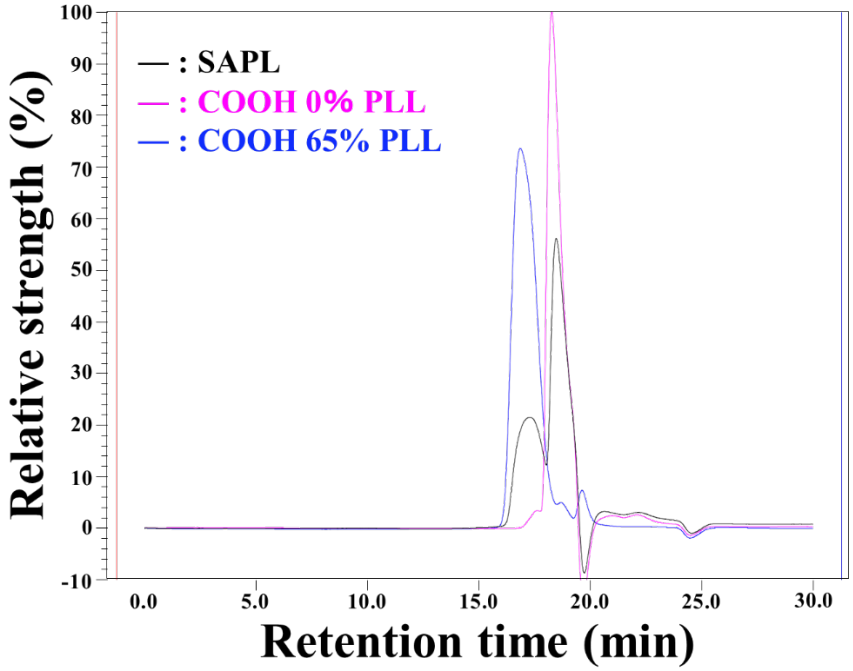

Figure 2.7. Refractive index spectra of succinic anhydride-treated poly-L-lysine (SAPL), poly-L-lysine (COOH 0% PLL), and 65 % carboxylated poly-L-lysine (COOH 65% PLL), obtained using a G4000PW$_{XL}$ column.

2.3.4 Temporal behaviors of main degradation products

To evaluate the temporal changes in the small-molecule products within the LYDEX gel degradation treatment solution, GPC was performed using a TSKgel G2500PW$_{XL}$ column (Figure 2.8).

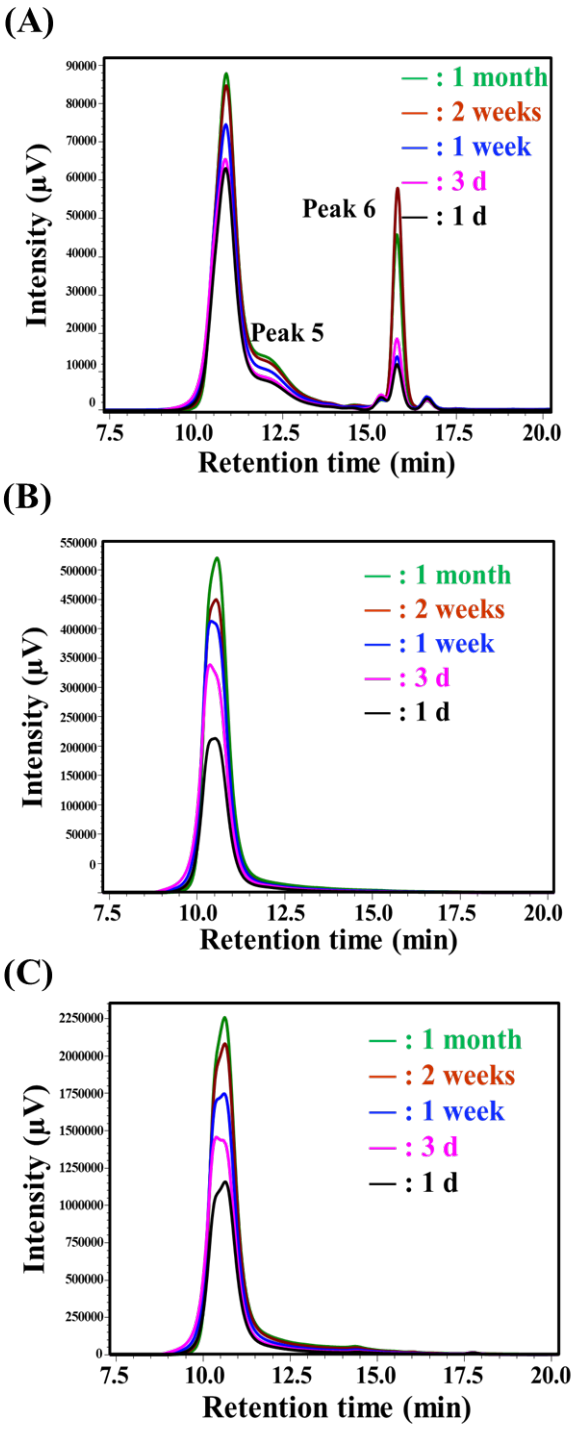

Figure 2.8. Gel permeation chromatography, using a G2500PW$_{XL}$ column, of the products within LYDEX degradation treatment solution; (A) refractive index detection, (B) ultraviolet (UV) detection at 323 nm, (C) UV detection at 210 nm.

Using the TSKgel G2500PW$_{XL}$ column, peaks 5 and 6 at 12.2- and 15.8-min RT, respectively, are the characteristic peaks, in addition to the peak at 10.7 min RT that elutes near the exclusion limit of the column. Of these peaks, 4 and 6 are consistent with the RT of NaCl, and their irregularities, rather than changes over time, suggest that NaCl and low-molecular-weight compounds may elute together.

Figure 2.9 shows the changes in the RI signals of peaks 1, 2, 3, and 5 with increasing degradation time, as shown in Figures 2.5 and 2.8. Peak 1 increases initially, but then slowly decreases. The trends of peaks 3 and 5 are similar, with slight increases even after 1 mo. The trend of peak 2 is similar to that of peak 1, increasing initially and remaining constant for a while, but then gradually decreasing. The Mw distribution values for each peak show no significant changes, suggesting the formation of a metastable substance over time (Table 2.2). First, peak 1 represents macromolecules with Mws of >1 million grams per mole, which initially form and then gradually degrade when dissolved. Peak 2 represents compounds with Mws of several hundred thousand grams per mole, and their formation, due to the degradation of the gel and compounds represented by peak 1, and their degradation in the dissolved state occur in parallel, gradually decreasing over time. In addition, peak 3 represents compounds with Mws of 10 000–20 000 g/mol, and peak 5 represents compounds with Mws of several thousand, but they are constantly increasing with the convergence to the formation of these compounds during the final stage of degradation.

Figure 2.10 shows the GP chromatogram of the degradation treatment solution (1 wk), obtained using a TSKgel G2500PW$_{XL}$ column. A large peak (10.8 min RT) is observed in the exclusion limit of the column, followed by a gentle peak to a shoulder centered at 11.8 min RT (Mw = 2500 g/mol) and peaks at 14.4, 15.3, 15.8, 16.6, and 17.2 min RT. The fractions below Mw = 2500 g/mol show almost no UV absorption at 323 and 210 nm and represent degradation

products of the oligodextran moiety generated by degradation, because no Schiff base (C=N bond) is present, as described above. Glucose reacts with proteins to produce glyoxal[60] (Mw = 58.04 g/mol), which is formed by autoxidation of glucose undergoing the Maillard reaction, glycolaldehyde[61] (Mw = 254.39 g/mol), which is derived from Schiff bases, and methylglyoxal[62] (Mw = 72.06 g/mol), 3-deoxyglucosone[63] (Mw = 162.14 g/mol), and glucosone[64] (Mw = 178.140 g/mol), which are formed by the Schiff base and degradation of Amadori rearrangement products. Therefore, AD-derived Amadori rearrangement products and their degradation products, which are smaller than glucose, suggested to be emerging.

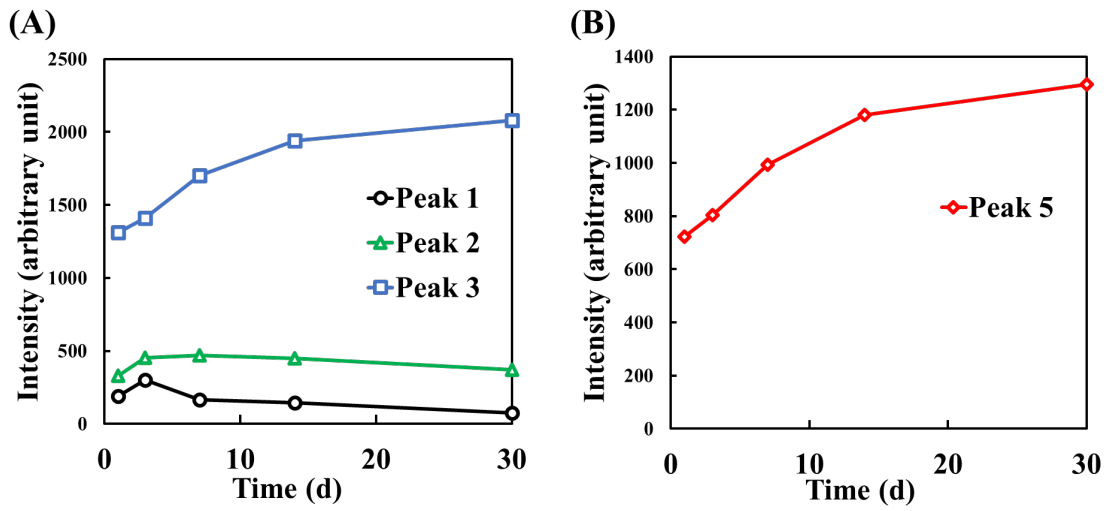

Figure 2.9. Changes in the degradation products (main peaks) over time in the degradation treatment solution; (A) Refractive index (RI) detection following elution from the G4000PW$_{XL}$ column and (B) RI detection following elution from the G2500PW$_{XL}$ column.

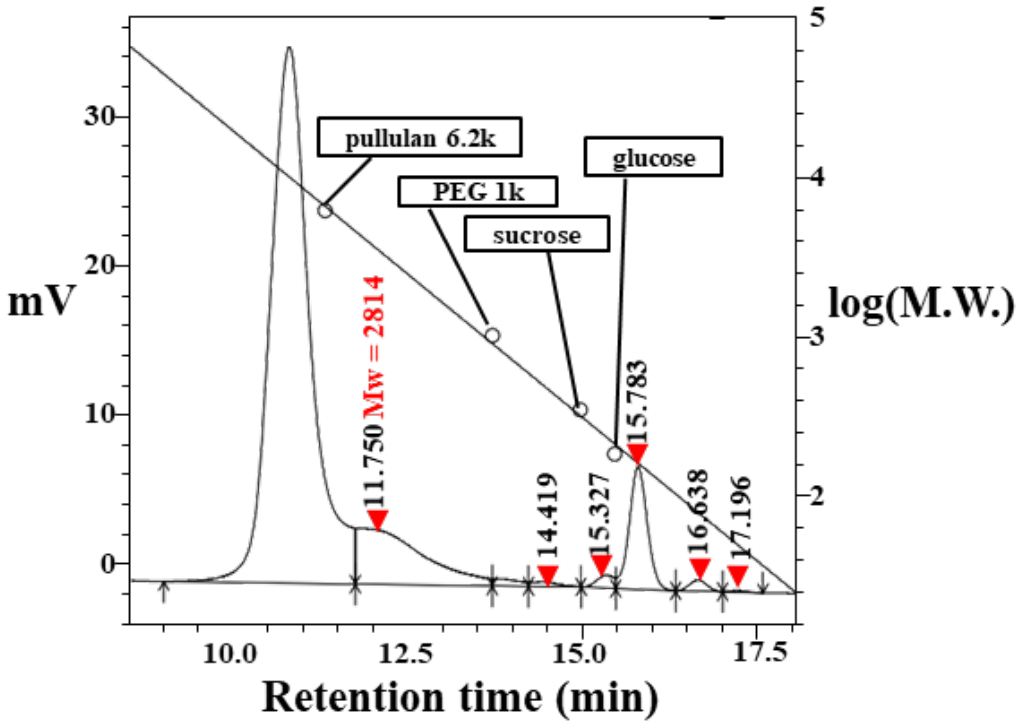

Figure 2.10. Gel permeation chromatogram of degradation solution (1 wk), obtained using a G2500PW$_{XL}$ column. Mw, molecular weight; PEG, polyethylene glycol.

Table 2.2. Changes in the molecular weight distribution (weight-average molecular weight (M_w) / number-average molecular weight (M_n)) of the major gel permeation chromatography peaks of LYDEX gel over time.

		Peak 1	*Peak 2*	*Peak 3*	*Peak 4*	*Peak 5*	*Peak 6*
1 d	M_w /M_n	1.06	2.24	1.35	1.05	1.22	1.01
3 d	M_w / M_n	1.06	2.36	1.35	1.04	1.24	1.01
1 wk	M_w / M_n	1.03	2.45	1.35	1.04	1.34	1.01
2 wk	M_w / M_n	—	2.69	1.35	1.03	1.23	1.01
1 mo	M_w / M_n	—	2.26	1.36	1.04	1.22	1.01

G4000PW$_{XL}$ and G2500PW$_{XL}$ columns were used for peaks 1–4 and peaks 5 and 6, respectively.

2.3.5 IR spectroscopy

The IR spectra of the samples that showed the major peaks after preparative isolation using GPC, dialysis, lyophilization, and concentration are shown in Figure 2.11. For comparison, AD and SAPL, which are components of LYDEX, were also measured in the same manner. AD exhibits no aldehyde group absorption (~1700 cm^{-1}), instead showing strong ether bond absorption, suggesting that the aldehyde group is converted to a hemiacetal (ether bond) via reaction with water, which is the characteristic absorption. The lack of aldehyde group absorption is consistent with the study by Maia et al.[44] and its absence for iodate-oxidized polysaccharides is generally due to the formation of gem-diol with hydrated hemiacetal groups[65].

The characteristic IR signals of amides are amide I (1600–1800 cm^{-1}), amide II (1470–1570 cm^{-1}), amide III (1250–1350 cm^{-1}), and amide A (3300–3500 cm^{-1}). SAPL is characterized by strong absorption, particularly at approximately 3400 and 1620 cm^{-1} due to the amide group, which are consistent with the reported signals of PLL[66]. The spectrum of the compounds represented by preparative peak 1 shows the characteristic absorptions reflecting the structures of AD and SAPL. For the compounds represented by preparative peak 2, similar to peak 1, the peaks reflecting the structures of AD and SAPL are observed, but the amide II band of SAPL at approximately 1500 cm^{-1} is completely absent, and the ether absorption increased slightly, suggesting that the AD component increased relative to that of the fraction represented by peak 1. For the compounds represented by preparative peak 3, the absorption of amide reduced and the absorption of ether, which reflects the structure of AD, is observed, thereby rendering the spectrum even closer to that of AD than that of peak 2.

For the compounds represented by preparative peak 5, as for preparative peak 3, absorption reflecting the structure of AD is strong, and the spectrum is close to that of AD, but

the amide absorption due to SAPL (~1620 cm^{-1}) is also observed. In summary, the spectrum of the compounds represented by preparative peak 1 is close to that of SAPL, the spectra of the compounds represented by preparative peaks 3 and 5 are close to that of AD, and the compounds represented by preparative

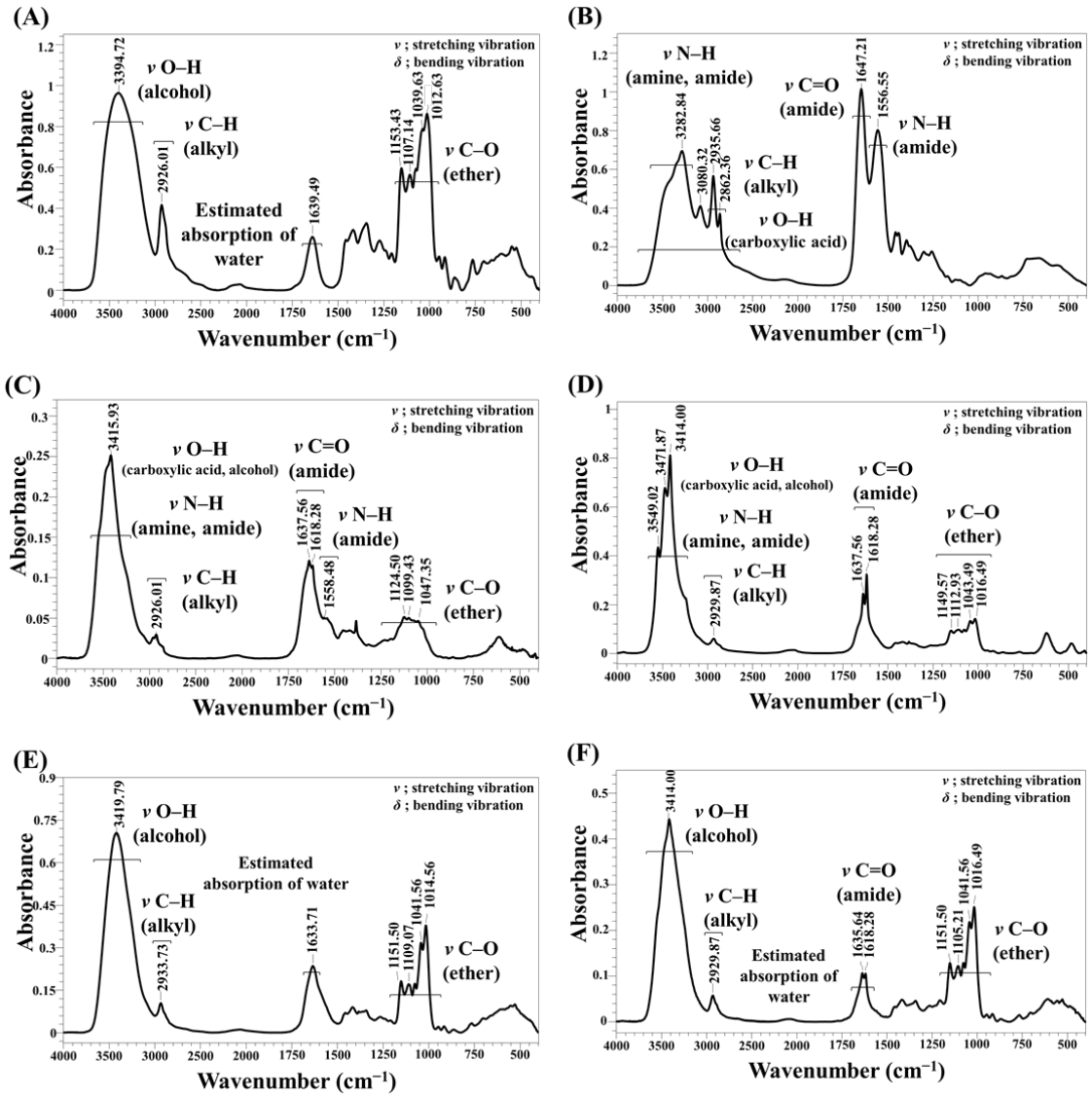

Figure 2.11. (A) Infrared (IR) spectrum of AD. (B) IR spectrum of SAPL. (C) IR spectrum of the fraction represented by preparative peak 1, (D) peak 2, (E) peak 3, and (F) peak 5.

peak 2 include AD and SAPL. Therefore, as the preparative peak shifts from 1 to 2 to 3 and 5 to the low-molecular-weight region, the structure shifts from relatively rich in the SAPL skeleton to rich in the AD skeleton. This refers not only to the whole structure but also to the substructure.

2.3.6 NMR spectroscopy

The ^{1}H NMR spectra of the preparative samples represented by peaks 2, 3, and 5 are shown in Figure 2.12. For comparison, AD and SAPL, the raw materials of LYDEX, were also measured in the same manner. Preparative peak 1 was not analyzed due to insufficient sensitivity for the small amount within the preparative volume. AD is characterized by methine and methylene signals representing protons adjacent to O atoms on the dextran backbone (α in the figure) and signals representing protons between hemiacetals (or acetals) (β in the figure). There are no signals attributed to the aldehyde protons. The C2–C3 and C3–C4 bonds of the glucose moiety are removed by oxidation, suggesting that C2 and C4, which are replaced by aldehydes, react with hydroxyl groups and are converted to the hemiacetal structure (ether bond)[67-69].

SAPL is characterized by signals such as those representing the adjacent methylene on the PLL backbone (a), the methylene adjacent to the carbonyl group on the succinate backbone (b), the methylene adjacent to the imine (c), and the proton on the C atom to which the amino group is attached (d). There are signals attributed to the α proton (e). Matsumura et al. reported the similar structural properties of succinylated PLLs at different carboxylation rates[70], although the carboxylation rate of SAPL is different from those reported previously.

The compounds represented by the preparative peaks 2, 3, and 5 exhibit the characteristic peaks (α, β, a, b, c, and d) of AD and SAPL in all samples, suggesting that the

structure is a hybrid of these skeletons. However, the structures of the degradation products represented by each preparative peak appear to shift from SAPL to AD skeleton-rich from preparative fraction 2 to 3 to 5 to the low molecular weight region, which is consistent with the IR spectra. The methine/methylene group increases from preparative fractions 2 to 3. Figures 2.7(D) and (E) show that the AD-derived peaks increase as the degradation of LYDEX progresses. The progress of the Maillard reaction deduced using previous studies[51] (Figure 2.2(A)) and the methylene group as one of the components of 3-deoxyosone that undergoes Strecker degradation via Amadori rearrangement[71] suggest that these peaks are due to an AD-derived degradation product. Conversely, as SAPL is stable in water and AD undergoes the Maillard reaction, alteration of the SAPL structure is unlikely, and the SAPL-derived methine/methylene group is observed. Thus, this increase suggests that the degradations of AD and SAPL are related to the Maillard reaction.

For preparative fractions 2, 3, and 5, the peak integrals of the glucose-derived signals of AD observed at 3.3–4.0 ppm are set to 100, and the peak integrals of the methylene-derived signals of SAPL observed at 1.2–1.9 ppm are compared. The SAPL/AD ratio is 4:2:1 for the preparative fractions 2:3:5.

Therefore, after AD and SAPL form a Schiff base, the main chain of AD is broken via Amadori rearrangement and molecular degradation commences, with AD degrading into Amadori rearrangement products and their degradation products; in addition, the Schiff bases of AD and SAPL are loosely bound via C–N, but SAPL retains most of the PLL structure, and as PLL is stable in aqueous solution[72], SAPL remains bound to a section of AD. This AD-bound SAPL becomes a polymer with an Mw of approximately 4000–5000 g/mol, which forms dimeric or trimeric aggregates, remaining undegraded.

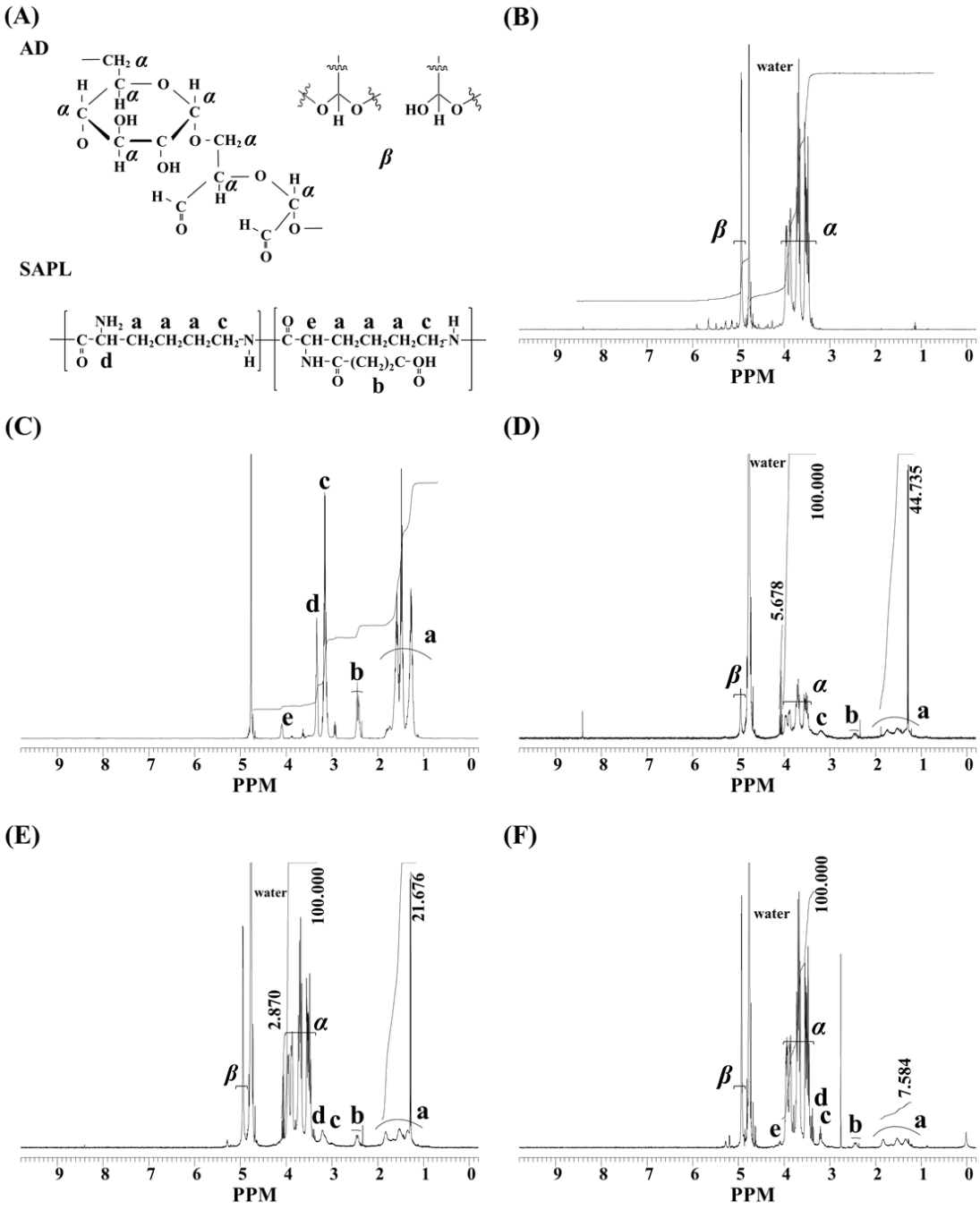

Figure 2.12. (A) Chemical structures of AD and SAPL. (B) ^{1}H NMR spectrum of AD. (C) ^{1}H NMR spectrum of SAPL. (D) ^{1}H NMR spectrum of the compounds represented by preparative peak 2, (E) peak 3, and (F) peak 5.

2.4 Conclusions

To elucidate the degradation mechanism of LYDEX in aqueous media, the main degradation products were analyzed, and the following degradation mechanisms were clarified. The analysis of degradation products using GPC showed that LYDEX became >60% water-soluble in 1 d, with mild subsequent solubilization. Degradation product analysis using GPC, followed by IR and ^{1}H NMR spectroscopy, revealed products with mixed structures containing SAPL and AD moieties.

According to the IR and ^{1}H NMR spectra, the later the GPC elution, the higher the percentage of the AD moieties, and in the fractions 2, 3, and 5 collected in this study, the SAPL/AD ratio changed from approximately 4 to 2 to 1, respectively, based on the ^{1}H NMR peak integrals. The methylene group increased from fraction 2 to 3 and was one of the components of 3-deoxyosone that underwent Strecker degradation via Amadori rearrangement, suggesting that it was related to the Maillard reaction.

The mixture of AD and SAPL became richer in AD as the Mw decreased. After the main chains of the solubilized degradation products of LYDEX were cleaved via Amadori rearrangement (Figure 2.2(B)), the structure of the AD-SAPL network, with Mws from several million to 145 000 g/mol, was potentially maintained for a while, wherein the SAPL skeleton remained undegraded and the AD portion degraded to oligodextran, with an Mw of > 2300 g/mol. However, the low-molecular-weight fractions of peaks 4 and 6 were not included in this analytical study because of irregular fluctuations that suggested potential contamination by NaCl or other substances. Specifically, peaks 4 and 6 increased with processing time, in addition to other degradation peaks in the GP chromatograms, as shown in Figure 2.9. In addition, the RTs of these peaks are consistent with that of NaCl and may therefore simply represent NaCl or organic compounds, such as sugars (alone), generated by LYDEX degradation.

Although LYDEX gel should not degrade further in saline solution, the *in vivo* degradation and absorption mechanism should be clarified in combination with data from *in vivo* kinetics and implantation studies for clinical application.

Macromolecules, such as polyvinylpyrrolidone and albumin, enter cells via endocytosis[73], and these macromolecules undergo digestion by endosomes formed there, which fuse with lysosomes. A Schiff base-bound Adriamycin-oxidized dextran (using a 70 kDa dextran) complex was used to study the intracellular form of Adriamycin, speculating that it is absorbed into tissue cells via endocytosis and then undergoes low-molecular-weight conversion by lysosomes[74].

This suggests that, similar to LYDEX, degradation products formed via gel microfragmentation due to self-degradation and high-molecular-weight degradation products are likely digested *in vivo* through phagocytosis by phagocytes, such as macrophages, absorbed into the spleen and liver, and degraded to low molecular weight via metabolism *in vivo*. When LYDEX gels are applied in the gastrointestinal tract, such as endoscopic wound dressings, AD and AD-derived degradation products may be reduced by enzymes to sugars, such as dextranase and isomaltose, several of which are utilized in the metabolic cycle *in vivo*, and several are eliminated. Regarding the pharmacokinetics of SAPL and SAPL-derived degradation products, low absorption of ^{14}C-radiolabeled ε-PLL in the gastrointestinal tract was observed in an absorption, distribution, metabolism, and excretion (ADME) study using oral administration[75], and SAPL and SAPL-derived degradation products may therefore pass through the fecal gastrointestinal tract without absorption.

Finally, hydrogels obtained by the reaction of AD with polymers bearing amino groups, such as collagen, have been previously reported. However, the *in vitro* degradation behavior of LYDEX by the reaction of AD with SAPL, as shown in this study, revealed LYDEX

self-degradability for the first time. This is extremely valuable for the study of molecular degradation mechanisms of polysaccharide hydrogels and the development of medical applications, such as hemostatic agents, sealants, and anti-adhesion materials.

2.5 References

1. Li, C., Wang, T., Hu, L., Wei, Y., Liu, J., Mu, X., Nie, J., & Yang, D. Photocrosslinkable bioadhesive based on dextran and PEG derivatives. *Materials Science and Engineering C*. **2014**, 35(1), 300–306. https://doi.org/10.1016/j.msec.2013.10.032
2. MacGillivray, T. E. Fibrin Sealants and Glues. *Journal of Cardiac Surgery*. **2003**, 18(6), 480–485. https://doi.org/10.1046/j.0886-0440.2003.02073.x
3. Canonico, S. The use of Human Fibrin Glue in the surgical operations. *Acta Biomedica de l'Ateneo Parmense*. **2003**, 74(SUPPL. 2), 21–25. https://pubmed.ncbi.nlm.nih.gov/15055028/
4. Hino, M., Ishiko, O., Honda, K. I., Yamane, T., Ohta, K., Takubo, T., & Tatsumi, N. Transmission of symptomatic parvovirus B19 infection by fibrin sealant used during surgery. *British Journal of Haematology*. **2000**, 108(1), 194–195. https://doi.org/10.1046/j.1365-2141.2000.01818.x
5. Ortel, T. L., Charles, L. A., Keller, F. G., Marcom, P. K., Oldham, H. N., Kane, W. H., & Macik, B. G. Topical thrombin and acquired coagulation factor inhibitors: Clinical spectrum and laboratory diagnosis. *American Journal of Hematology*. **1994**, 45(2), 128–135. https://doi.org/10.1002/ajh.2830450206
6. Siedentop, K. H., Park, J. J., Shah, A. N., Bhattacharyya, T. K., & O'Grady, K. M. Safety and efficacy of currently available fibrin tissue adhesives. *American Journal of Otolaryngology-Head and Neck Medicine and Surgery*. **2001**, 22(4), 230–235. https://doi.org/10.1053/ajot.2001.24817
7. Silver, F. H., Wang, M. C., & Pins, G. D. Preparation and use of fibrin glue in surgery. *In Biomaterials* (Vol. 16, Issue 12, pp. 891–903). **1995**, Elsevier. https://doi.org/10.1016/0142-9612(95)93113-R

8. Ramond, M. J., Valla, D., Gotlib, J. P., Rueff, B., & Benhamou, J. P. OBTURATION ENDOSCOPIQUE DES VARICES OESO-GASTRIQUES PAR LE BUCRYLATE®. I: ETUDE CLINIQUE DE 49 MALADES. *Gastroenterologie Clinique et Biologique*. **1986**, 10(8–9), 575–579. https://europepmc.org/article/med/3491014
9. Bhatia, S. K., Arthur, S. D., Chenault, H. K., & Kodokian, G. K. Interactions of polysaccharide-based tissue adhesives with clinically relevant fibroblast and macrophage cell lines. *Biotechnology Letters*. **2007**, 29(11), 1645–1649. https://doi.org/10.1007/s10529-007-9465-8
10. Erasmi, A. W., Sievers, H. H., Wohlschläger, C., Hewitt, C. W., Marra, S. W., Kann, B. R., Tran, H. S., Puc, M. M., Chrzanowski, F. A., Tran, J. L. V., Cilley, J. H., Simonetti, V. A., DelRossi, A. J., & Lenz, S. D. Inflammatory response after BioGlue application [6] (multiple letters). *In Annals of Thoracic Surgery* (Vol. 73, Issue 3, pp. 1025–1026). **2002**, Elsevier Inc. https://doi.org/10.1016/s0003-4975(01)03524-x
11. Fürst, W., & Banerjee, A. Release of glutaraldehyde from an albumin-glutaraldehyde tissue adhesive causes significant *in vitro* and *in vivo* toxicity. *Annals of Thoracic Surgery*. **2005**, 79(5), 1522–1528. https://doi.org/10.1016/j.athoracsur.2004.11.054
12. LeMaire, S. A., Schmittling, Z. C., Coselli, J. S., Ündar, A., Deady, B. A., Clubb, F. J., & Fraser, C. D. BioGlue surgical adhesive impairs aortic growth and causes anastomotic strictures. *Annals of Thoracic Surgery*. **2002**, 73(5), 1500–1506. https://doi.org/10.1016/S0003-4975(02)03512-9
13. Fancy, D. A., & Kodadek, T. Chemistry for the analysis of protein-protein interactions: Rapid and efficient cross-linking triggered by long wavelength light. *Proceedings of the National Academy of Sciences of the United States of America*, **1999**, 96(11), 6020–6024. https://doi.org/10.1073/pnas.96.11.6020

14. Elvin, C. M., Danon, S. J., Brownlee, A. G., White, J. F., Hickey, M., Liyou, N. E., Edwards, G. A., Ramshaw, J. A. M., & Werkmeister, J. A. Evaluation of photo-crosslinked fibrinogen as a rapid and strong tissue adhesive. *Journal of Biomedical Materials Research - Part A*. **2010**, 93(2), 687–695. https://doi.org/10.1002/jbm.a.32572
15. Elvin, Christopher M., Brownlee, A. G., Huson, M. G., Tebb, T. A., Kim, M., Lyons, R. E., Vuocolo, T., Liyou, N. E., Hughes, T. C., Ramshaw, J. A. M., & Werkmeister, J. A. The development of photochemically crosslinked native fibrinogen as a rapidly formed and mechanically strong surgical tissue sealant. *Biomaterials*. **2009**, 30(11), 2059–2065. https://doi.org/10.1016/j.biomaterials.2008.12.059
16. Elvin, Christopher M., Vuocolo, T., Brownlee, A. G., Sando, L., Huson, M. G., Liyou, N. E., Stockwell, P. R., Lyons, R. E., Kim, M., Edwards, G. A., Johnson, G., McFarland, G. A., Ramshaw, J. A. M., & Werkmeister, J. A. *A highly elastic tissue sealant based on photopolymerised gelatin. Biomaterials*. **2010**, 31(32), 8323–8331. https://doi.org/10.1016/j.biomaterials.2010.07.032
17. Mizuno, Y., Mizuta, R., Hashizume, M., & Taguchi, T. Enhanced sealing strength of a hydrophobically-modified Alaska pollock gelatin-based sealant. *Biomaterials Science*. **2017**, 5(5), 982–989. https://doi.org/10.1039/c6bm00829a
18. Chao, H. H., & Torchiana, D. F. BioGlue: Albumin/Glutaraldehyde Sealant in Cardiac Surgery. *Journal of Cardiac Surgery*. **2003**. 18(6), 500–503. https://doi.org/10.1046/j.0886-0440.2003.00304.x
19. Fuller, C. Reduction of intraoperative air leaks with Progel in pulmonary resection: A comprehensive review. *In Journal of Cardiothoracic Surgery* (Vol. 8, Issue 1, pp. 1–7). **2013**, BioMed Central. https://doi.org/10.1186/1749-8090-8-90
20. Kobayashi, H., Sekine, T., Nakamura, T., & Shimizu, Y. *In vivo* evaluation of a new sealant

material on a rat lung air leak Model. *Journal of Biomedical Materials Research*. **2001**, 58(6), 658–665. https://doi.org/10.1002/jbm.1066

21. Ishihara, M., Nakanishi, K., Ono, K., Sato, M., Kikuchi, M., Saito, Y., Yura, H., Matsui, T., Hattori, H., Uenoyama, M., & Kurita, A. Photocrosslinkable chitosan as a dressing for wound occlusion and accelerator in healing process. *Biomaterials*. **2002**, 23(3), 833–840. https://doi.org/10.1016/S0142-9612(01)00189-2
22. Ono, K., Saito, Y., Yura, H., Ishikawa, K., Kurita, A., Akaike, T., & Ishihara, M. Photocrosslinkable chitosan as a biological adhesive. *Journal of Biomedical Materials Research*. **2000**, 49(2), 289–295.
23. Liu, G., Shi, Z., Kuriger, T., Hanton, L. R., Simpson, J., Moratti, S. C., Robinson, B. H., Athanasiadis, T., Valentine, R., Wormald, P. J., & Robinson, S. Synthesis and characterization of chitosan/dextran-based hydrogels for surgical use. *Macromolecular Symposia*. **2009**, 279(1), 151–157. https://doi.org/10.1002/masy.200950523
24. Reyes, J. M. G., Herretes, S., Pirouzmanesh, A., Wang, D. A., Elisseeff, J. H., Jun, A., McDonnell, P. J., Chuck, R. S., & Behrens, A. A modified chondroitin sulfate aldehyde adhesive for sealing corneal incisions. Investigative *Ophthalmology and Visual Science*. **2005**, 46(4), 1247–1250. https://doi.org/10.1167/iovs.04-1192
25. Gilbert, T. W., Badylak, S. F., Gusenoff, J., Beckman, E. J., Clower, D. M., Daly, P., & Rubin, J. P. Lysine-derived urethane surgical adhesive prevents seroma formation in a canine abdominoplasty model. *Plastic and Reconstructive Surgery*. **2008**, 122(1), 95–102. https://doi.org/10.1097/PRS.0b013e31817743b8
26. Hill, A., Estridge, T. D., Maroney, M., Monnet, E., Egbert, B., Cruise, G., & Coker, G. T. Treatment of suture line bleeding with a novel synthetic surgical sealant in a canine iliac PTFE graft model. *Journal of Biomedical Materials Research*. **2001**, 58(3), 308–312.

27. Wallace, D. G., Cruise, G. M., Rhee, W. M., Schroeder, J. A., Prior, J. J., Ju, J., Maroney, M., Duronio, J., Ngo, M. H., Estridge, T., & Coker, G. C. A tissue sealant based on reactive multifunctional polyethylene glycol. *Journal of Biomedical Materials Research*. **2001**, 58(5), 545–555. https://doi.org/10.1002/jbm.1053

28. Sakai, S., Tsumura, M., Inoue, M., Koga, Y., Fukano, K., & Taya, M. Polyvinyl alcohol-based hydrogel dressing gellable on-wound via a co-enzymatic reaction triggered by glucose in the wound exudate. *Journal of Materials Chemistry B*. **2013**, 1(38), 5067−5075. https://doi.org/10.1039/c3tb20780c

29. Araki, M., Tao, H., Nakajima, N., Sugai, H., Sato, T., Hyon, S. H., Nagayasu, T., & Nakamura, T. Development of new biodegradable hydrogel glue for preventing alveolar air leakage. *Journal of Thoracic and Cardiovascular Surgery*. **2007**, 134(5), 1241–1248. https://doi.org/10.1016/j.jtcvs.2007.07.020

30. Araki, M., Tao, H., Sato, T., Nakajima, N., Sugai, H., Hyon, S. H., Nagayasu, T., & Nakamura, T. Creation of a uniform pleural defect model for the study of lung sealants. *Journal of Thoracic and Cardiovascular Surgery*. **2007**, 134(1), 145–151. https://doi.org/10.1016/j.jtcvs.2007.01.007

31. Hyon, S. H., Nakajima, N., Sugai, H., & Matsumura, K. Low cytotoxic tissue adhesive based on oxidized dextran and epsilon-poly- l -lysine. *Journal of Biomedical Materials Research - Part A*, **2014**, 102(8), 2511–2520. https://doi.org/10.1002/jbm.a.34923

32. Matsumura, K., Nakajima, N., Sugai, H., & Hyon, S. H. Self-degradation of tissue adhesive based on oxidized dextran and poly-l-lysine. *Carbohydrate Polymers*. **2014**, 113, 32–38. https://doi.org/10.1016/j.carbpol.2014.06.073

33. Naitoh, Y., Kawauchi, A., Kamoi, K., Soh, J., Okihara, K., Hyon, S. H., & Miki, T. Hemostatic effect of new surgical glue in animal partial nephrectomy models. *Urology*.

2013, 81(5), 1095–1100. https://doi.org/10.1016/j.urology.2013.01.002

34. You, K. E., Koo, M. A., Lee, D. H., Kwon, B. J., Lee, M. H., Hyon, S. H., Seomun, Y., Kim, J. T., & Park, J. C. The effective control of a bleeding injury using a medical adhesive containing batroxobin. *Biomedical Materials (Bristol)*. **2014**, 9(2), 025002. https://doi.org/10.1088/1748-6041/9/2/025002
35. Kamitani, T., Masumoto, H., Kotani, H., Ikeda, T., Hyon, S. H., & Sakata, R. Prevention of retrosternal adhesion by novel biocompatible glue derived from food additives. *Journal of Thoracic and Cardiovascular Surgery*. **2013**, 146(5), 1232–1238. https://doi.org/10.1016/j.jtcvs.2013.02.001
36. Takagi, K., Araki, M., Fukuoka, H., Takeshita, H., Hidaka, S., Nanashima, A., Sawai, T., Nagayasu, T., Hyon, S. H., & Nakajima, N. Novel powdered anti-adhesion material: Preventing postoperative intra-abdominal adhesions in a rat model. *International Journal of Medical Sciences*. **2013**, 10(4), 467–474. https://doi.org/10.7150/ijms.5607
37. Takagi, K., Tsuchiya, T., Araki, M., Yamasaki, N., Nagayasu, T., Hyon, S. H., & Nakajima, N. Novel biodegradable powder for preventing postoperative pleural adhesion. *Journal of Surgical Research*. **2013**, 179(1), e13–e19. https://doi.org/10.1016/j.jss.2012.01.056
38. Bang, B. W., Lee, E., Maeng, J. H., Kim, K., Hwang, J. H., Hyon, S. H., Hyon, W., & Lee, D. H. Efficacy of a novel endoscopically deliverable muco-adhesive hemostatic powder in an acute gastric bleeding porcine model. *PLoS ONE*. **2019**, 14(6), e0216829. https://doi.org/10.1371/journal.pone.0216829
39. Cadée, J. A., Van Luyn, M. J. A., Brouwer, L. A., Plantinga, J. A., Van Wachem, P. B., De Groot, C. J., Den Otter, W., & Hennink, W. E. *In vivo* biocompatibility of dextran-based hydrogels. *Journal of Biomedical Materials Research*. **2000**, 50(3), 397–404.
40. Ferreira, L., Rafael, A., Lamghari, M., Barbosa, M. A., Gil, M. H., Cabrita, A. M. S., &

Dordick, J. S. Biocompatibility of chemoenzymatically derived dextran-acrylate hydrogels. *Journal of Biomedical Materials Research - Part A*. **2004**, 68(3), 584–596. https://doi.org/10.1002/jbm.a.20102

41. Mehvar, R. Dextrans for targeted and sustained delivery of therapeutic and imaging agents. In Journal of Controlled Release (Vol. 69, Issue 1, pp. 1–25). *Elsevier*. **2000**. https://doi.org/10.1016/S0168-3659(00)00302-3
42. Khalikova, E., Susi, P., & Korpela, T. Microbial Dextran-Hydrolyzing Enzymes: Fundamentals and Applications. *Microbiology and Molecular Biology Reviews*. **2005**, 69(2), 306–325. https://doi.org/10.1128/mmbr.69.2.306-325.2005
43. Lévesque, S. G., & Shoichet, M. S. Synthesis of enzyme-degradable, peptide-cross-linked dextran hydrogels. *Bioconjugate Chemistry*. **2007**, 18(3), 874–885. https://doi.org/10.1021/bc0602127
44. Maia, J., Ferreira, L., Carvalho, R., Ramos, M. A., & Gil, M. H. Synthesis and characterization of new injectable and degradable dextran-based hydrogels. *Polymer*. **2005**, 46(23), 9604–9614. https://doi.org/10.1016/j.polymer.2005.07.089
45. Massia, S. P., & Stark, J. Immobilized RGD peptides on surface-grafted dextran promote biospecific cell attachment. *Journal of Biomedical Materials Research*. **2001**, 56(3), 390–399.
46. Matsumura, K., & Rajan, R. Oxidized Polysaccharides as Green and Sustainable Biomaterials. *Current Organic Chemistry*. **2021**, 25. https://doi.org/10.2174/1385272825666210428140052
47. Malaprade, L. Action of polyalcohols on periodic acid. Analytical application. *Bulletin de La Societe Chimique de France*. **1928**, 43, 683–696.
48. Drury, J. L., & Mooney, D. J. Hydrogels for tissue engineering: Scaffold design variables

and applications. In Biomaterials (Vol. 24, Issue 24, pp. 4337–4351). *Elsevier BV*. **2003**. https://doi.org/10.1016/S0142-9612(03)00340-5

49. Drobchenko, S. N., Isaeva-Ivanova, L. S., Kleiner, A. R., Lomakin, A. V., Kolker, A. R., & Noskin, V. A. An investigation of the structure of periodate-oxidised dextran. *Carbohydrate Research*. **1993**, 241(C), 189–199. https://doi.org/10.1016/0008-6215(93)80105-N
50. Maia, J., Carvalho, R. A., Coelho, J. F. J., Simões, P. N., & Gil, M. H. Insight on the periodate oxidation of dextran and its structural vicissitudes. *Polymer*. **2011**, 52(2), 258–265. https://doi.org/10.1016/j.polymer.2010.11.058
51. Chimpibul, W., Nagashima, T., Hayashi, F., Nakajima, N., Hyon, S. H., & Matsumura, K. Dextran oxidized by a malaprade reaction shows main chain scission through a maillard reaction triggered by schiff base formation between aldehydes and amines. Journal of Polymer Science, Part A: *Polymer Chemistry*. **2016**, 54(14), 2254–2260. https://doi.org/10.1002/pola.28099
52. Nonsuwan, P., Matsugami, A., Hayashi, F., Hyon, S. H., & Matsumura, K. Controlling the degradation of an oxidized dextran-based hydrogel independent of the mechanical properties. *Carbohydrate Polymers*. **2019**, 204, 131–141. https://doi.org/10.1016/j.carbpol.2018.09.081
53. Nonsuwan, P., & Matsumura, K. Amino-Carrageenan@Polydopamine Microcomposites as Initiators for the Degradation of Hydrogel by near-Infrared Irradiation for Controlled Drug Release. *ACS Applied Polymer Materials*. **2019**, 1(2), 286–297. https://doi.org/10.1021/acsapm.8b00209
54. Chimpibul, W., Nakaji-Hirabayashi, T., Yuan, X., & Matsumura, K. Controlling the degradation of cellulose scaffolds with Malaprade oxidation for tissue engineering. *Journal of Materials Chemistry B*. **2020**, 8(35), 7904–7913. https://doi.org/10.1039/d0tb01015d

55. Mo, X., Iwata, H., Matsuda, S., & Ikada, Y. Soft tissue adhesive composed of modified gelatin and polysaccharides. Journal of Biomaterials Science, *Polymer Edition*. **2000**, 11(4), 341–351. https://doi.org/10.1163/156856200743742

56. McGrath, R. Protein measurement by ninhydrin determination of amino acids released by alkaline hydrolysis. *Analytical Biochemistry*. **1972**, 49(1), 95–102. https://doi.org/10.1016/0003-2697(72)90245-X

57. Matsumura, K., & Hyon, S. H. Polyampholytes as low toxic efficient cryoprotective agents with antifreeze protein properties. *Biomaterials*. **2009**, 30(27), 4842–4849. https://doi.org/10.1016/j.biomaterials.2009.05.025

58. Hayashi, T., & Namiki, M. Role of sugar fragmentation in an early stage browning of amino-carbonyl reaction of sugar with amino acid. *Agricultural and Biological Chemistry*. **1986**, 50(8), 1965–1970. https://doi.org/10.1080/00021369.1986.10867692

59. Hodge, J. E. Dehydrated foods, Chemistry of Browning Reactions in Model Systems. *Journal of Agricultural and Food Chemistry*. **1953**, 1(15), 928–943. https://doi.org/10.1021/jf60015a004

60. Wells-Knecht, K. J., Zyzak, V., Litchfield, J. E., Thorpe, S. R., & Baynes, J. W. Mechanism of Autoxidative Glycosylation: Identification of Glyoxal and Arabinose as Intermediates in the Autoxidative Modification of Proteins by Glucose1". *In Biochemistry* (Vol. 34). **1995**. https://pubs.acs.org/sharingguidelines

61. Glomb, M. A., & Monnier, V. M. Mechanism of protein modification by glyoxal and glycolaldehyde, reactive intermediates of the Maillard reaction. *Journal of Biological Chemistry*. **1995**, 270(17), 10017–10026. https://doi.org/10.1074/jbc.270.17.10017

62. Thornalley, P. J. The glyoxalase system in health and disease. *In Molecular Aspects of Medicine*. **1993**, (Vol. 14, Issue 4, pp. 287–371). Pergamon. https://doi.org/10.1016/0098-

2997(93)90002-U

63. Kato, H., Hayase, F., Shin, D. B., Oimomi, M., & Baba, S. 3-Deoxyglucosone, an intermediate product of the Maillard reaction. *Progress in Clinical and Biological Research*. **1989**, 304, 69–84. https://europepmc.org/article/med/2780681
64. Kawakishi, S., Okawa, Y., & Uchida, K. Oxidative Damage of Protein Induced by the Amadori Compound-Copper Ion System. *Journal of Agricultural and Food Chemistry*. **1990**, 38(1), 13–17. https://doi.org/10.1021/jf00091a003
65. Sloan, J. W., Alexander, B. H., Lohmar, R. L., Wolff, I. A., & Rist, C. E. Determination of Dextran Structure by Periodate Oxidation Techniques. *Journal of the American Chemical Society*. **1954**, 76(17), 4429–4434. https://doi.org/10.1021/ja01646a045
66. De Campos Vidal, B., & Mello, M. L. S. Collagen type I amide I band infrared spectroscopy. *Micron*. **2011**, 42(3), 283–289. https://doi.org/10.1016/j.micron.2010.09.010
67. Aalmo, K. M., Grasdalen, H., Painter, T. J., & Krane, J. Characterisation by 1H- and 13C-n.m.r. spectroscopy of the products from oxidation of methyl α- and β-d-galactopyranoside with periodic acid in dimethyl sulphoxide. *Carbohydrate Research*. **1981**, 91(1), 1–11. https://doi.org/10.1016/S0008-6215(00)80985-4
68. Ishak, M. F., & Painter, T. J. Kinetic evidence for hemiacetal formation during the oxidation of dextran in aqueous periodate. *Carbohydrate Research*. **1978**, 64(C), 189–197. https://doi.org/10.1016/S0008-6215(00)83700-3
69. Yu, R. J., & Bishop, C. T. Novel oxidations of methyl glycopyranosides by periodic acid in dimethyl sulfoxide. *Canadian Journal of Chemistry*, **1967**, 45(19), 2195–2203. https://doi.org/10.1139/v67-355
70. Matsumura, K., Hayashi, F., Nagashima, T., & Hyon, S. H. Long-term cryopreservation of human mesenchymal stem cells using carboxylated poly-l-lysine without the addition of

proteins or dimethyl sulfoxide. *Journal of Biomaterials Science*, Polymer Edition, (2013, 24(12), 1484–1497. https://doi.org/10.1080/09205063.2013.771318

71. Tressl, R., Nittka, C., Kersten, E., & Rewicki, D. Formation of Isoleucine-Specific Maillard Products from [1-13C]-d-Glucose and [1-13C]-d-Fructose. *Journal of Agricultural and Food Chemistry*. **1995**, 43(5), 1163–1169. https://doi.org/10.1021/jf00053a009
72. Hiraki, J. Basic and applied studies on ε-polylysine. *Journal of Antibacterial and Antifungal Agents*. **1995**, 23, 349-354.
73. Silverstein, S. C., Steinman, R. M., & Cohn, Z. A. Endocytosis. *In Annual review of biochemistry* (Vol. 46, pp. 669–722). **1977**, Annual Reviews 4139 El Camino Way, P.O. Box 10139, Palo Alto, CA 94303-0139, USA. https://doi.org/10.1146/annurev.bi.46.070177.003321
74. Munechika, K., Sogame, Y., Kishi, N., Kawabata, Y., Ueda, Y., Yamanouchi, K., & Yokoyama, K. Tissue Distribution of Macromolecular Conjugate, Adriamycin Linked to Oxidized Dextran, in Rat and Mouse Bearing Tumor Cells. *Biological and Pharmaceutical Bulletin*. **1994**, 17(9), 1193–1198. https://doi.org/10.1248/bpb.17.1193
75. Hiraki, J., Ichikawa, T., Ninomiya, S. I., Seki, H., Uohama, K., Seki, H., Kimura, S., Yanagimoto, Y., & Barnett, J. W. Use of ADME studies to confirm the safety of ε-polylysine as a preservative in food. *Regulatory Toxicology and Pharmacology*. **2003**, 37(2), 328–340. https://doi.org/10.1016/S0273-2300(03)00029-1

Chapter 3

Evaluation of the optimal dose for maximizing the anti-adhesion performance of a self-degradable dextran-based material

3.1 Introduction

The adhesion of living tissue after a laparotomy occurs in >90% of patients[1,2], and such adhesion can lead to adhesive bowel obstruction. Thus, surgery can be difficult in such patients due to the resulting poor visibility and bleeding during reoperation. This adhesion is also believed to cause many sequelae, including chronic abdominal pain and infertility[3-5]. However, postoperative adhesions can occur not only in the abdomen, but also in other parts of the body, including the heart, teeth, and chest[6-8]. Although the adhesion of biological tissues is an essential aspect of wound healing, adhesion between tissues can lead to various issues, and hence, the use of anti-adhesion materials is desirable[9]. Thus, over recent decades, various anti-adhesive materials composed of biocompatible and biodegradable biomaterials have been developed[10,11]. For example, natural polymers, such as carboxymethylcellulose[12,13], hyaluronic acid[14,15], chitosan[16,17], gelatin[18,19,20], alginic acid[12,21,22], polylactic acid[23,24], polyvinyl alcohol[25,26], polycaprolactone[27], and polyethylene glycol[12] have been described. These anti-adhesion materials are typically used in the form of hydrogels[25,28,29] or films[30,31], although it is also possible to inhibit the adhesion mechanism using drugs[32]. Furthermore, delicate or minimally invasive surgery can be conducted to minimize

the adhesion caused by unnecessary tissue damage[33]. However, the majority of materials reported to date, including drug-loaded anti-adhesion barriers, are not yet ready for clinical use[34].

Currently, numerous anti-adhesion materials are being marketed in Japan, including the Seprafilm (sodium hyaluronate and carboxymethylcellulose) and Interseed (oxidized regenerated cellulose membrane) films, in addition to AdSpray (i.e., *N*-hydroxy succinimide (NHS)-modified carboxymethyl dextrin combined with sodium carbonate/sodium hydrogen carbonate), which forms a hydrogel upon spraying. Although film-type materials have been clinically validated as potential intraperitoneal physical barriers[35], they are extremely complicated to administer through the endoscopic port that is employed in a minimally invasive endoscopic procedure. This is of importance since such interventions are being increasingly employed to reduce patient discomfort[36]; hence, suitable materials must be developed for these applications. Moreover, although spray barriers are widely applicable in diverse surgical procedures, including laparoscopic surgery, they require complicated dissolution procedures[37].

Previously, our group reported a self-degradable adhesive with excellent functionality, named LYDEX, which is based on an aldehyde-functionalized dextran[38-45]. To date, this material has been investigated for various medical applications, including hemostatic agents[46,47], sealants[38,39], and endoscopic wound dressings[48]. Other reports on anti-adhesion materials highlighted that Seprafilm was more effective than Interseed in reducing pleural and intra-abdominal adhesions in a rat model[49,50]. In addition, compared to expanded polytetrafluoroethylene, Seprafilm efficiently reduced posterior sternal adhesions by inhibiting macrophage infiltration and fibrosis progression in a rabbit median sternotomy model[51]. Furthermore, the same model was used to examine whether changes in the composition of LYDEX affect its degradation rate and retention in the posterior sternum. The obtained results indicated that the degradation rate of LYDEX affects the progression of fibrosis in the posterior

sternum[52]. It should be noted here that the purpose of anti-adhesion materials is to act as a physical barrier to block contact between the surgical site and other sites, while also inhibiting fibrous band formation[53]. LYDEX adheres to the tissue through gelation. After gelation, the gel surface loses its adhesive function, although it continues to adhere to the tissue. In other words, LYDEX can form a physical barrier between the surgical site and other sites and act as an anti-adhesive, and thus can be developed into a new anti-adhesive.

In the intraperitoneal cavity, the repair of peritoneal defects caused by surgical operations begins approximately 12 h after surgery, and adhesions are formed mainly by macrophage migration and fibrin deposition over the subsequent 24–36 h[54]. As the degradation rate of LYDEX can be controlled simply by changing its composition[44], it was considered that the design of a suitable formulation could allow for the rapid degradation of LYDEX in the body following initial adhesion formation in the peritoneal defect, thereby reducing the period of excess remnant residue and the risk of infection in the peritoneum. Moreover, although the thickness of a gel is known to play a significant role in determining its degradation rate, no studies have focused on optimizing the thickness (dose) of the LYDEX gel. To address this knowledge gap, the aim of the current study is to investigate the effect of the LYDEX gel dose (film thickness) as a physical barrier in intraperitoneal adhesions using a rabbit-organ adhesion model.

3.2 Material and methods

3.2.1 Materials

ε-Poly-L-lysine (ε-PLL) (4 kDa, 25 wt.% aqueous solution, free base) was procured from JNC (Tokyo, Japan), and dextran (70 kDa) was procured from Meito Sangyo (Nagoya, Japan). Sodium periodate, succinic anhydride (SA), and all other chemicals were procured from

Nacalai Tesque (Kyoto, Japan), while Seprafilm was procured from Kaken Pharmaceutical (Kyoto, Japan). All chemicals and products were used without further purification unless otherwise stated.

3.2.2 Preparation of the aldehyde-functionalized dextran and succinic anhydride-treated ε-poly-L-lysine

Specimens of the aldehyde-functionalized dextran (AD) with oxidant/dextran ratios of 2.5:20, 3.0:20, and 4.0:20 (w/w) were prepared by oxidizing dextran in the presence of sodium periodate according to a previously reported method[55]. Subsequently, the AD was reacted with the primary amino group of ε-PLL at neutral pH to form a hydrogel (Figure 3.1). ε-PLL is a naturally occurring amino acid homopolymer consisting of 25–35 amino groups at the epsilon position and carboxyl groups at the α position of L-lysine, which are linked by amide bonds. Thus, considering the controllable reactivity and low toxicity[56] of succinic anhydride-treated ε-poly-L-lysine (SAPL), this polymer was also synthesized by acylating the ε-PLL amino groups with SA according to a previously reported method[41,57].

(A)

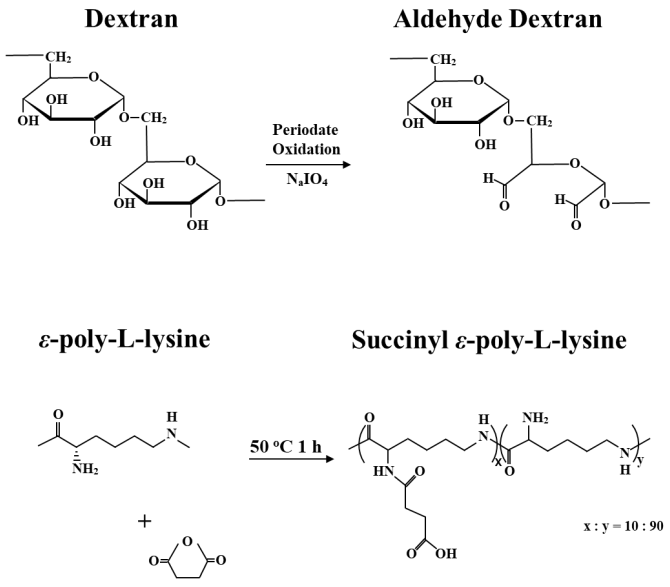

(B)

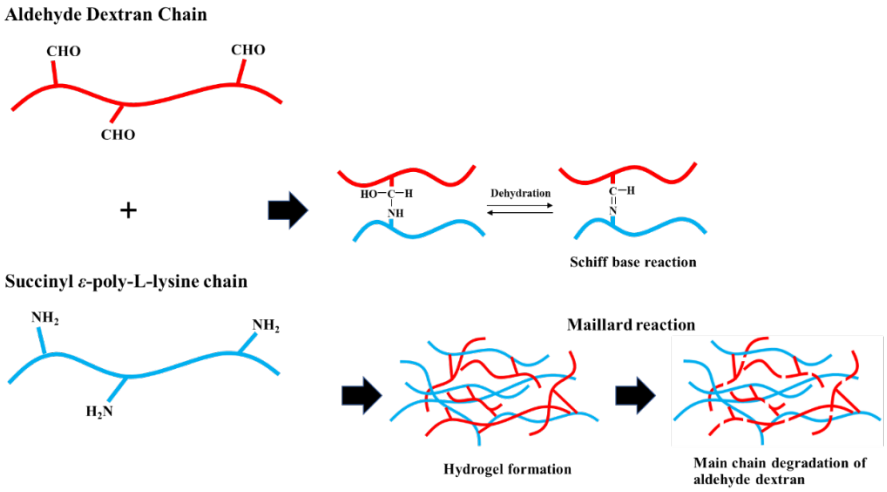

Figure 3.1. (A) Structure of aldehyde dextran and succinyl ε-poly-L-lysine. (B) Schematic of LYDEX hydrogel formation. LYDEX uses sodium periodate to introduce aldehyde groups into dextran, which react with amino groups to form imine bonds (Schiff bases) to form hydrogels. Then, the Maillard reaction cleaves the main chain of AD and degrades.

3.2.3 Characterization of AD and SAPL

3.2.3.1 Determination of the aldehyde and carboxyl group contents

The aldehyde content of AD was evaluated using a simple iodometric titration method according to a previous report[41]. The carboxyl group content of ε-PLL was evaluated by measuring the amount of residual amino groups using the ninhydrin method[58].

3.2.3.2 Evaluation of the hydrogel residue over time

The LYDEX specimen employed herein was composed of 4:1 AD/SAPL (w/w). Thus, to evaluate the hydrogel residue over time, the desired amount of LYDEX powder was placed into the well of a silicon molding plate (diameter = 10 mm; LADD Research Industries, Williston, VT, USA), and three volumes of a saline solution were added (c.f., the weight of LYDEX). After 3 min, the formed hydrogel was removed from the molding plate, placed into a brown glass bottle (30 mL capacity; Nichiden Rika Glass Co. Ltd., Kobe, Japan) containing a saline solution (12 mL), and allowed to degrade while shaking for 1, 7, 14, 28, 60, or 90 d in a water bath shaker (37 °C, 100 rpm). The degraded solution was filtered through a membrane filter (0.45 μm; Advantec Toyo, Tokyo Japan), and the residue was washed with distilled water for injection (~1 mL), dried under reduced pressure at room temperature, and weighed.

3.2.3.3 Measurement of the gel film thickness

LYDEX powder was placed on a base paper (area = 1 cm^2), and three volumes of a saline solution were added (c.f., the weight of LYDEX). After 3 min, the formed hydrogel was split in half with a spatula, and the thickness of the cross section was recorded and analyzed in three dimensions using a digital microscope (VHX-5000, Keyence, Osaka, Japan).

3.2.3.4 Evaluation of the adhesion strengths of LYDEX and Seprafilm

The adhesion strength of the LYDEX hydrogel was compared with that of Seprafilm as outlined in Figure 3.2 and referring to a previously reported method[59]. More specifically, collagen casings (#320; Nippi, Tokyo, Japan) were cut into 170 mm × 45 mm pieces, soaked in water, and stored at 4 °C until measurement. The water on the surface of the treated collagen casing was gently wiped off, the surface was further wiped with ethanol, and the sample was dried at 25 °C for 30 s. For the LYDEX experiments, the powder (40 μg, 2.5:20 AD/SAPL) was added to the adhesive layer of the collagen casing in two even portions, after which a saline solution (240 μL) was added. Subsequently, an additional collagen casing was placed on top of the formed gel with an adhesive area of 30 mm × 45 mm. For the Seprafilm experiments, the Seprafilm specimen was attached to the adhesive layer of the collagen casing dipped in saline, and another collagen casing dipped in saline was placed on top (adhesive area = 30 mm × 45 mm). After placing a weight of ~50 g on top of the prepared specimens for 5 min at 25 °C, their respective adhesion strengths were measured using a precision universal testing machine (AG-X Plus, Shimadzu Corp., Kyoto, Japan). For both the LYDEX and Seprafilm experiments, five specimens were tested and the average bond strength was determined (n = 5).

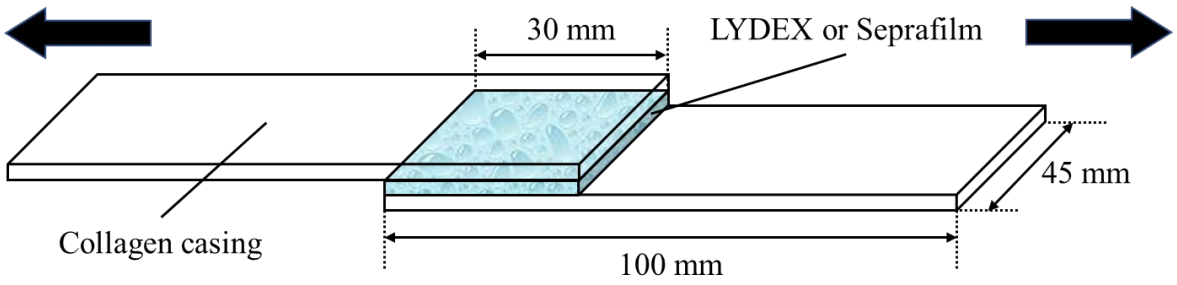

Figure 3.2. Schematic representation of the samples used to measure the bond strength.

3.2.4 *In vivo* evaluation of adhesion prevention

3.2.4.1 Animals

All experiments were performed at the Chitose Laboratory of the Japan Food Analysis Center according to the guidelines of the Animal Welfare Committee. Mature male Japanese white rabbits (>2.5 kg; Kitayama Labes, Co. Ltd., Nagano, Japan) were housed individually in fiber-reinforced polymer cages and kept in a room with a temperature of 20–26 °C and with 12 h/d lighting. The rabbits were fed a limited amount of gamma-irradiated rabbit and guinea pig feed (LRC4, Oriental Yeast Company, Tokyo, Japan) and were allowed to freely drink tap water.

3.2.4.2 Surgical procedure

The test animals were intramuscularly anesthetized with a triple mixture of anesthetics (medetomidine hydrochloride [Dmitol, Nippon Zenyaku Kogyo, Fukushima, Japan]; midazolam [midazolam injection 10 mg “Sandoz,” Sandoz Pharmaceuticals, Tokyo, Japan]; and butorphanol tartrate [Betorphanol, Meiji Seika Pharma, Tokyo, Japan] at a 0.15:2.0:2.0 ratio (mg/mL)). The animals were intramuscularly administered the anesthetic at a dose of 2 mL/kg body weight for general anesthesia.

Subsequently, the abdomen of the rabbit was sheared, and a midline incision of ~10 cm was made through the abdominal skin and wall to expose the colon (from the cecal colostomy to a portion of the colon). The serosa was incised from around the colon string near the cecal colostomy, exposing the muscular layer of the colon with an area of ~1 cm × 2 cm. The exposed area was sutured in two places and was designated as "treatment site 1." The colon, which was approximately 3 cm away from treatment site 1, was treated in the same way as treatment site 1 and designated as "treatment site 2." The fascia of the abdominal wall adjacent to each treatment site was incised and dissected (~7 cm × 6 cm) and designated as "abdominal wall injury site."

Either LYDEX or Seprafilm was applied to one of the treatment sites, and the remaining treatment site was left untreated to serve as a control (Figure 3.3).

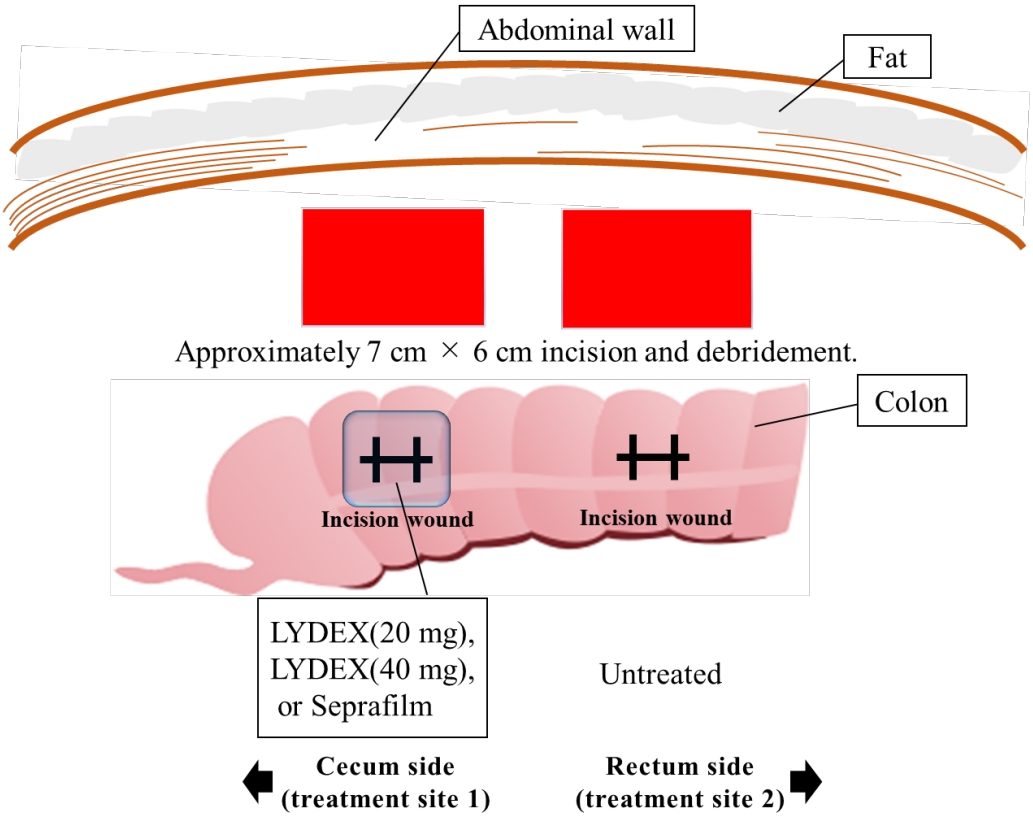

Figure 3.3. Schematic detailing the adhesion model

3.2.4.3 Experimental design

LYDEX prepared using an oxidant/dextran ratio of 2.5:20, which was molecularly designed to have the same degradation period (2 weeks) as the existing anti-adhesion materials, was applied to the animal organ adhesion models, and its anti-adhesion effect was compared with that of Seprafilm. Rabbits were used as the organ adhesion model because multiple treatments on the same organ are possible. To explore the possibility of application in the field of gastrointestinal surgery, the colon was selected as the treatment organ. The application period was 4 weeks, and

each group consisted of 8 animals.

Thus, LYDEX was applied to an area of ~4 cm × 2 cm to completely cover the treated area (~2 cm × 1 cm), and the amount of powder applied was either 20 or 40 mg/cm^2. After application, the samples were sprayed with water and allowed to gel for ~2 min. For the Seprafilm experiments, this specimen was applied to completely cover the treated area, and ~4 cm × 5 cm of Seprafilm was wrapped around the colon. To maintain contact between the treatment and abdominal wall injury sites, the exposed colon was returned to its original position. Subsequently, a colon string ~1 cm away from treatment site 1 on the cecal colostomy side and another ~1 cm away from treatment site 2 on the rectal side were gently fixed to the abdominal wall injury site using sutures. At the end of the application period, the treated area was observed for abnormalities. The evaluation criteria for adhesions (Table 1) were established with reference to previous studies[49,50], and the degree of adhesion was scored according to the area and strength of adhesion. The degree of adhesion was evaluated as the sum of the grades indicating the extent and intensity of adhesion (maximum score 8). The mean degree of adhesion was calculated as the average of n = 8 cases based on the indicators listed in Table 3.1.

Table 3.1. Evaluation criteria for adhesion

Extent of Adhesion	**Strength of Adhesion**
0: No adhesion	0: No adhesion
1: Adhesion over 1/4 of the treated area	1: Thin film separable by blunt dissection
2: Adhesion over 1/2 of the treated area	2: Less than 50% of the treated area needs to be
3: Adhesion over 3/4 of the treated area	3: More than 50% of the treated area needs to be
4: Adhesion over all of the treated area	4: All of the treated area needs to be dissected

3.2.4.4 Histopathological examinations

A portion of the treated area was removed, sectioned, and fixed in a 10% neutral buffered formalin solution. The sections were then embedded in paraffin, and thin sections were prepared. Histopathological specimens were prepared by hematoxylin and eosin (HE), periodic acid Schiff (PAS), and Masson trichrome (MT) staining. PAS staining was used only for the evaluation of residual LYDEX because it is a test method for the detection of polysaccharides. In contrast, MT staining is employed for detecting collagen fibers. The prepared histopathological specimens were observed under an optical microscope, and the parameters related to adhesion (HE staining); the residual specimen (HE staining, PAS staining); fibrosis (HE staining, PAS staining); and cell invasion (HE staining) were histopathologically evaluated. The residual organs were stored in a 10% neutral buffered formalin solution.

3.2.4.5 Statistical analysis

All statistical analyses of the recorded data were performed using a Microsoft Excel statistical software package (BellCurve for Excel, Social Survey Research Information Co., Ltd., Tokyo, Japan). All data were expressed as mean ± standard deviation (SD). Student's t-test was used for comparison between two groups, while one-way analysis of variance (ANOVA) with a post-hoc Tukey–Kramer test was used for comparison between more than three groups, based on the report by Takai et al.[52]. Statistical significance was defined at the $P < 0.05$ level.

3.3 Results and discussion

3.3.1 Characterization of AD and SAPL

To prepare different compositions of AD, dextran was oxidized by sodium periodate using predetermined amounts of these reagents to obtain oxidant/dextran ratios of 2.5:20, 3.0:20,

and 4.0:20 (w/w). The aldehyde contents of the three AD samples were determined by titration with iodine, and it was confirmed that AD specimens with aldehyde contents of 0.28, 0.30, and 0.40 mol/aldehyde glucose unit were obtained. Subsequently, to control the reactivity with AD, a few of the amino groups of ε-PLL were acylated by the introduction of COOH groups upon reaction with SA. To produce SAPL, a predetermined amount of SA was added to achieve 10 ± 5 mol% succinylation. The results of a ninhydrin assay indicated that the product contained the intended SA content for a succinylation degree of <12 mol%. These results are consistent with those of previous studies[41,43]; hence, the corresponding materials were selected for use in subsequent experiments owing to the adequate degradability properties of the obtained polymer.

3.3.2 Gel degradation over time

As described above, three LYDEX gel specimens were prepared using the prepared AD and SAPL samples with aldehyde contents of 0.28, 0.30, and 0.40, and their degradation processes were observed (Figure 3.4). As indicated, a higher aldehyde ratio resulted in a longer gel degradation time, which is consistent with previous findings[43]. After the aldehyde group of AD and the amino group of SAPL form a Schiff base, the main chain (1,6-glycosidic bond) of AD becomes unstable due to occurrence of the Maillard reaction (Amadori transition) and molecular degradation begins[42]. It is speculated that a high ratio of aldehyde groups in AD increases the number of cross-linking points between AD and SAPL, thereby maintaining the gel structure even if the Schiff bases are degraded to a slight extent. More specifically, the gel disappeared after 7 d for an aldehyde ratio of 0.28 and after ~30 d for an aldehyde ratio of 0.30, while ~18% of the gel remained after ~90 d for an aldehyde ratio of 0.40. In comparison, it should be noted that Seprafilm is advertised to act as a wound barrier for ~7 d[53]. Thus, although the test conditions employed in this study provided a harsher environment than those found in the intraperitoneal

region, I decided to use the LYDEX gel with an aldehyde ratio of 0.28 (i.e., prepared using an oxidant/dextran ratio of 2.5:20) owing to its ability to completely degrade within 7 d.

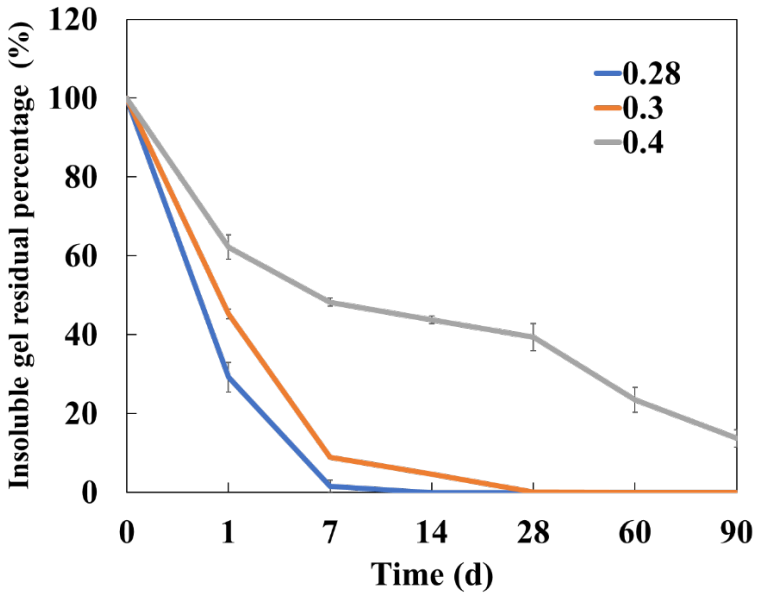

Figure 3.4. Residual fraction of the LYDEX gel over time as a function of the aldehyde content in the AD.

3.3.3 Effect of the film thickness on degradation

To evaluate how the dose (film thickness) of the LYDEX gel affects its performance as a physical barrier to adhesion, I investigated the degradation processes of 20, 40, and 60 mg/cm^2 LYDEX gel films (2.5:20 oxidant/dextran ratio) over 28 d (Figure 3.5). It was observed that the 20 and 40 mg/cm^2 gels underwent full degradation within ~1 and 3 d, respectively, while for a dose of 60 mg/cm^2, 2.2% of the gel remained after 14 d. These results therefore indicate that the degradation time increased with increasing gel thickness (or an increased dose). Digital microscopy (VHX-5,000, Keyence, Osaka, Japan) indicated that the thicknesses of the gels produced using 20, 40, and 60 mg/cm^2 doses of this LYDEX gel were 860, 1,520, and 2,010 μm, respectively (Figure 3.6).

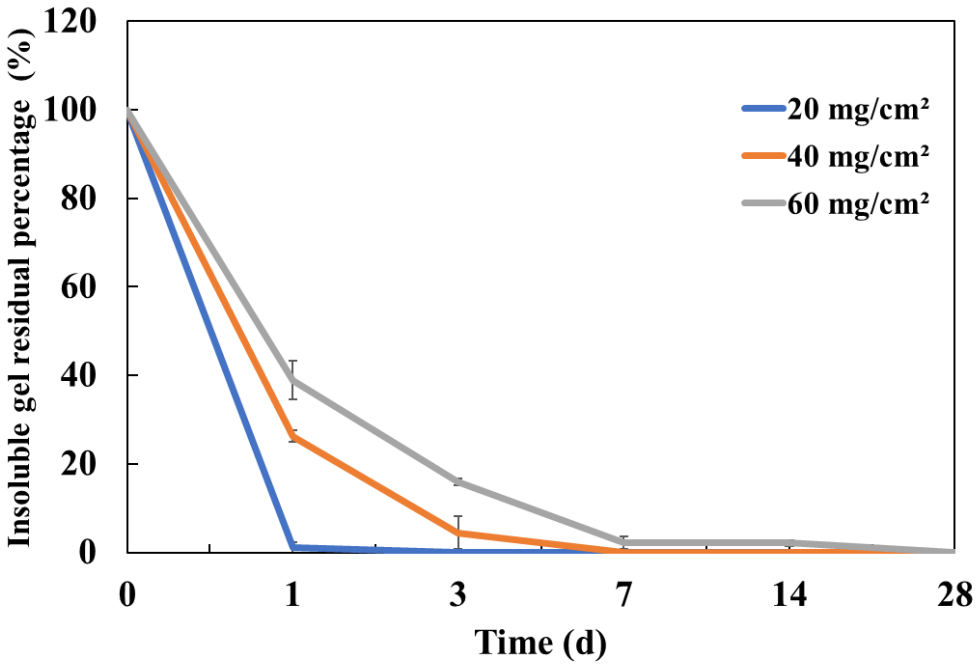

Figure 3.5. Amounts of residual LYDEX gel present over time for the three gel doses (or gel thicknesses).

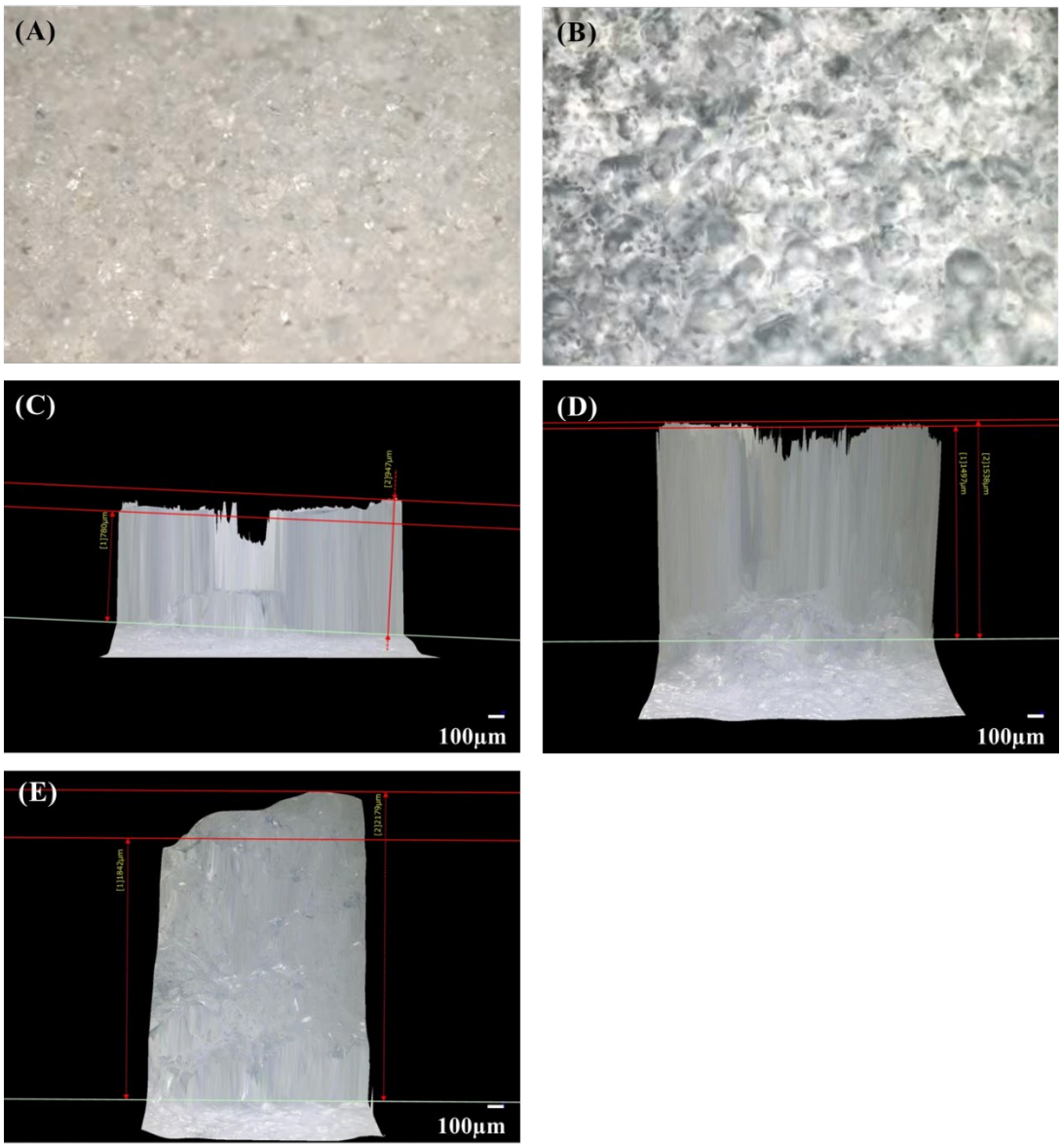

Figure 3.6. Morphologies and film thicknesses of the LYDEX gel films. (A) LYDEX powder, (B) immediately after gelation, and with (C) 20, (D) 40, (E) and 60 mg/cm^2 doses of the LYDEX gel.

3.3.4 Adhesive strengths of LYDEX and Seprafilm

Seprafilm does not require suture fixation owing to its high adhesion strength toward wet tissue; furthermore, LYDEX adheres to wet tissue in a similar manner. Thus, using a collagen casing sheet, the adhesive strengths of LYDEX and Seprafilm were measured in terms of their tensile shear strengths of bonding to evaluate whether the adhesion strength is suitable for an anti-adhesion material. Ideally, the adhesive strength should be sufficiently high to prevent displacement when it is applied to the affected area. Seprafilm was used in the sheet form, and LYDEX was used in the form of a powder (2.5:20 oxidant/dextran ratio). The results are presented in Table 3.2. More specifically, the average adhesion strength of Seprafilm was determined to be 550.07 ± 23.88 gf (n = 5), while that of LYDEX was 905.43 ± 93.21 gf ($p < 0.01$), i.e., 1.64 times stronger than that of Seprafilm. In addition, our results indicated that the LYDEX film was 10 times stronger than the fibrin glue used as a surgical adhesive in a previous study[41], thereby indicating the suitability of LYDEX for application to wet surfaces such as soft tissues. Moreover, it should be noted that the reactivities of the amino and aldehyde groups in SAPL are relatively high[41], and it is unlikely that the AD reacted with the collagen molecules during measurement.

Table 3.2. Shearing bond strengths of LYDEX and Seprafilm toward swollen collagen sheets at 25 ℃

Adhesive	***Shearing Bonding Strength (gf)***					***Average ± SD (gf)***
LYDEX	922.74	857.02	923.19	1054.21	769.98	905.43 ± 93.21***
Seprafilm	588.59	515.14	554.77	539.20	552.65	550.07 ± 23.88

Different from Seprafilm at *** $p < 0.01$.

3.3.5 Animal experiments

To evaluate how the dose (film thickness) of the LYDEX gel affects its performance as a physical barrier, I created an animal model of abdominal wall injury and colostomy in rabbits and compared the use of Seprafilm with different doses of LYDEX (20 and 40 mg/cm^2). Based on preliminary animal studies showing sufficient anti-adhesion efficacies at 40 mg/cm^2, in addition to different cytotoxicity results[41] and membrane thickness results (Figure 3.6), I selected doses of 20 and 40 mg/cm^2 for investigation. As shown in Figure 3.7, our initial observations indicated that compared to the Seprafilm treatment group (Figure 3.7(A)), a similar degree of adhesion inhibition was observed in the 20 mg/cm^2 LYDEX treatment group (Figure 3.7(B)), while a higher degree of adhesion inhibition was found in the 40 mg/cm^2 LYDEX treatment group (Figure 3.7(C)). No noteworthy changes other than the presence or absence of adhesions were observed at the treated sites in either group. In the anti-adhesion efficacy study, 4 out of 8 cases (50%) showed no adhesions at the Seprafilm-treated site (mean degree of adhesion = 2.1). Similarly, in the 20 mg/cm^2 LYDEX treatment group, no adhesions were observed in 4 out of 8 cases (50%) (mean degree of adhesion = 1.3), indicating that the anti-adhesion effect was similar to that of the Seprafilm group. Moreover, in the 40 mg/cm^2 LYDEX group, adhesions were observed in only 1 out of 7 cases (14%) (mean degree of adhesion = 0.4), indicating superior anti-adhesion performance at this higher dosage [$P < 0.01$ (Seprafilm vs Control), $P < 0.01$ (LYDEX 20 mg/cm^2 vs Control), $P < 0.01$ (LYDEX 40 mg/cm^2 vs Control)]. It should be noted here that the anti-adhesion mechanism is important when considering the use of such a material as a physical barrier between a surgical site and other organs until tissue healing is complete. As presented in Table 3.3 and Figure 3.8, our results indicated that a higher dose resulted in a lower degree of adhesion.

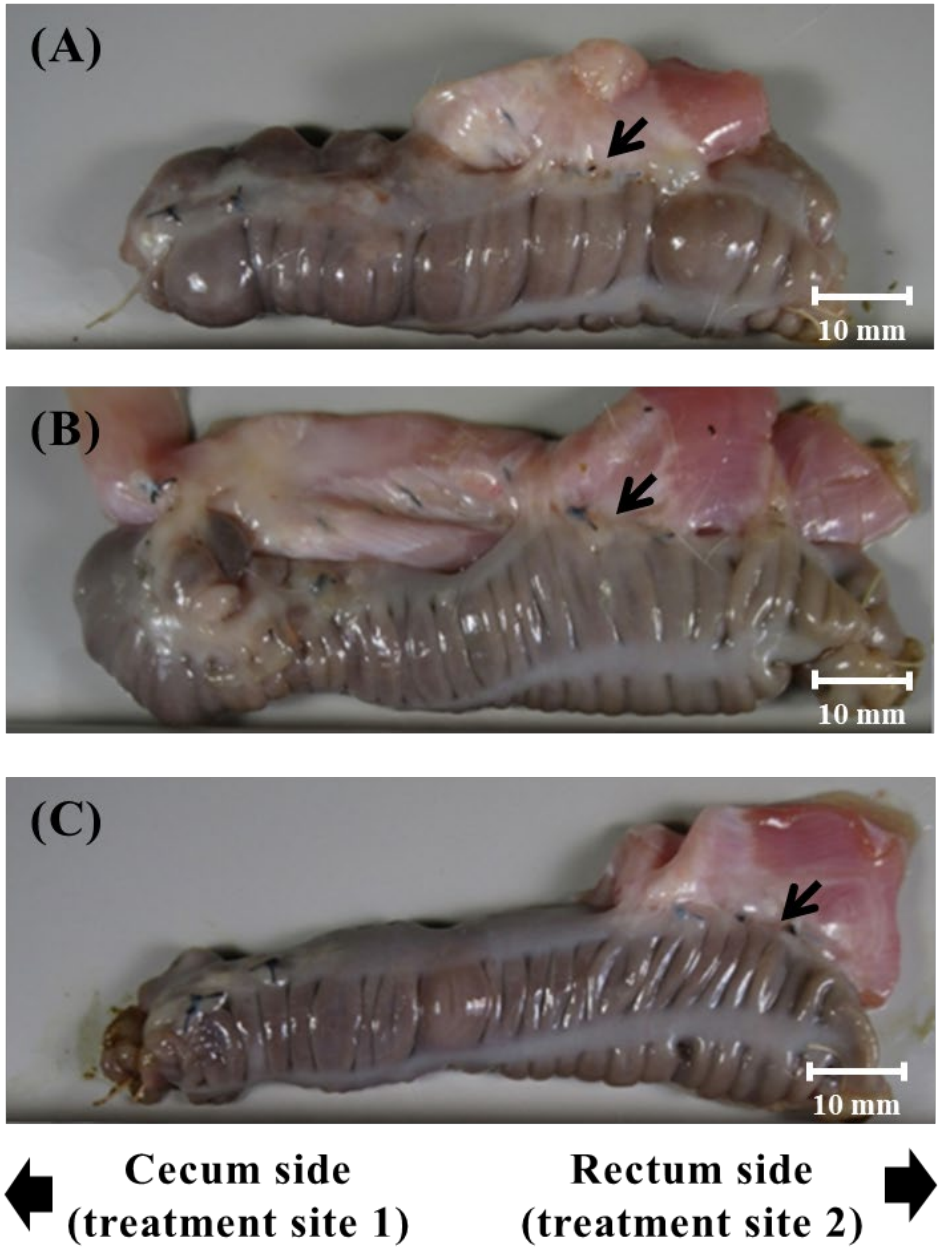

Figure 3.7. Gross observation images. The cecum side (treatment site 1) corresponds to the specimen application site, and the rectal side (treatment site 2) is the control site. Adhesion between the treated control site and the abdominal wall is indicated by arrows. (A) Seprafilm, (B) LYDEX, 20 mg/cm^2, and (C) LYDEX, 40 mg/cm^2.

Table 3.3. Summary of the degrees of adhesion

	Treatment control site	LYDEX or Seprafilm application site
LYDEX (40 mg)	7/7 [a)] (7.1)	1/7 [a)] (0.4)
LYDEX (20 mg)	8/8 (7.4)	4/8 (1.3)
Seprafilm	8/8 (7.4)	4/8 (2.1)

Results are expressed as the number of animals with adhesions/total number of animals, with the mean degree of adhesion for each group being shown in parentheses. [a)] To properly evaluate the anti-adhesion effect, the gross and histopathological examination results obtained for one case in the LYDEX (40 mg) group were excluded from the evaluation. The animal in question showed no adhesions at the treated control site on gross examination. Therefore, the total number of animals was 7.

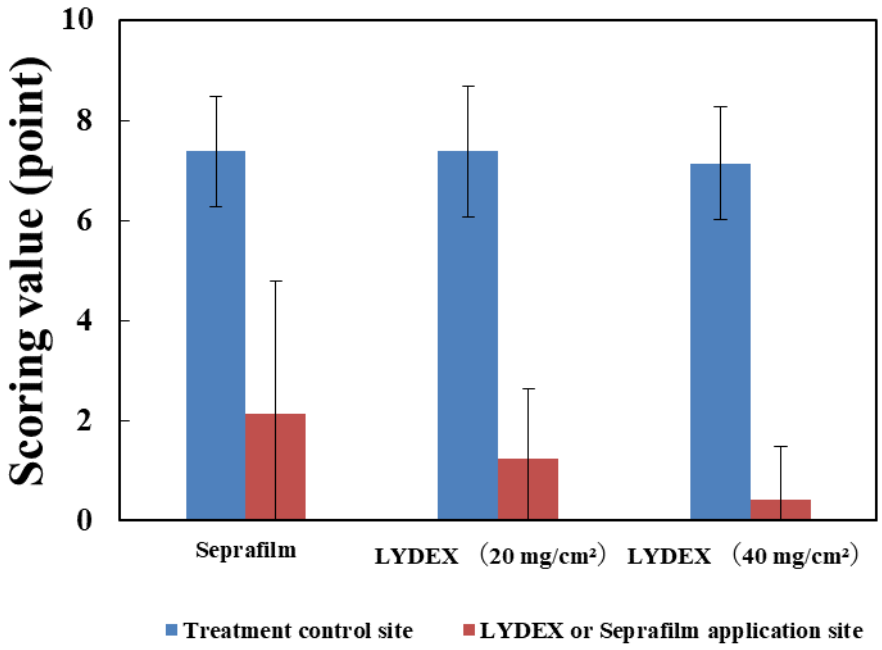

Figure 3.8. Mean values of the degree of adhesion. The number of animals used in each group was 8. In one case (LYDEX, 40 mg/cm^2), no adhesion was observed at the control site, and hence, the total number of animals was 7. *P < 0.01.

As shown in Figure 3.9, the histopathology results were consistent with the gross examination results in the cases where histopathologic adhesions were observed. In the 40 mg/cm^2 LYDEX treatment group, mild adhesions were observed in 1 of the 7 sites and not in the remaining 6 sites. Fibrosis was also absent in 2 of the 6 sites and was only slightly present in the remaining 5 sites. In the 20 mg/cm^2 LYDEX treatment group, slight-to-mild adhesions were observed in 4 of the 8 sites, and no adhesions were observed in the remaining 4 sites. One site showed no fibrosis, and the remaining 7 sites showed only slight fibrosis. No LYDEX (PAS-positive) remained at these sites. In the Seprafilm treatment group, slight-to-moderate adhesions were observed in 4 of the 8 sites, and no adhesions were observed in the remaining 4 sites. In the

20 mg/cm^2 LYDEX, 40 mg/cm^2 LYDEX, and Seprafilm treatment groups, macrophage infiltration was observed at the treated sites, and no inflammatory cell infiltration was detected, thereby suggesting that neither LYDEX nor the approved product exhibited inflammatory properties.

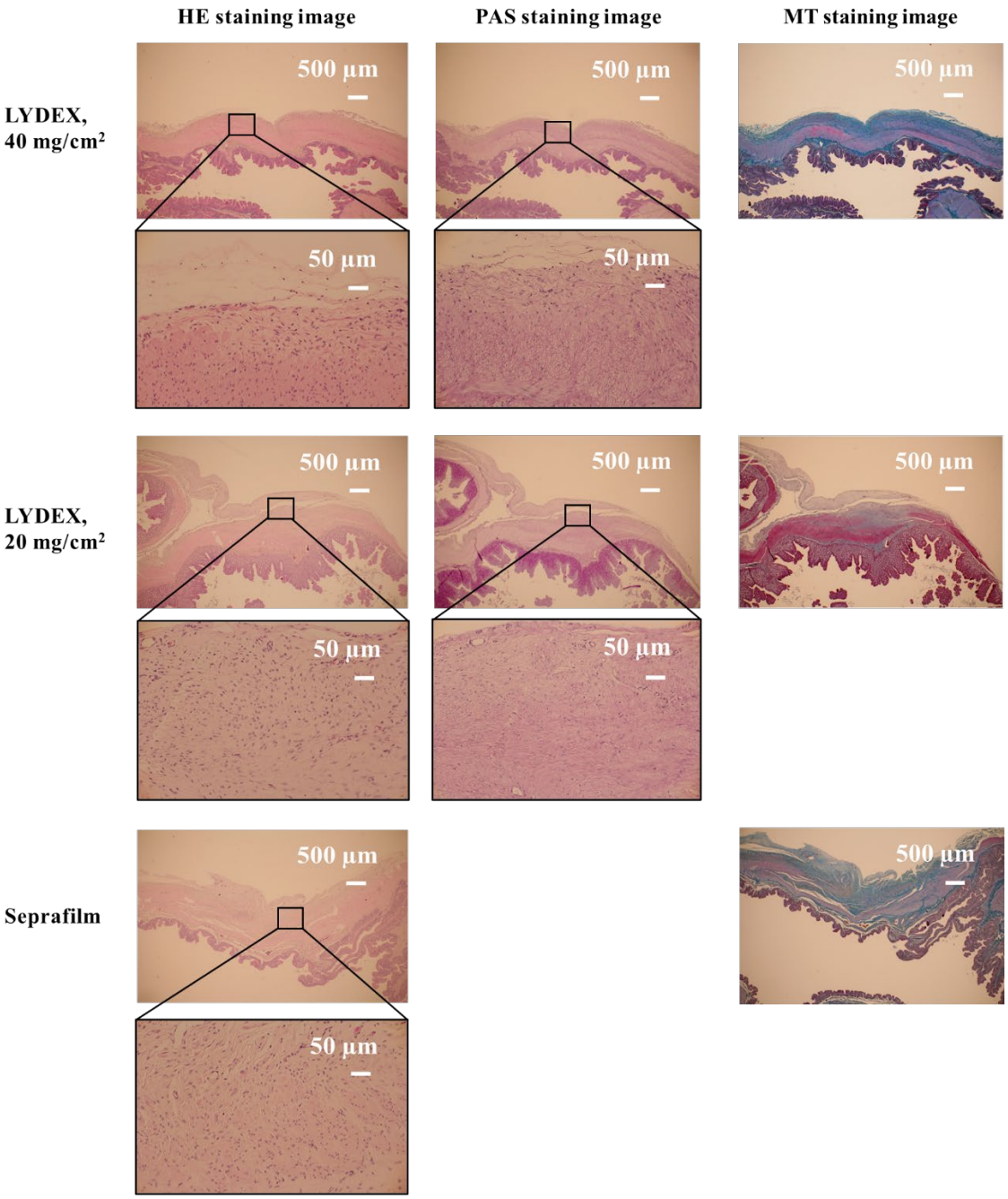

Figure 3.9. Images of the areas treated with LYDEX and Seprafilm after HE, PAS, and MT staining. The insets show enlarged views of the framed areas.

3.4 Conclusions

Postoperative adhesions are a common complication; hence, various anti-adhesive materials, such as Seprafilm, have been developed in recent years to prevent adhesions between surgical sites and their adjacent tissues[60]. However, only a few materials have been proven to be safe and effective in clinical trials[35,37,61,62]. In this study, to further investigate the application of LYDEX, which has already been shown to be effective in preventing adhesions, I used a rabbit-organ adhesion model to examine how the dose (film thickness) of the LYDEX gel affects its application as a physical barrier in intraperitoneal adhesions.

LYDEX is a self-degrading adhesive that degrades via the Maillard reaction, and its degradation rate can be easily controlled by varying the oxidant/dextran ratio employed for the preparation of AD[41]. Such polysaccharide materials have been studied for use in drug delivery and tissue engineering scaffolds owing to their degradability and biocompatibility[10,63-65]. As shown in Figure 3.4, the degradation period varied depending on the aldehyde ratio, and it was newly revealed in this study that the degradation rate of the gel also depends on the film thickness (Figure 3.5). It should also be noted that *in vivo*, 40 mg of the LYDEX gel (oxidant/dextran ratio = 2.5:20) was significantly more effective in preventing adhesions than the commonly employed anti-adhesion membrane, Seprafilm (Figure 3.8). These results suggest that the degradation rate can be more broadly tailored to the indicated site by considering both the aldehyde ratio and gel film thickness.

During laparoscopic surgery, which is a minimally invasive procedure that is rapidly replacing open abdominal surgery, the administration of sheet-type anti-adhesive materials through the endoscope port is extremely challenging. Therefore, hydrogels have been developed for many non-sheet-type anti-adhesion applications. However, the low tensile strengths of hydrogels limit their use in load-bearing applications and may lead to the premature dissolution

or leakage of the hydrogels from the target site[66]. In contrast, our developed LYDEX powder immediately forms a gel in the presence of water via Schiff base formation, resulting in strong adhesion. After gelation, it becomes a physical barrier between the injured site and the surrounding organs, in addition to exerting an anti-adhesion effect. In addition, its rapid solidification (within ~2 min) [50] may overcome the limitations of other hydrogels. Furthermore, as the powder is sprayed onto the targeted area and subsequently subjected to gelation, it forms an adhesion barrier on any regular or irregular surface and can be sprayed into deep sites or under the incision wounds of the abdominal wall. Importantly, it should be noted that conventional sheet-type anti-adhesion materials cannot be evenly applied to uneven surfaces.

Recently, AdSpray (Terumo Corporation, Tokyo), which consists of (NHS)-modified carboxymethyl dextrin and sodium carbonate/sodium hydrogen carbonate, has been clinically used as a spray-type bioabsorbable anti-adhesive system[37,54]. In this system, the two powders are dissolved in distilled water for injection under vigorous shaking, loaded into a syringe, and mixed with compressed air; however, this preparation process is complex. In contrast, LYDEX powder is superior in the context of laparoscopic surgery because AD and SAPL do not react when mixed in the absence of moisture; hence, the two components can be first combined in a single vial and then placed in a special applicator for use[50]. It should be noted that to promote the clinical application of such systems, it is important to obtain unlimited coverage of the target peritoneum for both open and laparoscopic surgeries. In addition, the anti-adhesion material should be biodegradable and biocompatible, as it is no longer needed once the objective is achieved[67,68].

The intraperitoneal repair of peritoneal defects caused by surgical manipulation begins approximately 12 h after surgery, wherein the mesothelial cells and fibroblasts begin to cover the affected area. On the third day, macrophages infiltrate the tissue, and as the lesion regresses, the mesothelial layer reforms and covers the lesion by days 7–10[69,70]. At the same time, adhesions are

mainly formed by macrophage migration and by the deposition of inflammatory exudates composed of fibrin matrix over a period of 24–36 h[54]. Considering these mechanisms of peritoneal repair, adhesion, and development, a material that covers the peritoneal defect for approximately one week without causing an inflammatory reaction and is absorbed *in vivo* after peritoneum repair would be useful in preventing adhesion. In this context, I note that AdSpray is intraperitoneally absorbed after ~3 d[54], while Seprafilm acts as a wound barrier for ~7 d after adhering to the moist tissue. The latter is therefore more suitable in the context of its biodegradation, and hence, it was considered reasonable to select LYDEX (oxidant/dextran ratio = 2.5:20) for investigation owing to its ability to undergo biodegradation within 7 d.

Furthermore, it has been reported that dextran exhibits an anti-adhesive effect by regulating immune cells[71], and since no infiltration of inflammatory cells was observed at LYDEX doses of 20 or 40 mg/cm^2 (Figure 3.9), it was inferred that AD has the same effect. Therefore, LYDEX can be considered suitable for use as an anti-adhesive material from the viewpoints of its biodegradability, adhesiveness, and anti-inflammatory properties. Furthermore, as LYDEX has been reported to exhibit potential for use as a base material for drug delivery systems, it may be even more effective when loaded with anti-inflammatory agents[72,73], which are known to possess anti-adhesion effects.

In the context of biocompatibility, it was previously demonstrated that the degradation products of LYDEX undergo a Maillard reaction and a subsequent degradation process, followed by molecular degradation *in vivo* via phagocytosis by phagocytes such as macrophages[42] (Figure 3.9). In general, it is necessary to evaluate the *in vivo* degradation and absorption of the degradation products after phagocytosis by labeling with radioisotopes. However, as the smallest components of AD and SAPL are sugars and amino acids, which are utilized *in vivo*, the degradation products may be widely distributed *in vivo* for a long period of time.

Finally, in this study into the optimal dose (film thickness) of LYDEX for achieving a suitable anti-adhesion performance for *in vivo* applications, it was found that the thickness of the gel film affects the degradation period and anti-adhesion efficacy. Overall, our observations suggest that it is possible to design LYDEX-based films for use at a wide range of *in vivo* application sites. These results present in this study are therefore expected to promote the clinical application of this novel anti-adhesive material that exhibits both hemostatic and sealant performances, thereby rendering LYDEX an extremely versatile material for applications that have not previously been possible using other anti-adhesion products. The application of LYDEX as an anti-adhesive material is not limited to the abdominal field, and currently, our group is also researching its potential in the field of ophthalmology. Furthermore, as a new field, our group has begun research and development into the application of LYDEX in the field of regenerative medicine, and our group aims to realize the clinical application of LYDEX in various fields as soon as possible.

3.5 References

1. Menzies, D., Frcs, M. B., Registrar, S., Ellis, H., Dm, C., & Frcs, M. Intestinal obstruction from adhesions--how big is the problem? *Annals of The Royal College of Surgeons of England*. **1990**, *72*(1), 60. /pmc/articles/PMC2499092/?report=abstract
2. Okabayashi, K., Ashrafian, H., Zacharakis, E., Hasegawa, H., Kitagawa, Y., Athanasiou, T., & Darzi, A. Adhesions after abdominal surgery: A systematic review of the incidence, distribution and severity. *Surgery Today*. **2014**, *44*(3), 405–420. https://doi.org/10.1007/S00595-013-0591-8/TABLES/2
3. Kamel, R. M. Prevention of postoperative peritoneal adhesions. *European Journal of Obstetrics & Gynecology and Reproductive Biology*. **2010**, *150*(2), 111–118. https://doi.org/10.1016/J.EJOGRB.2010.02.003
4. Ouaïssi, M., Gaujoux, S., Veyrie, N., Denève, E., Brigand, C., Castel, B., Duron, J. J., Rault, A., Slim, K., & Nocca, D. Post-operative adhesions after digestive surgery: Their incidence and prevention: Review of the literature. *Journal de Chirurgie Viscerale*. **2012**, *149*(2), 114–126. https://doi.org/10.1016/J.JVISCSURG.2011.11.006
5. van Goor, H. Consequences and complications of peritoneal adhesions. *Colorectal Disease*, *9*(SUPPL. 2). **2007**, 25–34. https://doi.org/10.1111/J.1463-1318.2007.01358.X
6. Ayed, A. K., Chandrasekaran, C., & Sukumar, M. Video-assisted thoracoscopic surgery for primary spontaneous pneumothorax: clinicopathological correlation. *European Journal of Cardio-Thoracic Surgery : Official Journal of the European Association for Cardio-Thoracic Surgery*. **2006**, *29*(2), 221–225. https://doi.org/10.1016/J.EJCTS.2005.11.005
7. Nkere, U. U. Postoperative adhesion formation and the use of adhesion preventing techniques in cardiac and general surgery. *ASAIO Journal (American Society for Artificial Internal Organs : 1992)*. **2000**, *46*(6), 654–656. https://doi.org/10.1097/00002480-200011000-00003

8. Songer, M. N., Ghosh, L., & Spencer, D. L. Effects of sodium hyaluronate on peridural fibrosis after lumbar laminotomy and discectomy. *Spine*. **1990**, *15*(6), 550–554. https://doi.org/10.1097/00007632-199006000-00022

9. Lin, L. X., Yuan, F., Zhang, H. H., Liao, N. N., Luo, J. W., & Sun, Y. L. Evaluation of surgical anti-adhesion products to reduce postsurgical intra-abdominal adhesion formation in a rat model. *PLOS ONE*. **2017**, *12*(2), e0172088. https://doi.org/10.1371/JOURNAL.PONE.0172088

10. Matsumura, K., & Rajan, R. Oxidized Polysaccharides as Green and Sustainable Biomaterials. *Current Organic Chemistry*. **2021**, *25*(13), 1483–1496. https://doi.org/10.2174/1385272825666210428140052

11. Siswomihardjo, W. Biocompatibility issues of biomaterials. *Advanced Structured Materials*, **2016**, *58*, 41–65. https://doi.org/10.1007/978-3-319-14845-8_3

12. Baek, S., Park, H., Park, Y., Kang, H., & Lee, D. Development of a Lidocaine-Loaded Alginate/CMC/PEO Electrospun Nanofiber Film and Application as an Anti-Adhesion Barrier. *Polymers 2020.* **2020**, *Vol. 12, Page 618*, *12*(3), 618. https://doi.org/10.3390/POLYM12030618

13. Çipe, G., Köksal, H. M., Yildirim, S., Celayir, M. F., & Baykan, A. Efficacy of hyaluronic acid - carboxymethyl cellulose membrane (Seprafilm (R)) and polylactic acid barrier film (Surgiwrap (TM)) for the prevention of adhesions after thyroid surgery: an experimental model. *TURKISH JOURNAL OF MEDICAL SCIENCES*. **2011**, *41*(1), 73–79. https://doi.org/10.3906/SAG-0911-400

14. Jeong, J. Y., Chung, P. K., & Yoo, J. C. Effect of sodium hyaluronate/ carboxymethyl cellulose (Guardix-sol) on retear rate and postoperative stiffness in arthroscopic rotator cuff repair patients: A prospective cohort study. *Journal of Orthopaedic Surgery*. **2017**, *25*(2).

https://doi.org/10.1177/2309499017718908

15. Yeul Ji, G., Hyun Oh, C., Gwan Moon, B., Yi, S., Bo Han, I., Hwa Heo, D., Kim, K.-T., Ah Shin, D., Nyun Kim, K., & Author, C. Efficacy and Safety of Sodium Hyaluronate with 1,4-Butanediol Diglycidyl Ether Compared to Sodium Carboxymethylcellulose in Preventing Adhesion Formation after Lumbar Discectomy. *Korean Journal of Spine*. **2015**, *12*(2), 41–47. https://doi.org/10.14245/KJS.2015.12.2.41
16. Chang, J. J., Lee, Y. H., Wu, M. H., Yang, M. C., & Chien, C. T. Electrospun anti-adhesion barrier made of chitosan alginate for reducing peritoneal adhesions. *Carbohydrate Polymers*. **2012**, *88*(4), 1304–1312. https://doi.org/10.1016/J.CARBPOL.2012.02.011
17. Chen, C. H., Chen, S. H., Mao, S. H., Tsai, M. J., Chou, P. Y., Liao, C. H., & Chen, J. P. Injectable thermosensitive hydrogel containing hyaluronic acid and chitosan as a barrier for prevention of postoperative peritoneal adhesion. *Carbohydrate Polymers*. **2017**, *173*, 721–731. https://doi.org/10.1016/J.CARBPOL.2017.06.019
18. Horii, T., Tsujimoto, H., Miyamoto, H., Yamanaka, K., Tanaka, S., Torii, H., Ozamoto, Y., Takamori, H., Nakamachi, E., Ikada, Y., & Hagiwara, A. Physical and biological properties of a novel anti-adhesion material made of thermally cross-linked gelatin film: Investigation of the usefulness as anti-adhesion material. *Journal of Biomedical Materials Research Part B: Applied Biomaterials*. **2018**, *106*(2), 689–696. https://doi.org/10.1002/JBM.B.33880
19. Shahram, E., Sadraie, S. H., Kaka, G., Khoshmohabat, H., Hosseinalipour, M., Panahi, F., & Naimi-Jamal, M. R. Evaluation of chitosan–gelatin films for use as postoperative adhesion barrier in rat cecum model. *International Journal of Surgery*. **2013**, *11*(10), 1097–1102. https://doi.org/10.1016/J.IJSU.2013.09.012
20. Tian, F., Dou, C., Qi, S., Zhao, L., Chen, B., Yan, H., & Zhang, L. Preventive effect of

dexamethasone gelatin sponge on the lumbosacral epidural adhesion. *International Journal of Clinical and Experimental Medicine*. **2015**, *8*(4), 5478. /pmc/articles/PMC4483993/

21. Baek, S., Park, H., Chen, K., Park, H., & Lee, D. Development of an implantable PCL/alginate bilayer scaffold to prevent secondary infections. *Korean Journal of Chemical Engineering*. **2020**, *37*(4), 677–687. https://doi.org/10.1007/S11814-019-0459-8
22. Kim, D., Choi, G. J., Baek, S., Abdullah, A., Jang, S., Hong, S. A., Kim, B. G., Lee, J., Kang, H., & Lee, D. Characterization of anti-adhesion properties of alginate/polyethylene oxide film to reduce postsurgical peritoneal adhesions. *Science of Advanced Materials*. **2017**, *9*(9), 1669–1677. https://doi.org/10.1166/SAM.2017.3166
23. Hinoki, A., Saito, A., Kinoshita, M., Yamamoto, J., Saitoh, D., & Takeoka, S. Polylactic acid nanosheets in prevention of postoperative intestinal adhesion and their effects on bacterial propagation in an experimental model. *The British Journal of Surgery*. **2016**, *103*(6), 692–700. https://doi.org/10.1002/BJS.10122
24. Liu, S., Qin, M., Hu, C., Wu, F., Cui, W., Jin, T., & Fan, C. Tendon healing and anti-adhesion properties of electrospun fibrous membranes containing bFGF loaded nanoparticles. *Biomaterials*. **2013**, *34*(19), 4690–4701. https://doi.org/10.1016/J.BIOMATERIALS.2013.03.026
25. Bae, S. H., Son, S. R., Kumar Sakar, S., Nguyen, T. H., Kim, S. W., Min, Y. K., & Lee, B. T. Evaluation of the potential anti-adhesion effect of the PVA/Gelatin membrane. *Journal of Biomedical Materials Research Part B: Applied Biomaterials*. **2014**, *102*(4), 840–849. https://doi.org/10.1002/JBM.B.33066
26. Qiu, R., Li, J., Sun, D., Li, H., Qian, F., & Wang, L. 20(S)-Ginsenoside Rg3-loaded electrospun membranes to prevent postoperative peritoneal adhesion. *Biomedical Microdevices*. **2019**, *21*(4), 1–11. https://doi.org/10.1007/S10544-019-0425-6/FIGURES/8

27. Fu, S. Z., Li, Z., Fan, J. M., Meng, X. H., Shi, K., Qu, Y., Yang, L. L., Wu, J. B., Fan, J., Luo, F., & Qian, Z. Y. Biodegradable and thermosensitive monomethoxy poly(ethylene glycol)-poly(lactic acid) hydrogel as a barrier for prevention of post-operative abdominal adhesion. *Journal of Biomedical Nanotechnology*. **2014**, *10*(3), 427–435. https://doi.org/10.1166/JBN.2014.1726

28. Bang, S., Lee, E., Ko, Y. G., Kim, W. Il, & Kwon, O. H. Injectable pullulan hydrogel for the prevention of postoperative tissue adhesion. *International Journal of Biological Macromolecules*. **2016**, *87*, 155–162. https://doi.org/10.1016/J.IJBIOMAC.2016.02.026

29. Lauder, C. I. W., Strickland, A., & Maddern, G. J. Use of a Modified Chitosan–Dextran Gel to Prevent Peritoneal Adhesions in a Porcine Hemicolectomy Model. *Journal of Surgical Research*. **2012**, *176*(2), 448–454. https://doi.org/10.1016/J.JSS.2011.10.029

30. Ten Broek, R. P. G., Stommel, M. W. J., Strik, C., Van Laarhoven, C. J. H. M., Keus, F., & Van Goor, H. Benefits and harms of adhesion barriers for abdominal surgery: A systematic review and meta-analysis. *The Lancet*. **2014**, *383*(9911), 48–59. https://doi.org/10.1016/S0140-6736(13)61687-6/ATTACHMENT/23FE39A9-C25F-4BFD-A215-1F6688EAD001/MMC1.PDF

31. Ward, B. C., & Panitch, A. Abdominal Adhesions: Current and Novel Therapies. *Journal of Surgical Research*. **2011**, *165*(1), 91–111. https://doi.org/10.1016/J.JSS.2009.09.015

32. Sandoval, M. A., & Hernandez-Vaquero, D. Preventing peridural fibrosis with nonsteroidal anti-inflammatory drugs. *European Spine Journal*. **2008**, *17*(3), 451. https://doi.org/10.1007/S00586-007-0580-Y

33. Han, E. S., Scheib, S. A., Patzkowsky, K. E., Simpson, K., & Wang, K. C. The sticky business of adhesion prevention in minimally invasive gynecologic surgery. *Current Opinion in Obstetrics and Gynecology*. **2017**, *29*(4), 266–275.

https://doi.org/10.1097/GCO.0000000000000372

34. Imai, A., Takagi, H., Matsunami, K., & Suzuki, N. Non-barrier agents for postoperative adhesion prevention: Clinical and preclinical aspects. *Archives of Gynecology and Obstetrics*. **2010**, *282*(3), 269–275. https://doi.org/10.1007/S00404-010-1423-3/FIGURES/4
35. Diamond, M. P., Bieber, E., Coddington, C., Franklin, R., Grunert, G., Gunn, D., Lotze, E., Rowe, G., Grainger, D., Tjaden, B., Holtz, G., Patton, G., Johns, D. A., Johnson, K., Kettel, M., Morales, A., Leach, R., Blacker, C., & Putman, J. M. Reduction of adhesions after uterine myomectomy by Seprafilm membrane (HAL-F): a blinded, prospective, randomized, multicenter clinical study. *Fertility and Sterility*. **1996**, *66*(6), 904–910. https://doi.org/10.1016/S0015-0282(16)58716-0
36. Tsapanos, V. S., Stathopoulou, L. P., Papathanassopoulou, V. S., & Tzingounis, V. A. The role of Seprafilm™ bioresorbable membrane in the prevention and therapy of endometrial synechiae. *Journal of Biomedical Materials Research: An Official Journal of The Society for Biomaterials, The Japanese Society for Biomaterials, and The Australian Society for Biomaterials and the Korean Society for Biomaterials*. **2002**, *63*(1), 10–14.
37. Suto, T., Watanabe, M., Endo, T., Komori, K., Ohue, M., Kanemitsu, Y., Itou, M., Takii, Y., Yatsuoka, T., Shiozawa, M., Kinugasa, T., Ueno, H., Takayama, T., Masaki, T., Masuko, H., Horie, H., & Inomata, M. The Primary Result of Prospective Randomized Multicenter Trial of New Spray-Type Bio-absorbable Adhesion Barrier System (TCD-11091) Against Postoperative Adhesion Formation. *Journal of Gastrointestinal Surgery*. **2017**, *21*(10), 1683–1691. https://doi.org/10.1007/S11605-017-3503-1/TABLES/5
38. Araki, M., Tao, H., Nakajima, N., Sugai, H., Sato, T., Hyon, S. H., Nagayasu, T., & Nakamura, T. Development of new biodegradable hydrogel glue for preventing alveolar air leakage. *Journal of Thoracic and Cardiovascular Surgery*. **2007**,134(5), 1241–1248.

https://doi.org/10.1016/j.jtcvs.2007.07.020

39. Araki, M., Tao, H., Sato, T., Nakajima, N., Sugai, H., Hyon, S. H., Nagayasu, T., & Nakamura, T. Creation of a uniform pleural defect model for the study of lung sealants. *Journal of Thoracic and Cardiovascular Surgery*. **2007**, *134*(1), 145–151. https://doi.org/10.1016/j.jtcvs.2007.01.007

40. 40 39. Chimpibul, W., Nagashima, T., Hayashi, F., Nakajima, N., Hyon, S. H., & Matsumura, K. Dextran oxidized by a malaprade reaction shows main chain scission through a maillard reaction triggered by schiff base formation between aldehydes and amines. *Journal of Polymer Science, Part A: Polymer Chemistry*. **2016**, *54*(14), 2254–2260. https://doi.org/10.1002/pola.28099

41. Hyon, S. H., Nakajima, N., Sugai, H., & Matsumura, K. Low cytotoxic tissue adhesive based on oxidized dextran and epsilon-poly- l -lysine. *Journal of Biomedical Materials Research - Part A*. **2014**, *102*(8), 2511–2520. https://doi.org/10.1002/jbm.a.34923

42. Hyon, W., Shibata, S., Ozaki, E., Fujimura, M., Hyon, S. H., & Matsumura, K. Elucidating the degradation mechanism of a self-degradable dextran-based medical adhesive. *Carbohydrate Polymers*. **2022**, *278*, 118949. https://doi.org/10.1016/J.CARBPOL.2021.118949

43. Matsumura, K., Nakajima, N., Sugai, H., & Hyon, S. H. Self-degradation of tissue adhesive based on oxidized dextran and poly-l-lysine. *Carbohydrate Polymers*. **2014**, *113*, 32–38. https://doi.org/10.1016/j.carbpol.2014.06.073

44. Nakajima, N., Sugai, H., Tsutsumi, S., & Hyon, S. H. Self-Degradable Bioadhesive. *Key Engineering Materials*. **2007**, *342–343*(1), 713–716. https://doi.org/10.4028/WWW.SCIENTIFIC.NET/KEM.342-343.713

45. Nonsuwan, P., Matsugami, A., Hayashi, F., Hyon, S. H., & Matsumura, K. Controlling the

degradation of an oxidized dextran-based hydrogel independent of the mechanical properties. *Carbohydrate Polymers*. **2019**, *204*, 131–141. https://doi.org/10.1016/j.carbpol.2018.09.081

46. Naitoh, Y., Kawauchi, A., Kamoi, K., Soh, J., Okihara, K., Hyon, S. H., & Miki, T. Hemostatic Effect of New Surgical Glue in Animal Partial Nephrectomy Models. *Urology*. **2013**, *81*(5), 1095–1100. https://doi.org/10.1016/J.UROLOGY.2013.01.002
47. You, K. E., Koo, M. A., Lee, D. H., Kwon, B. J., Lee, M. H., Hyon, S. H., Seomun, Y., Kim, J. T., & Park, J. C. The effective control of a bleeding injury using a medical adhesive containing batroxobin. *Biomedical Materials (Bristol)*. **2014**, *9*(2), 025002. https://doi.org/10.1088/1748-6041/9/2/025002
48. Bang, B. W., Lee, E., Maeng, J. H., Kim, K., Hwang, J. H., Hyon, S. H., Hyon, W., & Lee, D. H. Efficacy of a novel endoscopically deliverable muco-adhesive hemostatic powder in an acute gastric bleeding porcine model. *PLOS ONE*. **2019**, *14*(6), e0216829. https://doi.org/10.1371/JOURNAL.PONE.0216829
49. Takagi, K., Araki, M., Fukuoka, H., Takeshita, H., Hidaka, S., Nanashima, A., Sawai, T., Nagayasu, T., Hyon, S. H., & Nakajima, N. Novel powdered anti-adhesion material: Preventing postoperative intra-abdominal adhesions in a rat model. *International Journal of Medical Sciences*. **2013**, *10*(4), 467–474. https://doi.org/10.7150/ijms.5607
50. Takagi, K., Tsuchiya, T., Araki, M., Yamasaki, N., Nagayasu, T., Hyon, S. H., & Nakajima, N. Novel biodegradable powder for preventing postoperative pleural adhesion. *Journal of Surgical Research*. **2013**, *179*(1), e13–e19. https://doi.org/10.1016/j.jss.2012.01.056
51. Kamitani, T., Masumoto, H., Kotani, H., Ikeda, T., Hyon, S. H., & Sakata, R. Prevention of retrosternal adhesion by novel biocompatible glue derived from food additives. *Journal of Thoracic and Cardiovascular Surgery*. **2013**, *146*(5), 1232–1238. https://doi.org/10.1016/j.jtcvs.2013.02.001

52. Takai, F., Takeda, T., Yamazaki, K., Ikeda, T., Hyon, S. H., Minatoya, K., & Masumoto, H. Management of retrosternal adhesion after median sternotomy by controlling degradation speed of a dextran and ε-poly (l-lysine)-based biocompatible glue. *General Thoracic and Cardiovascular Surgery*. **2020**, *68*(8), 793–800. https://doi.org/10.1007/S11748-020-01297-3/FIGURES/5

53. Diamond, Michael P., Burns, E. L., Accomando, B., Mian, S., & Holmdahl, L. Seprafilm® adhesion barrier: (1) A review of preclinical, animal, and human investigational studies. *Gynecological Surgery*. **2012**, *9*(3), 237–245. https://doi.org/10.1007/S10397-012-0741-9/TABLES/1

54. Cezar, C., Korell, M., Tchartchian, G., Ziegler, N., Senshu, K., Herrmann, A., Larbig, A., & De Wilde, R. L. How to avoid risks for patients in minimal-access trials: Avoiding complications in clinical first-in-human studies by example of the ADBEE study. *Best Practice & Research Clinical Obstetrics & Gynaecology*. **2016**, *35*, 84–96. https://doi.org/10.1016/J.BPOBGYN.2015.11.004

55. Mo, X., Iwata, H., Matsuda, S., & Ikada, Y. Soft tissue adhesive composed of modified gelatin and polysaccharides. *Journal of Biomaterials Science, Polymer Edition*. **2000**, *11*(4), 341–351. https://doi.org/10.1163/156856200743742

56. Chao, H. H., & Torchiana, D. F. BioGlue: Albumin/Glutaraldehyde Sealant in Cardiac Surgery. *Journal of Cardiac Surgery*. **2003**, *18*(6), 500–503. https://doi.org/10.1046/J.0886-0440.2003.00304.X

57. Matsumura, K., & Hyon, S. H. Polyampholytes as low toxic efficient cryoprotective agents with antifreeze protein properties. *Biomaterials*. **2009**, *30*(27), 4842–4849. https://doi.org/10.1016/j.biomaterials.2009.05.025

58. McGrath, R. Protein measurement by ninhydrin determination of amino acids released by

alkaline hydrolysis. *Analytical Biochemistry*. **1972**, *49*(1), 95–102. https://doi.org/10.1016/0003-2697(72)90245-X

59. Kakinoki, S., Taguchi, T., Saito, H., Tanaka, J., & Tateishi, T. Injectable in situ forming drug delivery system for cancer chemotherapy using a novel tissue adhesive: Characterization and *in vitro* evaluation. *European Journal of Pharmaceutics and Biopharmaceutics*. **2007**, *66*(3), 383–390. https://doi.org/10.1016/J.EJPB.2006.11.022
60. Kusuki, I., Suganuma, I., Ito, F., Akiyama, M., Sasaki, A., Yamanaka, K., Tatsumi, H., & Kitawaki, J. Usefulness of moistening Seprafilm before use in laparoscopic surgery. *Surgical Laparoscopy, Endoscopy and Percutaneous Techniques*. **2014**, *24*(1). https://doi.org/10.1097/SLE.0B013E31828F6EC1
61. Azziz, R. Microsurgery alone or with INTERCEED Absorbable Adhesion Barrier for pelvic sidewall adhesion re-formation. The INTERCEED (TC7) Adhesion Barrier Study Group II. *Surgery, Gynecology & Obstetrics.* **1993**, *177*(2), 135–139.
62. Becker, J. M., Dayton, M. T., Fazio, V. W., Beck, D. E., Stryker, S. J., Wexner, S. D., Wolff, B. G., Roberts, P. L., Smith, L. E., Sweeney, S. A., & others. Prevention of postoperative abdominal adhesions by a sodium hyaluronate-based bioresorbable membrane: a prospective, randomized, double-blind multicenter study. *Journal of the American College of Surgeons*. **1996**, *183*(4), 297–306.
63. Chimpibul, W., Nakaji-Hirabayashi, T., Yuan, X., & Matsumura, K. Controlling the degradation of cellulose scaffolds with Malaprade oxidation for tissue engineering. *Journal of Materials Chemistry B*. **2020**, *8*(35), 7904–7913. https://doi.org/10.1039/D0TB01015D
64. Lee, K. Y., & Mooney, D. J. Alginate: Properties and biomedical applications. *Progress in Polymer Science*. **2012**, *37*(1), 106–126. https://doi.org/10.1016/J.PROGPOLYMSCI.2011.06.003

65. Nonsuwan, P., & Matsumura, K. Amino-Carrageenan@Polydopamine Microcomposites as Initiators for the Degradation of Hydrogel by near-Infrared Irradiation for Controlled Drug Release. *ACS Applied Polymer Materials*. **2019**, *1*(2), 286–297. https://doi.org/10.1021/acsapm.8b00209

66. Wu, W., Cheng, R., das Neves, J., Tang, J., Xiao, J., Ni, Q., Liu, X., Pan, G., Li, D., Cui, W., & Sarmento, B. Advances in biomaterials for preventing tissue adhesion. *Journal of Controlled Release*. **2017**, *261*, 318–336. https://doi.org/10.1016/J.JCONREL.2017.06.020

67. Del Giudice, G., Fragapane, E., Bugarini, R., Hora, M., Henriksson, T., Palla, E., O'Hagan, D., Donnelly, J., Rappuoli, R., & Podda, A.Vaccines with the MF59 Adjuvant Do Not Stimulate Antibody Responses against Squalene. *Clinical and Vaccine Immunology*. **2006**, *13*(9), 1010. https://doi.org/10.1128/CVI.00191-06

68. Yeo, Y., & Kohane, D. S. Polymers in the prevention of peritoneal adhesions. *European Journal of Pharmaceutics and Biopharmaceutics*, **2008**, *68*(1), 57–66. https://doi.org/10.1016/J.EJPB.2007.03.027

69. Ergul, E., & Korukluoglu, B. Peritoneal adhesions: Facing the enemy. *International Journal of Surgery*. **2008,** *6*(3), 253–260. https://doi.org/10.1016/J.IJSU.2007.05.010

70. Maciver, A. H., McCall, M., & James Shapiro, A. M. Intra-abdominal adhesions: Cellular mechanisms and strategies for prevention. *International Journal of Surgery.* **2011**, *9*(8), 589–594. https://doi.org/10.1016/J.IJSU.2011.08.008

71. Rein, M. S., & Hill, J. A. 32% dextran 70 (Hyskon) inhibits lymphocyte and macrophage function *in vitro*: a potential new mechanism for adhesion prevention. *Fertility and Sterility*. **1989**, *52*(6), 953–957. https://doi.org/10.1016/S0015-0282(16)53158-6

72. Kraft, F., Schmidt, C., Van Aken, H., & Zarbock, A. Inflammatory response and extracorporeal circulation. *Best Practice & Research Clinical Anaesthesiology*. **2015**, *29*(2),

113–123. https://doi.org/10.1016/J.BPA.2015.03.001

73. Zacharia, E., Papageorgiou, N., Ioannou, A., Siasos, G., Papaioannou, S., Vavuranakis, M., Latsios, G., Vlachopoulos, C., Toutouzas, K., Deftereos, S., Providência, R., & Tousoulis, D. Inflammatory Biomarkers in Atrial Fibrillation. *Current Medicinal Chemistry*. **2017**, *26*(5), 837–854. https://doi.org/10.2174/0929867324666170727103357

Chapter 4

General Conclusion

Invasive techniques such as sutures and staples are used to join wounds, but have drawbacks such as secondary tissue damage[1]. A promising and attractive option to mitigate the drawbacks of invasive techniques and to close or connect tissues is the use of tissue adhesives. Tissue adhesives are not only used as an adjunct during suturing in surgery, but also function as hemostatic agents, sealants (to ensure watertightness by forming a barrier layer that prevents fluid and/or gas leakage through an incision), and tissue adhesions to firmly join and secure two surfaces[2,3]. Already in clinical application, tissue Adhesives include cyanoacrylate adhesives made from synthetic materials, fibrin glue adhesives made from naturally derived materials, and biopolymer-aldehyde adhesives made from naturally derived materials and synthetic materials. However, these tissue adhesives do not fully meet the required properties such as low adhesion under wet conditions and low cytocompatibility[4-6]. Cyanoacrylate is mainly used for skin closure, but its use as a tissue adhesive is limited due to its toxic degradation products (formaldehyde)[7]. Fibrin glues have excellent biocompatibility and versatility because they are composed of biogenic components5; however, they have low mechanical properties[8] and there is concern about the transmission of diseases that may be associated with blood products.

A common challenge for synthetic adhesives is to find polymers that are non-toxic and exhibit good gel strength. For this reason, the variety of polymers currently in use is small, with

most adhesives being based on polyurethane or PEG[9-16]. Recently, research and development on adhesive materials using biomimetic techniques has expanded rapidly. In particular, the introduction of L-b-3,4-dihydroxyphenyl-a-alanine (DOPA), which is involved in the adhesive behavior of mussel adhesion proteins, into synthetic polymers such as PEG has been investigated[17-20]. Although this research area has shown many prospects for adhesive strength, the use of toxic oxidants is a major concern.

To meet the requirements for an ideal tissue adhesive as described in Chapter 1, our group has also developed a new self-degrading dextran-based medical adhesive, LYDEX, with high adhesive performance and flexibility, low toxicity, and no risk of viral infection[21]. LYDEX is composed of two components: dextran (AD) oxidized with periodate to introduce aldehyde groups and ε-poly-L-lysine (SAPL) treated with succinic anhydride. After gelation and adhesion by Schiff base bonding between the aldehyde group of AD and the amino group of SAPL, molecular degradation accompanied by Maillard reaction is initiated, but the detailed degradation mechanism has not yet been clarified.

In Chapter 2, the degradation mechanism was elucidated by analyzing the main products of LYDEX by instrumental measurements, with the aim of elucidating in detail the degradation products under typical solution conditions *in vitro*. The degradation of LYDEX gels with a sodium periodate/dextran content of 2.5/20 was observed using gel permeation chromatography and infrared and ^{1}H NMR spectra. These analyses identified degradation products with a mixed structure of SAPL and AD, suggesting a link to the Maillard reaction. The mixture of AD and SAPL became richer in AD as the Mw decreased. After the main chains of the solubilized degradation products of LYDEX were cleaved via Amadori rearrangement, the structure of the AD-SAPL network, with Mws from several million to 145 000 g/mol, was

potentially maintained for a while, wherein the SAPL skeleton remained undegraded and the AD portion degraded to oligodextran, with an Mw of > 2300 g/mol.

In vivo, the degradation products and macromolecular degradation products formed by microfragmentation of LYDEX gel by autolysis are likely to undergo molecular degradation *in vivo* via phagocytosis by macrophages and other phagocytes, as indicated by the data from the transplantation study in Chapter 3, and be absorbed into the spleen and liver, where they are likely to be reduced to low molecular weight by *in vivo* metabolism.

In Chapter 3, in order to advance the development stage toward clinical application of anti-adhesion materials, one of the applications of LYDEX, the optimal dosage (film thickness) of LYDEX to obtain appropriate anti-adhesion performance in *in vivo* applications was investigated. It was clearly shown that the gel film thickness affects the degradation period and the anti-adhesion effect.

It is newly revealed in this study that the degradation period varies with the aldehyde ratio and that the degradation rate of the gel also depends on the thickness of the membrane. It is also noteworthy that *in vivo*, 40 mg of LYDEX gel (oxidant/dextran ratio = 2.5:20) was significantly more effective in preventing adhesions than Seprafilm, a commonly employed anti-adhesion membrane.

The results of this study suggest that LYDEX-based films can be designed for use in a wide range of *in vivo* application sites. Therefore, these results are expected to facilitate the clinical application of this novel anti-adhesion material that combines hemostatic and sealant performance[22-25], making LYDEX an extremely versatile material for applications not possible with previous anti-adhesion materials.

Finally, in this study, the self-degradability of LYDEX was revealed for the first time through the observation of the *in vitro* degradation behavior of LYDEX by the reaction of AD

and SAPL. Although it is not easy to elucidate the degradation mechanism of polymeric compounds, the fact that the degradation mechanism of polysaccharide hydrogels by oxidation has been elucidated by estimating the degradation products over time has increased the probability of its medical applications. In addition, I believe that this report will contribute to the development of new material by combining the control method of degradation and deterioration and the degradation mechanism of polysaccharide hydrogels (polymeric compounds) by oxidation.

Reference

1. Lauto, A., Mawad, D., Foster, L. J. R. Adhesive biomaterials for tissue reconstruction. *J. Chem. Technol. Biotechnol*. **2008**, 83, 464−472. https://doi.org/10.1002/jctb.1771
2. Spotnitz, W. D., Burks, S. Hemostats, sealants, and adhesives: components of the surgical toolbox. *Transfusion*. **2008**, 48, (7), 1502-16. https://doi.org/10.1111/j.1537-2995.2008.01703.x
3. Spotnitz, W. D., Burks, S. State-of-the-art review: Hemostats, sealants, and adhesives II: Update as well as how and when to use the components of the surgical toolbox. *Clin. Appl. Thromb. Hemost*. **2010**, 16, (5), 497-514. https://doi.org/10.1177/1076029610363589
4. Petersen, B., Barkun, A., Carpenter, S., Chotiprasidhi, P., Chuttani, R., Silverman, W., Hussain, N., Liu, J., Taitelbaum, G., Ginsberg, G. G., Technology Assessment Committee., American Society for Gastrointestinal Endoscopy. Tissue adhesives and fibrin glues. *Gastrointest Endosc*. **2004**, 60, (3), 327−333. https://doi.org/10.1016/S0016-5107(04)01564-0
5. Spotnitz, W. D. Fibrin sealant: The only approved hemostat, sealant, and adhesive-a laboratory and clinical perspective. *ISRN Surg*. **2014**, 2014, 203943. https://doi.org/10.1155/2014/203943
6. Chivers, R. A., Wolowacz, R. G. The strength of adhesivebonded tissue joints. *Int. J. Adhes. Adhes*. **1997**, 17, 127−132. https://doi.org/10.1016/S0143-7496(96)00041-3
7. Bhatia, S. K., Traumatic Injuries Chapter 10 Traumatic Injuries. *Biomater. Clini. Applications*. **2010**, 213-258. https://doi.org/10.1007/978-1-4419-6920-0_10
8. Mandell, S.P., Gibran, N.S. Fibrin sealants: surgical hemostat, sealant and adhesive. *Expert Opin. Biol. Ther*. **2014**, 14, (6), 821–830. https://doi.org/10.1517/14712598.2014.897323

9. Ferreira, P., Pereira, R., Coelho, J. F., Silva, A. F., Gil, M. H. Modification of the biopolymer castor oil with free isocyanate groups to be applied as bioadhesive. *Int. J. Biol. Macromo*l. **2007**, 40, (2), 144-152. https://doi.org/10.1016/j.ijbiomac.2006.06.023

10. Eto, M., Morita, S., Sugiura, M., Yoshimura, T., Tominaga, R., Matusda, T. Elastomeric surgical sealant for hemostasis of cardiovascular anastomosis under full heparinization. *Eur. J. Cardiothorac. Surg*. **2007**, 32, (5), 730-734. https://doi.org/10.1016/j.ejcts.2007.06.046

11. Gilbert, T. W., Badylak, S. F., Gusenoff, J., Beckman, E. J., Clower, D. M., Daly, P., Rubin, J. P. Lysine-derived urethane surgical adhesive prevents seroma formation in a canine abdominoplasty model. *Plast. Reconstr. Surg*. **2008**, 122, (1), 95–102. https://doi.org/10.1097/PRS.0b013e31817743b8

12. Kim, K. D., Wright, N.M. Polyethylene glycol hydrogel spinal sealant (DuraSeal Spinal Sealant) as an adjunct to sutured dural repair in the spine: results of a prospective, multicenter, randomized controlled study. *Spine (Phila Pa 1976)*. **2011**, 36 (23), 1906-1912. https://doi.org/10.1097/BRS.0b013e3181fdb4db

13. Strong, M. J., Carnahan, M. A., D'Alessio, K., Butlin, J. D. G., Butt, M. T., Asher, A. L. Preclinical characterization and safety of a novel hydrogel for augmenting dural repair. *Mater. Res. Express 2*. **2015**, 095401. https://doi.org/10.1088/2053-1591/2/9/095401

14. Hill, A., Estridge, T. D., Maroney, M., Monnet, E., Egbert, B., Cruise, G., Coker, G.T. Treatment of suture line bleeding with a novel synthetic surgical sealant in a canine iliac PTFE graft model. *J. Biomed. Mater. Res*. **2001**, 58, (3), 308–312. https://doi.org/10.1002/1097-4636(2001)58:3<308::AID-JBM1022>3.0.CO;2-P

15. Fuller, C. Reduction of intraoperative air leaks with Progel in pulmonary resection: a comprehensive review. *J. Cardiothorac. Surg*. **2013**, 8, 90. https://doi.org/10.1186/1749-8090-8-90

16. Khoynezhad, A., DelaRosa, J., Moon, M. R., Brinkman, W. T., Thompson, R. B., Desai, N. D., Malaisrie, S. C., Girardi, L. N., Bavaria, J. E., Reece, T. B., PROTECT Investigators. Facilitating hemostasis after proximal aortic surgery: Results of the PROTECT trial. *Ann. Thorac. Surg*. **2018**, 105, (5), 1357-1364. https://doi.org/10.1016/j.athoracsur.2017.12.013

17. Ryu, J. H., Lee, Y., Kong, W. H., Kim, T. G., Park, T. G., Lee, H. Catechol-functionalized chitosan/pluronic hydrogels for tissue adhesives and hemostatic materials. *Biomacromolecules*. **2011**, 12, (7), 2653-2659. https://doi.org/10.1021/bm200464x

18. Kim, Y. -M., Kim, C. -H., Park, M. -R., Song, S. -C. Development of an injectable dopamine-conjugated poly(organophophazene) hydrogel for hemostasis. *Bull. Korean. Chem. Soc*. **2016**, 37, 372-377. https://doi.org/10.1002/bkcs.10686

19. Mehdizadeh, M., Weng, H., Gyawali, D., Tang, L., Yang, J. Injectable citrate-based mussel-inspired tissue bioadhesives with high wet strength for sutureless wound closure. *Biomaterials*. **2012**, 33, (32), 7972-7983.

20. Fan, C., Fu, J., Zhu, W., Wang, D. -A. A mussel-inspired double-crosslinked tissue adhesive intended for internal medical use. *Acta Biomater*. **2016**, 33, 51-63. https://doi.org/10.1016/j.biomaterials.2012.07.055

21. Nakajima, N., Sugai, H., Tsutsumi, S., Hyon, S.-H. Self-degradable bioadhesive. *Key Eng. Mater*. **2007**, 342-343, 713-716. https://doi.org/10.4028/www.scientific.net%2FKEM.342-343.713

22. Araki, M., Tao, H., Nakajima, N., Sugai, H., Sato, T., Hyon, S.-H., Nagayasu, T., Nakamura, T. Development of new biodegradable hydrogel glue for preventing alveolar air

leakage. *J. Thorac. Cardiovasc. Surg*. **2007**, 134, (5), 1241-1248. https://doi.org/10.1016/j.jtcvs.2007.07.020

23. Araki, M., Tao, H., Sato, T., Nakajima, N., Sugai, H., Hyon, S.-H., Nagayasu, T., Nakamura, T. Creation of a uniform pleural defect model for the study of lung sealants. *J. Thorac. Cardiovasc. Surg*. **2007**, 134, (1), 145–151. https://doi.org/10.1016/j.jtcvs.2007.01.007
24. Naitoh, Y., Kawauchi, A., Kamoi, K., Soh, J., Okihara, K., Hyon, S.-H., Miki, T. Hemostatic effect of new surgical glue in animal partial nephrectomy models. *Urology.* **2013**, 81, (5), 1095-1100. https://doi.org/10.1016/j.urology.2013.01.002
25. You KE, et al., The effective control of a bleeding injury using a medical adhesive containing batroxobin. Biomed Mater. **2014** Apr;9(2):025002. https://doi.org/10.1088/1748-6041/9/2/025002

Achievement

Journal publications:

1. Hyon, W., Shibata, S., Ozaki, E., Fujimura, M., Hyon, S. H., & Matsumura, K. Elucidating the degradation mechanism of a self-degradable dextran-based medical adhesive. *Carbohydrate Polymers*. **2022**, 278, 118949. https://doi.org/10.1016/J.CARBPOL.2021.118949
2. Hyon, W., Hyon, S. H. Matsumura, K. Evaluation of the optimal dose for the anti-adhesion performance of a self-degradable dextran-based material. *Carbohydrate Polymer Technologies and Applications*. **2022**. 100255. https://doi.org/10.1016/j.carpta.2022.100255.

Others Journal publications:

1. Jin, H., Choi, W., Matsumura K., Hyon, S. H., Gen, Y., Hayashi, M., Kawabata, T., Ijiri, M., Miyoshi, K. Cryopreservation of pig spermatozoa using carboxylated poly-L-lysine as cryoprotectant. *J. Reprod Dev*. **2022**. 68(5), 312-317. https://doi.org/10.1262/jrd.2022-058.
2. 近田 英一, 玄 優基, 玄 丞烋. 医療機器原材料としての生体内分解吸収性ポリマー“BioDegmer®”‐グリコール酸/乳酸共重合体を中心に. *バイオマテリアル*. **2022**. 40, 2, 132-137.
3. Takeuchi, H., Nishioka, M., Maezawa, T., Kitano, Y., Terada-Yoshikawa, K., Tachibana, R., Kato M., Hyon, S. H., Gen, Y., Tanaka, K., Toriyabe, K., Nii, M., Kondo, E., Ikeda, T., Carboxylated poly-l-lysine as a macromolecular cryoprotective agent enables the development of defined and xeno-free human sperm cryopreservation reagents. *Cells*. **2021**. 10(6), 1435. https://doi.org/10.3390/cells10061435.

4. Bang, B. W., Lee, E., Maeng, J. H., Kim, K., Hwang, J. H., Hyon, S. H., Hyon, W., & Lee, D. H. Efficacy of a novel endoscopically deliverable muco-adhesive hemostatic powder in an acute gastric bleeding porcine model. *PLOS ONE*. **2019**, 14(6), e0216829. https://doi.org/10.1371/JOURNAL.PONE.0216829.
5. Fujikawa, T., Imamura, S., Tokumaru, M., Ando, T., Gen, Y., Hyon S. H., Kubota, C., Cryoprotective effect of antifreeze polyamino-acid (Carboxylated Poly-l-Lysine) on bovine sperm: A technical note. *Cryobiology*. **2018**. 82, 159-162. https://doi.org/10.1016/j.cryobiol.2018.02.009.
6. 松村 和明, 玄 優基, 玄 丞侑. カテキンとその医療応用. *バイオマテリアル*. **2019**. 37, 1, 38-41.
7. 玄 優基, 玄 丞侑. 安全性と機能性に優れた医療用接着剤 LYDEX. *別冊 BIO Clinica*. **2017**. 6, 3, 100-107.
8. 玄 優基, 玄 丞侑. 安全性と機能性に優れた医療用接着剤 LYDEX. *BIO Clinica*. **2017**. 32, 11, 85-92.
9. Fujikawa, T., Ando, T., Gen, Y., Hyon, S.H., Kubota, C. Cryopreservation of bovine somatic cells using antifreeze polyamino-acid (carboxylated poly-L-lysine). *Cryobiology*. **2017**. 76, 140-145. https://doi.org/10.1016/j.cryobiol.2017.01.010.

Conferences:

1. Hyon, W., Hyon, S. H., Matsumura, K. Elucidation of the degradation mechanism for a novel self-degradation adhesive, 257th ACS National Meeting & Exposition, 31 March to 4 Aoril, 2019, Orland, Florida, United State of America, Orange County Convention Center
2. Hyon, W., Matsumura, K., Hyon, S. H. A novel anti-adhesion material using LYDEX®, TERMIS EU 2019, 27-31 May 2019, Rhodes, Greece, Rodos Palace Hotel

※ *"Gen, Y" and "Hyon, W" are the same person and "Hyon, W" is my passport name.*

Acknowledgement

I would like to express our sincere gratitude to Dr. Kazuaki Matsumura, Professor of Frontier Research Area of Materials Chemistry, School of Advanced Science and Technology, Japan Advanced Institute of Science and Technology, for his great guidance and encouragement in conducting this research. I thank Toray Research Center, Inc. for their assistance with IR and ^{1}H NMR spectroscopy. I thank the Japan Food Analysis Center for their cooperation in animal testing. I would like to thank Dr. Suong-Hyu Hyon, President of BMG Inc., and his staff for not only providing us with the experimental equipment and experimental space, but also for their support and valuable advice during the experiments of this study. Finally, I would like to express our sincere gratitude to the animals that served as material for this research, and I pray that they may rest in peace.

Yuki Gen